Cape Peninsula University of Technology

FORWARD OSMOSIS MEMBRANES FOR DIRECT FERTIGATION WITHIN THE SOUTH AFRICAN WINE INDUSTRY

by

ROBYN AUGUSTINE

Thesis submitted in fulfilment of the requirements for the degree

Master of Engineering: Chemical Engineering

in the Faculty of

Engineering

at the

Cape Peninsula University of Technology

Supervisor: Associate Prof. Marshall Sheldon

Cape Town

December 2017

DECLARATION

I, Robyn Augustine, declare that the contents of this thesis represent my own unaided work and that the thesis has not previously been submitted for academic examination towards any qualification. Furthermore, it represents my own opinions and not necessarily those of the Cape Peninsula University of Technology.

Signed **Date**

ABSTRACT

Water scarcity in South Africa (SA) and more specifically Cape Town, Western Cape, has escalated to disaster levels in 2018. Agriculture and irrigation account for 62% of SA's accessible potable water (Thopil & Pouris, 2016), and although the agriculture sector plays a pivotal role in SA's socio-economic development, the future of the sector is dependent on critical issues such as climate variability and population growth (Besada & Werner, 2015). Wine production in SA is an important agricultural activity, contributing great economic value to the agri-food sector. However, despite this, the wine industry is responsible for vast water consumption and the unsafe disposal of winery wastewater, which are critical issues from an environmental and economic standpoint.

The ever-imminent crisis pertaining to the limited supply of fresh water from conventional water resources has necessitated the need to develop alternative water resources to supplement an increased water supply, which include the reuse of wastewater, ground water, brackish water (BW) and seawater (SW) desalination. When fresh water supplies are limited, agricultural irrigation is penalised. The reuse of agricultural wastewater as a substitution for potable water irrigation may prove beneficial in areas where water shortages are severe.

Forward osmosis (FO) is a developing desalination technology that has received increased attention as a promising lower-energy desalination technology. FO technology relies on the natural osmotic process, driven by a concentration gradient as opposed to significant hydraulic pressures like reverse osmosis (RO). Water is extracted from a lower concentrated feed solution (FS) to a highly concentrated draw solution (DS). The term "lower energy" is only applicable for applications where the recovery of the DS is not required. FO technology offers several advantages. However, the lack of suitable membrane modules and DSs hinder its practical application. FO offers novelty applications in which specialised DSs are selected to serve as the final product water, most notably concentrated fertilisers for direct fertigation.

The aim of this study was to evaluate the performance and compatibility of commercially available cellulose triacetate (CTA) and aquaporin biomimetic FO membranes with commonly used fertilisers for direct fertigation within the SA wine industry, using a fertiliser drawn forward osmosis (FDFO) system.

Straight (1 M KCl) and blended (N/P/K) fertilisers were used as the draw solutes against alternative feed water resources; deionized (DI) water as the control, synthetic winery wastewater (SWW) and synthetic brackish water (BW5). The osmotic pressure (OP) of alternative feed water resources and fertiliser draw solutes was analysed using an osmometer. The initial OP of DI water as control, SWW, BW5, 1 M KCl and 2/0.15/1 M blended N/P/K solutions were 0, 61, 414, 4 668 and 9 978 kPa, respectively. Second and third generation aquaporin biomimetic membranes (ABMs) were evaluated in the FDFO desalination study, namely ABM_A01 and ABM_A02. The comparative performance of the FO membranes (CTA and ABM) using fertiliser DSs was assessed in terms of water flux (J_w), reverse solute flux (J_s) and percentage water recovery.

The ABM_A02 membrane proved superior for the reclamation of water with the purpose of reducing the final nutrient concentration for direct fertigation using a straight 1 M KCl DS. The ABM_A02 generated an exceptional J_w of 14.25 and 12.97 $L.m^{-2}.h^{-1}$ with DI water as the control and SWW FSs, respectively, when compared to the commercial CTA membrane and ABM_A01 membrane. However, the performance of the ABM_A02 membrane is limited to feed waters containing significant total dissolved solids (TDS), only achieving a J_w of 4.33 $L.m^{-2}.h^{-1}$ when BW5 was used as a FS. A substantial increase in the experimental J_w of 15.54 and 11.31 $L.m^{-2}.h^{-1}$ was observed for the CTA and ABM_A02 membrane using a blended N/P/K fertiliser DS with FSs, DI water and BW5, respectively. The study demonstrated that both straight (1 M KCl) and blended (N/P/K) fertilisers commonly used in the winery industry in the Western Cape can be used as suitable draw solutions. The average J_s generated with a 1 M KCl DS and DI feed water was 0.94, 36.18 and 6.72 $g.m^{-2}.h^{-1}$ for the CTA, ABM_A01 and ABM_A02 membranes, respectively.

The performance of the ABM resulted in significantly higher J_w and J_s in comparison to the commercial CTA membrane, suggesting that the incorporation of aquaporins (AQPs), modifying the structural parameters of the thin film composite (TFC) polyamide membrane, had an improved effect on membrane performance.

Keywords: Draw solution, Concentration polarisation, Feed solution, Fertiliser drawn forward osmosis, Forward osmosis, Osmotic pressure, Water flux and Reverse solute diffusion.

ACKNOWLEDGEMENTS

I wish to thank:

- My supervisor, Associate Professor Marshall Sheldon, for her excellent supervision, wisdom, patience, and dedication to this project.
- Dr. Debbie de Jager for her constant assistance and support.
- My confidante and partner, Miss Zandile Jingxi, for her moral support throughout this project.
- Dr. Lukhanyo Mekuto for his assistance in finalizing my thesis.
- The postgraduate students at Cape Peninsula University of Technology (CPUT) for their support and encouragement.
- The administrative and technical chemical engineering staff at CPUT; Mrs. Elizma Alberts, Mr. Alwyn Bester and Mrs. Hannelene Small for their assistance and contributions to this project.
- My parents and sister for their never-ending support and constant encouragement.

The financial assistance of the National Research Foundation towards this research is acknowledged. Opinions expressed in this thesis and the conclusions arrived at, are those of the author, and are not necessarily attributed to the National Research Foundation.

DEDICATION

For my parents and sister, whose unconditional love and support give me the strength to accomplish all things. Everything I am is because of you.

TABLE OF CONTENTS

LIST OF TABLES

LIST OF FIGURES

GLOSSARY

Term	Explanation
Biochemical oxygen demand (BOD)	The amount of oxygen required by micro-organisms growing in aerobic conditions for the biodegradation of compounds (Bassa & Chetty, 2002).
Biomimetic membrane	Incorporates biological elements or borrows concepts, ideas or inspiration from biological systems (Shen *et al*., 2014).
Draw solution (DS)	The highly concentrated solution is referred to as the draw solution (DS). The DS exhibits a greater osmotic pressure (OP) than that of the saline feed solution (FS) (McCutcheon & Elimelech, 2006; Fang *et al*., 2012).
Feed solution (FS)	The concentrated solution on the side of the semi-permeable membrane which exhibits a lower osmotic potential (OP) than that of the draw solution (DS) (McCutcheon & Elimelech, 2006).
Forward osmosis (FO)	The forward osmosis (FO) process is driven by the natural osmotic pressure (OP) difference across a semi-permeable membrane (Phuntsho, 2012; Qasim *et al*., 2015).
Lees	Winery sediment produced from the fermentation process (i.e. yeasts, tartrates, and pulp) (Van Schoor, 2005).

Osmotic pressure (OP)	The movement of a pure solvent across a membrane while maintaining a condition of equilibrium, this equivalent pressure is known as osmotic pressure (OP) (Phuntsho, 2012).
Sodium adsorption ratio (SAR)	The measurement of the amount of sodium (Na) present in the wastewater relative to the amount of calcium (Ca) and magnesium (Mg) present in the wastewater. The sodium adsorption ratio (SAR) represents the quality of a solution with regard to the Na content. SAR is defined as: $$SAR = \frac{[Na]}{\sqrt{\frac{([Ca] + [Mg])}{2}}}$$ Na divided by the square root of (Ca + Mg)/2, where all values are concentrations expressed in mmol.dm^{-3} (Quist-Jensen *et al*., 2015).

LIST OF ABBREVIATIONS

Abbreviation	Explanation
$(NH_4)_2CO_3$	Ammonium carbonate
$(NH_4)_2SO_4$	Ammonium sulphate
ABM	Aquaporin biomimetic membrane
AOSB	Atlantic ocean seaboard
AQP	Aquaporin
BGW	Brackish ground water
BOD	Biological oxygen demand ($mg.L^{-1}$)
BSF	Biological sand filters
BW	Brackish water
BW5	Synthetic brackish water (5 000$mg.L^{-1}$ NaCl)
C	Carbon
C_2H_6O	Ethanol
$C_6H_{12}O_6$	Glucose
$C_7H_6O_5$	Gallic acid
$C_8H_8O_3$	Vanillin
CA	Cellulose acetate
CaCl	Calcium chloride
CH_3COOH	Acetic acid
Cl	Chloride
$CO(NH_2)_2$	Urea
COD	Chemical oxygen demand ($mg.L^{-1}$)
CP	Concentration polarization
CTA	Cellulose triacetate
DAFF	Department of Agriculture, Forestry, and Fisheries
DI	Deionised
DS	Draw solution
DWAF	Department of Water Affairs and Forestry
ECP	External concentration polarization
FDFO	Fertiliser drawn forward osmosis
FO	Forward osmosis
FS	Feed solution

GDP	Gross domestic product
GM	Genetically modified
H_2O	Water
H_2S	Hydrogen sulphide
H_2SO_4	Sulphuric acid
H_3PO_4	Phosphoric acid
ICP	Internal concentration polarization
IOSB	Indian ocean seaboard
IP	Interfacial polymerization
K	Potassium
K_2SO_4	Potassium sulphate
KCl	Potassium chloride
KNO_3	Potassium nitrate
$MgCl_2$	Magnesium chloride
$MgSO_4$	Magnesium sulphate
N	Nitrogen
NaCl	Sodium chloride
NaOH	Sodium hydroxide
NF	Nanofiltration
NH_4NO_3	Ammonium nitrate
ODMP	Osmotically driven membrane process
OE	Osmotic equilibrium
OMBRs	Osmotic membrane bioreactors
OP	Osmotic pressure
P	Phosphorous
P_2O_5	Phosphorous pentoxide
PDMP	Pressure driven membrane process
PFD	Process flow diagram
PRO	Pressure retarded osmosis
PSE	Polyethersulfone
PSF	Polysulfone
RO	Reverse osmosis
RSFS	Reverse solute flux selectivity
SA	South Africa
SANAS	South African National Accreditation System
SAR	Sodium adsorption ratio

SBR	Sequencing batch reactor
SEM	Scanning electron microscope
SSW	Synthetic seawater (35 000mg.L^{-1} NaCl)
SW	Seawater
SWW	Synthetic winery wastewater
TDS	Total dissolved solids (mg.L^{-1})
TEP	Transparent exopolymer particles
TFC	Thin film composite
TSS	Total suspended solids
USA	United States of America
WC	Western Cape
WMA	Water management area

LIST OF SYMBOLS

Symbol	Explanation
A	Pure water permeability coefficient ($L.m^{-2}.h^{-1}.bar^{-1}$)
A_m	Effective membrane area (m^2)
C	Mass concentration ($g.L^{-1}$)
C_t	Reverse solute concentration ($g.L^{-1}$)
EC	Electrical conductivity ($mS.cm^{-1}$ or $\mu S.cm^{-1}$)
i	van't Hoff's solute factor (dimensionless)
J_s	Reverse solute flux ($g.m^{-2}.h^{-1}$)
J_w	Experimental water flux ($L.m^{-2}.h^{-1}$)
M	Molar concentration ($mol.L^{-1}$)
M_w	Molecular weight ($g.mol^{-1}$)
$\overline{M_w}$	Average molecular weight ($g.mol^{-1}$)
n	Moles (mol)
R	Universal gas constant ($J.g.mol^{-1}.K^{-1}$)
S	Structural parameter (µm)
T	Temperature (K)
TDS	Total dissolved solids ($mg.L^{-1}$)
Greek symbols	
π	Osmotic pressure (kPa)
ρ	Density of pure solvent ($g.L^{-1}$)
Subscript	
b	Bulk
d	Draw solution
f	Feed solution

LIST OF UNITS

Unit	Explanation
cm	Centimeter
hL	Hectolitre
h	Hour
µm	Micromter
mm	Millimeter
$mS.cm^{-1}$	Microsiemen per centimeter
nm	Nanometer

RESEARCH OUTPUTS

Conference Presentation

Augustine, R. 2017. Forward osmosis membranes for direct fertigation within the South African wine industry. WISA Water Sustainability Symposium **"**From Scarce to Sufficient"**,** 7 to 9 May 2017, Cape Town, South Africa.

Poster Presentation

Sheldon, M.S., Jingxi E.Z., **Augustine, R**. & De Jager, D. 2017. FORWARD OSMOSIS: An alternative desalination technology for the textile industry. WISA Water Sustainability Symposium **"**From Scarce to Sufficient"**,** 7 to 9 May 2017, Cape Town, South Africa.

Publications

Sheldon, M.S., Jingxi, E.Z., De Jager, D., **Augustine, R**., Korenak, J., Hélix-Nielsen, C. & Petrinic, I. 2017. Forward osmosis in a South African context: Part A: Dye solutions as draw solutions in the textile industry*. Water SA 3477.*Under review.

Augustine, R., Sheldon, M.S., Petrinic, I. & Hélix-Nielsen, C. 2018. Exploring alternative feed water resources for a fertiliser drawn forward osmosis system. *Water SA 3583.* Under review.

CHAPTER ONE
INTRODUCTION

1.1. Background

Wine production is one of the most important agricultural activities throughout the world, contributing immensely to economic revenue in the agri-food sector (Brito *et al.,* 2006; Devesa-Rey *et al.,* 2011). A total volume of 252.9 x 10^6 hL of wine was produced worldwide in the year 2012 (Conradie *et al*., 2014). South Africa (SA) remains one of the top producing wine countries, contributing a total of 10 x 10^6 hL of wine (Conradie *et al*., 2014). The SA wine industry has made great strides in recent years, with exports having more than doubled between 2005 and 2015 (WOSA, 2016). However, despite vast improvements within the SA wine industry, changes in climatic patterns threaten to affect wine and fruit production. These impacts are already being felt within the SA wine industry (Mozell & Thach, 2014). Water shortages within SA present a formidable challenge, with the agricultural sector consuming about 60% of SA's accessible freshwater for irrigation (Goga & Pegram, 2014). High water demand for food production has stressed many catchment areas and deteriorated water quality in SA (Thiam *et al.,* 2015).

The wine industry is not only water intensive but also produces large volumes of winery wastewater (Melamane, 2007; Melamane *et al.,* 2007; Conradie *et al*., 2014; Kyzas *et al.,* 2014). In general, winery wastewaters are acidic with a high organic load (Melamane, 2007; Melamane *et al.,* 2007; Conradie *et al*., 2014; Kyzas *et al.,* 2014), which can cause considerable environmental pollution (Van Schoor 2005; Melamane *et al.,* 2007; Mosse *et al.,* 2011; Conradie *et al*., 2014; Kyzas *et al.,* 2014). In the past, small volumes of winery wastewater had minimal effects on the immediate environment, but with increasing wine production both in SA and elsewhere in the world, the disposal of winery wastewater and contamination problems related to winery wastewater treatment have raised concerns about the possibilities of establishing viable wastewater treatment systems (Devesa-Rey *et al.,* 2011). Research and development relating to winery wastewater treatment continue to seek more cost-effective and sustainable winery wastewater treatment options (Van Schoor, 2005; Melamane *et al.,* 2007; Devesa-Rey *et al.,* 2011; Kyzas *et al.,* 2014; Laing, 2016).

Drinking water has become an increasingly marginal resource. Global and local water stress may be alleviated by the replacement of potable water by alternative water

sources, specifically for use in industrial processes (Lutchmiah *et al*., 2014). Water availability in the areas surrounding the wine industry in SA could be partially improved by the reuse of treated winery wastewater to replace potable water for irrigation purposes (Melamane *et al.,* 2007). However, the seasonal nature of winery wastewater raises specific problems for treatment processes (Melamane *et al.,* 2007; Kyzas *et al.,* 2014). The attractive features of membrane separation techniques, coupled with the urgent need to address water scarcity and energy shortage, have led to increased research in membrane separation technology (Klaysom *et al*., 2013; Qasim *et al*., 2015).

Forward osmosis (FO) is a developing desalination process that has grown substantially in the last ten years, receiving increased attention in both academic research and industrial development (Cath *et al.,* 2006; Zhao *et al.,* 2012; Lutchmiah *et al*., 2014; Shaffer *et al.,* 2015). FO is thought to have great potential in wastewater treatment for the production of potable water in an energy-efficient manner. FO technology may prove to be a feasible treatment option for the reclamation of potable water from winery wastewater as it possesses considerable advantages. These include a low fouling tendency; minimal pre-treatment of the feed; reduced cake layer formation, which in turn simplifies membrane cleaning; and low pressure operation, which implies lower energy and also simplifies design and equipment use (Klaysom *et al.,* 2013; Lutchmiah *et al.,* 2014; Shaffer *et al.,* 2015). Despite its substantial potential, the shortcomings of FO technology remain a crucial factor hindering its practical application. Internal concentration polarization (ICP), fouling and reverse solute diffusion are inherent in osmotically-driven membrane processes (ODMPs). These shortcomings result in reduction of the overall driving force across the FO membrane and are governed by factors such as membrane orientation and inadequate membrane design (Akther *et al.,* 2015; Shaffer *et al.,* 2015). The ideal FO membrane should exhibit high water flux, high solute rejection, low concentration polarization (CP), high chemical resistance and be mechanically robust (Qasim *et al*., 2015; Shaffer *et al.,* 2015). The membrane properties of the support and active layers are critical for achieving ideal FO membranes.

The viability of FO technology has been demonstrated in a variety of applications, including desalination, wastewater reclamation, wastewater treatment, osmotic membrane bioreactors (OMBR), and liquid food processing (Yong *et al*., 2012). Potential applications of FO in the food, water, and energy sector have been the focus of many earlier studies (Shaffer *et al.,* 2015). However, FO is gaining significant interest in novel areas where the separation and recovery of the draw solutes are not necessary (Phuntsho *et al*., 2011; Phuntsho 2012; McGovern, 2014; Phuntsho *et al*., 2014). While inorganic and thermolytic salts prove to be optimal draw solutes, the use of specialised

draw solutes for niche applications chosen to serve as the final product eliminates the energy-intensive draw recovery stage. Most notably, concentrated fertilisers for agriculture use and concentrated nutrients in hydration bags (Shaffer *et al*., 2015).

The aim of this research project was to evaluate the performance parameters of commercially available FO membranes within the SA wine industry, with the purpose of producing a fertiliser solution for direct fertigation.

1.2. Research problem statement

Despite significant advances in the understanding of FO technology, several limitations and challenges remain. Some of these limiting factors include CP, membrane fouling and reverse solute diffusion, which are governed by factors such as membrane orientation and inadequate membrane design. Membrane selection and development is crucial for process efficiency and is a key factor hindering the successful application of FO technology.

1.3. Aims and objectives

The aim of the research project was to evaluate various commercially available FO membranes and assess their compatibility with commonly used fertilisers for direct fertigation within the SA wine industry, using a fertiliser drawn forward osmosis (FDFO) system.

The objectives of the research project included:

i. Identifying alternative feed solutions (FSs) and evaluating their potential as suitable FSs.
ii. Identifying fertilisers for the use of draw solutions (DSs) in a FDFO process and evaluating their potential as suitable DSs.
iii. Identifying suitable membranes and assessing their potential for application in a FDFO system by investigating:
    - Water flux,
    - Reverse solute flux and,
    - Percentage water recovery rate.

1.4. Research questions

i. Which FS and DS will produce the highest osmotic pressure difference (Δπ)?
ii. Which DS will produce the highest flux?
iii. Is the biomimetic FO membrane a compatible membrane for the production of a fertiliser solution?
iv. Will the application of the FO desalination process be successful in the SA wine industry?

1.5. Significance of the research

The research project will contribute to the understanding of current FO challenges such as membrane development and the improvement of existing FO membranes. In FO technology the phenomenon of CP is a significant barrier that dramatically reduces the performance of FO. The effects of CP on flux behaviour and fouling in FO will be made evident within the SA wine industry.

1.6. Delineation of the research

The research project will not include:

i. The effect of temperature on the flux.
ii. Modelling of the water transport across the membrane.
iii. Evaluating the rejection and salt recovery across the semi-permeable membrane.

CHAPTER TWO
LITERATURE REVIEW

2.1. The food, water, and energy crisis

Food, water, and energy security are imperative for a self-sufficient economy. South Africa (SA) is currently facing severe water shortages, which – paired with insufficient available arable land (Von Bormann & Gulati, 2014; Woltersdorf *et al.,* 2016) and a dependence on coal-fired power – suggests that SA's economy is testing the limits of its resource constraints (Von Bormann & Gulati, 2014; Thopil & Pouris, 2016). Approximately 90% of electricity in SA is generated from coal-fired plants, many of which are located in semi-arid areas. Coal-fired plants use a combination of wet and dry cooling methods (Thopil & Pouris, 2016). Management constraints and inequality of access to resources are intensified by the uneven distribution of natural resources and the location of economic development in SA (Von Bormann & Gulati, 2014; Thiam *et al.,* 2015). Challenges resulting from resource constraints point towards an imminent crisis in the provision of nutritious food, clean water, and electricity. Increasing resource price inflation and instability have highlighted the interconnected and interdependent nature of food resources, water, and energy (Von Bormann & Gulati, 2014). If the challenges regarding food, water, and energy are addressed in isolation, the risk of food, water, and energy security will ultimately become evident, contributing to growing social insecurity (Von Bormann & Gulati, 2014).

Complex forces, both global and domestic, are contributing to an already strained existing food supply. At a macro-level, food security is inevitably linked to global market dynamics of demand and supply. Financial and political forces within the global system further complicate food availability and make changes hard to anticipate (Von Bormann & Gulati, 2014; Besada & Werner, 2015). At a local level, food security is impacted by the following (Von Bormann & Gulati, 2014; Besada & Werner, 2015; Thiam *et al.,* 2015):

i. Population growth,
ii. Availability of arable lands,
iii. Soil degradation,
iv. Water resources, and
v. Climate variability.

SA is likely to experience increased temperatures and altered precipitation as a result of climate change. Crop production is directly impacted by climate variability. The advent of climate change will modify agricultural productivity and increase climate variability, leading to changes in food production and international trade patterns (Calzadilla *et al*., 2014).

Water scarcity is a broad issue that concerns both national and international government. Currently, more than one billion people lack access to fresh drinking water and 2.4 billion people lack access to adequate sanitation (Thopil & Pouris, 2016). It is estimated that by the year 2025, more than 60% of the world's population will live in countries with significant water imbalances, largely in Asia, Africa and Latin America (Thopil & Pouris, 2016). Water imbalances already experienced in these regions have led to increased attention in the allocation and utilisation of water within the food-water-energy nexus (Thopil & Pouris, 2016).

SA is located in a semi-arid region and is considered one of the 30 driest countries in the world (Thopil & Pouris, 2016). SA is currently facing severe water shortage. SA's mean annual rainfall is 497 mm per annum, well below the global annual average of 860 mm per annum. To put things further into perspective, Botswana and Namibia have an annual rainfall of 400 and 254 mm per annum, respectively with populations of two and 2.28 million, while SA has a population of 50 million people (Thopil & Pouris, 2016). SA's relatively low rainfall and vast population size have placed a skewed level of stress on the limited water resources (Thopil & Pouris, 2016). Given the level of water scarcity in the country, water-intensive energy production and an increase in agricultural production in response to growing demand will challenge the existing balance between the water-energy nexus (Von Bormann & Gulati, 2014).

SA has reached a state where fresh water resources within its boundaries are nearly fully utilised. This, paired with adverse challenges in the quality, quantity, and accessibility of water resources, may necessitate the recycling of wastewater, the development of suitable wastewater treatment processes, as well as water reclamation from alternative water resources to argument existing supplies (Von Bormann & Gulati, 2014). Meeting higher water quality requirements often requires advanced treatment technologies to purify and treat wastewater, but these processes are often associated with high energy requirements (Von Bormann & Gulati, 2014). Thus a movement toward green technologies that are capable of providing clean water and clean energy from abundantly available renewable resources may provide a potential solution to the world's most challenging problems of water and energy scarcity (Klaysom *et al*., 2013).

2.1.1. Water usage in South Africa (SA)

The majority of water resources in SA are used for agriculture and irrigation. Agriculture and irrigation account for 62% of SA's accessible water resources (Thopil & Pouris, 2016). Rural and urban usage accounts for 18% while large industries and power generation accounts for only 8%. Figure 2.1 illustrates the water usage in SA for the year 2011 in billion cubic meters.

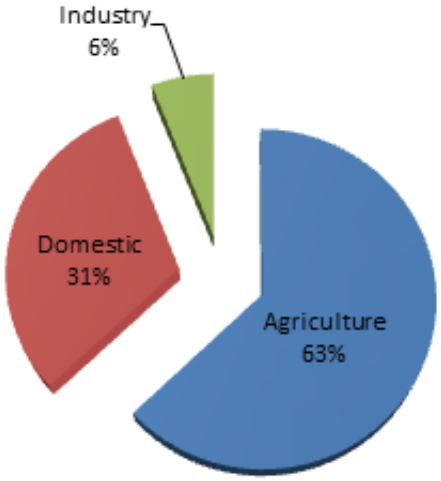

Figure 2.1: Water usage in SA (2011 billion cubic meters) (adapted from Thopil & Pouris, 2016)

In order to facilitate effective water management practices, SA has been divided into 19 catchment-based water management areas (WMAs). Of the 19 WMAs, nine experience moderate water shortage while six face severe water shortage. Although water usage in large industries and power generation is only 8%, the regions where these industries are located fall into the moderate to severely water constrained WMAs (Thopil & Pouris, 2016).

2.2. The South African (SA) agriculture

Agriculture is the foundation of many developing economies. As one of these, developing economies, SA needs to ensure a healthy agricultural industry. The agriculture sector plays a pivotal role in SA's socio-economic development. However, the future of the sector is dependent on critical issues such as climate variability, population growth, changes in consumer needs and shifts in the global economy and related markets (DAFF, 2012; DAFF, 2015a). As one of the most employment-intensive sectors of the economy, the agricultural sector's potential impact on employment and poverty relief is much larger than its actual weight as the economy suggests. Despite its relatively small contribution to the gross domestic product (GDP), the sector plays a central role in terms

of food security, social welfare, job creation and ecotourism (Goldblatt, 2010). The agriculture sector provides, either directly or indirectly, a total of 8.5 million people with employment, representing about 7% of formal employment (DAFF, 2012; DAFF, 2015a) and contributes to 3% of the GDP. The agricultural sector, therefore, has significant social and economic implications for SA (Nkondo *et al.,* 2012; Dryden & Campbell, 2013). DAFF (2015a) estimates the total gross value of agriculture production in 2013 for field crops, horticulture, and animal products at 192 017 million rands.

SA has a dual agricultural economy that encompasses the less developed subsistence sector as well as the well-developed commercial sector. Agricultural activities range from intensive crop production to mixed farming (DAFF, 2012; DAFF, 2015a). Approximately 12% of SA's surface area can be used for crop production. Of the total available arable land, only 22% comprises of high potential arable land, and some 1.3 million hectares are under irrigation (DAFF, 2015a).

The health of the agriculture sector in SA is dependent on the sustainability of farming methods. Intensive farming practices are dependent on water, fuel, feed, inorganic fertilisers, pesticides, herbicides, and increasingly on genetically modified (GM) seeds (Goldblatt, 2010). In 1904, AgriSA was established as the South African Agriculture Union. AgriSA serves approximately 32 000 large and small commercial farmers with a mission to promote the development, profitability, stability, and sustainability of agriculture in SA (DAFF, 2012).

2.3. The South African (SA) wine industry

SA is described as the most exciting New World wine-producing country due to a combination of old vines, new regions and winemaking talent (Vinexpo, 2013; Fleming *et al*., 2014). In SA it is estimated that 98 597 hectares of wine-producing grapes are cultivated (SAWIS, 2016). The majority of SA vineyards are located in the Western Cape (WC), with the Stellenbosch wine region dominating 16.48% of the hectares of vines and Paarl, Robertson, Swartland, Breedekloof, Olifants River, Worcester, Northern Cape and Klein Karoo (SAWIS, 2016) yielding the rest of the wine-producing grapes. Figure 2.2 illustrates the distribution of wine grape vineyards in the WC region.

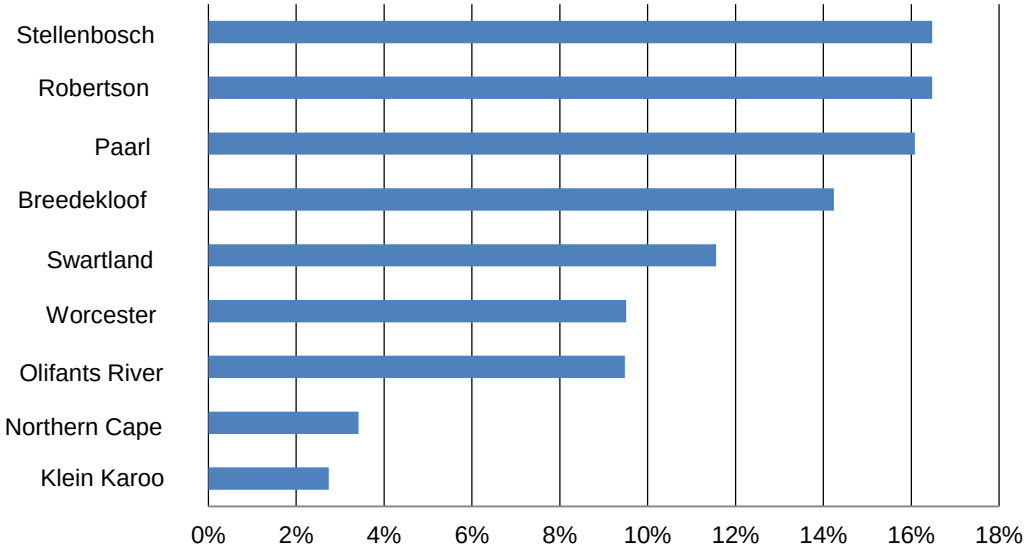

Figure 2.2: The distribution of wine grape vineyards (hectares) per wine region, 2015 (adapted from SAWIS, 2016)

In 2015 the major wine producing countries ranked from the highest to the lowest for wine production in litres (L) were as follows: Italy, France, Spain, the United States of America (USA), Argentina, Chile, SA and China (SAWIS, 2016). In 2015 the total wine production of the SA wine industry, which ranks 8th in terms of world production, was estimated at 1.2 x 10^{9} L per year. This includes wine, wine for brandy, distilling wine, grape juice concentrate and grape juice (SAWIS, 2016). In SA there are a total 3 232 primary grape producers and a total of 566 wine cellars that crush grapes (SAWIS, 2016). The average winery crushes approximately one to 100 tons of grapes, with white wine making up more than 70% of SA's wine production (Conradie *et al*., 2014; SAWIS, 2016). Table 2.1 illustrates the number of primary wineries in SA according to production capacity. In 2015 the total wine consumption in SA was estimated to be 4.25 x 10^{6} hL, which included natural wine, fortified wine and sparkling wine (SAWIS, 2016). The SA wine industry exported 43.4% of its total wine production in the year 2015, a total of 4.2 x 10^{6} hL (SAWIS, 2016).

The winemaking industry remains one of SA's leading agri-exporters, accounting for 1.2% of the national GDP in 2013 (VinPro, 2015). However, despite a vibrant export market, focus remains on the mounting pressures of the wine industry's profitability, noting that increased rates in wine production costs have significantly surpassed the growth in income procured from grape production (VinPro, 2015). Increases in wine production in SA have intensified pressures that the industry exerts on natural resources

such as water, soil, and vegetation (Grismer *et al.,* 2003; Van Schoor, 2005; Conradie *et al*., 2014).

Table 2.1: Number of primary wineries in SA per production capacity in 2015 (SAWIS, 2016)

Capacity (tons of grapes crushed)	Number of wineries
1-100	1 230
>100-500	1 168
>500-1 000	426
>1 000-5 000	395
>5 000-10 000	12
>10 000	1

2.3.1. The winemaking process

Vinification encompasses all the steps in the winemaking process, during the elaboration of wine from grapes through fermentation (Devesa-Ray *et al*., 2011). Winemaking is seasonal (Melamane *et al*., 2007; Guglielmi *et al*., 2009; Devesa-Ray *et al*., 2011; Conradie *et al*., 2014; Kyzas *et al*., 2014) and predominantly performed during the autumn dormancy (i.e. vintage period) (Devesa-Ray *et al*., 2011). The fundamentals of winemaking have remained the same over time (Conradie *et al*., 2014), but the process differs in terms of region, financial status of the winery, procedures, practices, and the types of grapes used (Laing, 2016). The winemaking industry generates large amounts of waste during the annual vintage period (Kyzas *et al*., 2014). This waste is characterised by a high content of biodegradable compounds and suspended solids (Devesa-Ray *et al*., 2011). Waste generated from the vinification process consists of plant remains from destemmed grapes, sediments obtained from clarification, bagasse from pressing and lees obtained from the various decanting steps (Devesa-Ray *et al*., 2011).

2.3.2. Winery wastewater treatment and recycling

Waste minimisation is an important aspect of any industry, as it not only reduces the consumption of potable water but also decreases the total volume of wastewater generated (Melamane *et al*., 2007). Large quantities of low-quality wastewater are generated from the various operations associated with the vinification process. This wastewater poses an environmental threat if not treated correctly (Van Schoor, 2005; Conradie *et al*., 2014). Wastewater generated from the vinification process varies from one winery to another (Agustina *et al*., 2008; Conradie *et al*., 2014).

The volume and composition of winery wastewater are dependent on the use of water, production period and unique winemaking techniques of the winery concerned (Melamane *et al*., 2007; Conradie *et al*., 2014; Laing, 2016). It has been estimated that SA produces approximately one billion L of winery wastewater per annum (Sheridan *et al*., 2011; Welz *et al*., 2012). Winery wastewater produced in SA has been predominately disposed of through land irrigation. The potential occurrence of unpleasant odours and seepage as a result of land irrigation are some of the secondary environmental risks associated with such irrigation. Over-irrigation may result in saturated, anaerobic soils (Van Schoor, 2005; Myburgh & Howell, 2014; Laing, 2016).

With SA being a water-scarce country, all efforts should be made to treat winery wastewater for further use, which puts the spotlight on wastewater treatment options (Dillon, 2011). The use of treated wastewater further contributes to sustainable farming and reduces financial overheads. The choice of wastewater treatment plant is often determined by factors such as the size of the winery operation in terms of tonnage harvested and the resultant wastewater generated (Dillon, 2011). Wastewater treatments are usually conducted on site, unless, as in certain instances, winery wastewater is channelled into local municipal lines and becomes the responsibility of the municipality (Van Schoor, 2005; Dillon, 2011). Between 70 and 80% of wineries are currently engaged in primary wastewater treatments, which involve the separation and screening of solid organic materials (Dillon, 2011). This process removes solid waste but does not change the composition of the wastewater, unlike treatments involving biological and disinfection action. Many effective treatment options exist with the main objective of reducing the organic matter and suspended solids within the wastewater stream. However, these are usually associated with high capital installation and running costs. Current winery wastewater treatment options include (Van Schoor, 2005; Dillon, 2011; Laing, 2016):

i. Primary treatment involving mechanical screening and delta separator.
ii. Primary treatment using lime dosing.
iii. Secondary treatment using a bioreactor system.
iv. Secondary treatment using a sequencing batch reactor (SBR).
v. Tertiary treatment involving a wetland for final polishing.

A number of studies in SA (Ramond *et al*., 2013; Welz & le Roes-Hill, 2014; Welz *et al*., 2014) have investigated the bioremediation capacity of biological sand filter (BSF) mesocosms for the treatment of winery wastewater, with the principle objective of chemical oxygen demand (COD), and phenolic and salt removal.

2.3.3. Origin of winery wastewater and associated pollutants

The winemaking process is seasonal. Activities relating to the winemaking process occur predominately during the harvest period (Guglielmi *et al*., 2009; Conradie *et al*., 2014). Throughout the year, the water volume and pollution load vary in relation to the different processes taking place (Van Schoor 2005; Arienzo *et al*., 2009; Conradie *et al*., 2014; Kyzas *et al.,* 2014). Wineries differ in size, operational procedures and management practices. They undertake similar but highly site-specific practices. These variables result in the production of different qualities and quantities of wastewater (Van Schoor, 2005; Agustina *et al*., 2008; Conradie *et al*., 2014; Ioannou *et al*., 2013). The chemical characteristics of winery wastewater are influenced by practices such as the type of wine produced, the wine production period, the winemaking style, the type of equipment used and the frequency of washing and methods of tank disinfection (Agustina *et al*., 2008; Arienzo *et al*., 2009; Laing, 2016). Winery wastewater originates primarily from the various washing operations during the crushing and pressing of grapes, as well as from the rinsing of the fermentation zones, barrels, washing equipment, and bottles (Petruccioli *et al.,* 2002; Van Schoor, 2005; Strong & Burgress, 2008; Ioannou *et al*., 2013; Erdogan, 2014). Wineries must be kept meticulously clean to avoid contamination and spoilage (Kyzas *et al.,* 2014). Table 2.2 illustrates the various winemaking practices and their associated wastewater generation source. Winery wastewater is produced predominately in the vintage season; the vintage season encompasses all activities from the harvesting of grapes to their pressing and fermentation into wine (Laing, 2016). The season lasts roughly three months after harvesting (Laing, 2016).

2.3.4. Characteristics of winery wastewater

Analysis of the characteristics of winery wastewater indicate that its composition varies greatly around the world and even between different wineries within the same country (Conradie *et al*., 2014; Mosse *et al*., 2011). Discrepancies in winery wastewater composition further complicate the question of finding a general solution for the treatment of winery wastewater at different wineries. It is important to understand the detailed composition of winery wastewater when considering its correct treatment and reuse efficiency.

Table 2.2: Winemaking practices and their associated wastewater generation source (adapted from Musee *et al*., 2007; Laing, 2016)

Procedure	Process description	Wastewater generation source
Crushing and Pressing	Crushing and pressing occurs interchangeably. The process of crushing simply breaks grape berries while pressing encompasses the separation of grape juice from the grape berry solids. These processes produce musts and solids. Juice is released and the process of maceration occurs.	Washing of equipment (i.e. presses and solid residues) and washing of the production room.
Fermentation	The fermentation process lasts approximately 15 days for each tank from the time it was filled with 80% must.	No wastewater generated from the fermentation process itself. Wastewater is generated by the pre-washing of the fermentation vessels and by the cleaning of the winery.
Decanting	The decanting process lasts approximately 2 days for red grapes and 5 days for white grapes. During the decanting step the supernatant wine is separated from the wine lees. Thereafter it is fed to tanks for further stabilisation.	Wastewater is generated from the washing of the tanks, from the cleaning of the decanting pump, from the washing of the production room and from losses during wine decanting.
Maturation and stabilisation	Maturation and stabilisation occur in tanks and lasts approximately 15 days.	The pre-washing of the stabilisation vessels generates wastewater.
Filtration	Wine quality is enhanced after stabilisation though the filtration process. Thereafter the wine is emptied in tanks; the process lasts approximately 10 days.	Wastewater is generated from the washing of tanks, the washing of filters, the cleansing of the transportation pumps, the washing of the production room and from possible spillages during its transfer.
Transportation and disposal	Wine produced is discharged from tanks and either sold in bulk or bottled and transported to its final destination. This period is approximately one semester (i.e. 6 months).	Wastewater is generated from the washing of the storage tanks, the washing of the transportation pumps and the washing of the packing room.

In general, winery wastewater consists of organic matter and salts; it contains moderate nutrient concentrations and has a low pH (Melamane *et al*., 2007; Conradie *et al*., 2014; Kyzas *et al*., 2014). Organic waste makes up most of the waste matter generated in the cellar. The organic material found in winery wastewater is generated from the grapes and wine: after the grapes have been destemmed and pressed, what is left is grape marc that consists of grape skins and pips. The high level of COD and variations in pH are attributed to residues on the floor of the cellar and in the press (Van Schoor, 2005; Conradie *et al*., 2014). Lees that form on the bottom of wine tanks or barrels after fermentation of the grape juice also contribute to the organic compounds and COD of the winery wastewater. Table 2.3 illustrates the general chemical characteristics of winery wastewater and the minimum and maximum quantities of their constituents, as reported in literature.

Table 2.3: Summary of the reported chemical characteristics of winery wastewater (adapted from Laing, 2016)

Parameter	Minimum	Maximum	References
pH	3.50	6.11	4, 5
Chemical oxygen demand (COD) ($mg.L^{-1}$)	400	27 200	1, 2, 4, 5
Total suspended solids (TSS) ($g.L^{-1}$)	0.10	1.50	1, 2, 4, 6
Polyphenols ($mg.L^{-1}$)	5.10	1 450	1, 2
Ethanol ($g.L^{-1}$)	1.20	4.90	3
Glucose and fructose ($g.L^{-1}$)	0.10	5.00	3
Glycerol ($g.L^{-1}$)	0.16	0.32	3
Tartaric acid ($mg.L^{-1}$)	0.12	1 680	3
Malic acid ($mg.L^{-1}$)	0.11	70	3
Lactic acid ($mg.L^{-1}$)	0.13	250	3
Acetic acid ($mg.L^{-1}$)	50	663	3
Total nitrogen ($mg.L^{-1}$)	0.001	71	1, 2, 4
Total phosphorus ($mg.L^{-1}$)	1.00	176	1, 2, 4

1. Petruccioli *et al*., 2000; 2. Petruccioli *et al*., 2002; 3. Agustina *et al*., 2008; 4. Arienzo *et al*., 2009; 5. Mahajan *et al*., 2009; 6. Mosse *et al*., 2011.

2.3.5. Feasibility of winery wastewater for irrigation

Untreated winery wastewater does not meet the requirements set out by the National Water Act (Act no. 36 of 1998) for safe discharge into water sources. Therefore, winery wastewater needs to undergo treatment before its release into water sources or disposal in an alternative manner (Van Schoor, 2005). The alternative method for the disposal of treated winery wastewater most commonly employed by SA wineries is land irrigation (Van Schoor, 2005; Laing, 2016). The requirements of treated winery wastewater for land irrigation are set out in the National Water Act, 1998. The water intended for land

irrigation use must be registered with The Department of Water Affairs and Forestry (DWAF) before irrigation may commence (Van Schoor, 2005). Table 2.4, below, indicates specific parameters for the composition of treated winery wastewater if it is to be used for land irrigation purposes.

Table 2.4: Quality requirements of treated winery wastewater for land irrigation use (adapted from Van Schoor, 2005; Laing, 2016)

	Required wastewater limits for various volumes use for irrigation per day			
		Pastures/Lawns		**Other crops**
Parameter	**50m^3.d^{-1}**	**50 - 500m^3.d^{-1}**	**500 – 2 000m^3.d^{-1}**	**0 - 50m^3.d^{-1}**
Chemical oxygen demand (COD) (mg.L^{-1})	<5 000 after removal of alge	<400 after removal of alge	<75	<100
Electrical conductivity (EC) (mS.m^{-1})	<200	<200	<150	<150
pH	6≤pH≤9	6≤pH≤9	5.5≤pH≤9.5	6≤pH≤9
Sodium adsorption ratio (SAR)	<5	<5	N.A	<5
Suspended solids (SS) (mg.L^{-1})	N.A	N.A	<25	N.A

Most wineries have begun to treat winery wastewater on site, through various means, usually for irrigation on pastures or discarding into SA rivers (Sheridan *et al.,* 2011). The current use of winery wastewater for irrigation is imperative for the development of sustainable winery wastewater treatment plans. It must also be determined whether the current irrigation practice is beneficial or detrimental for grape production (Van Schoor, 2005). Under ideal conditions irrigation with winery wastewater should be no more complicated than irrigating a crop with water that contains added fertiliser (i.e. fertigation). However, the seasonal variability of winery wastewater composition may cause imbalances. Imbalances may stem from mismatches between combinations of wastewater composition; irrigation methods and delivery rate; and the inability of the land to absorb and fully neutralize the wastewater. The rehabilitation of contaminated soil is both costly and time consuming therefore, imbalances as the result of winery wastewater irrigation must be avoided. If winery wastewater could be used in a sustainable manner, it would offer the following benefits (Myburgh & Howell, 2014):

i. Reduction in the energy presently required for wastewater treatment, e.g. using pumps to aerate the water in ponds.

ii. The presence of major plant nutrients in the wastewater, e.g. nitrogen (N), phosphorus (P), and potassium (K), could reduce the cost of fertilisation.
iii. Where irrigation water is limited, the reuse of wastewater will have a positive impact on grape yields if additional irrigation could be supplied in the form of treated winery wastewater.
iv. If possible, the water saving and higher yields acquired from irrigation with treated winery wastewater will contribute to the sustainability and economic viability of wine production.

2.3.6. Fertiliser usage in South Africa (SA)

Fertiliser consumption in SA represents about 0.5% of the total global consumption (DAFF, 2015b). Maize accounts for 41% of total fertiliser application while sugar cane, the second largest consumer, accounts for 18%. Horticulture and fruit crops account for 20% of total fertiliser consumption. However, their contribution to the total value of crop production is much greater (DAFF, 2015b). SA has become increasingly dependent on imports to satisfy local fertiliser demand, this raises concern among local fertiliser consumers. In 1990, less than 20% of the fertiliser used was imported; in 1999, 40% of the local demand was met by imports, and in 2008 more than 65% of SA's nutritional fertiliser consumed was imported (Grain SA, 2011).

2.3.7. Grapevine nutrition and fertigation

Nutrition is a cost-sensitive issue in vineyards. For many end uses, grape berry appearance and composition are significant drivers for production technology. However, yield remains the primary driver (Treeby, 2006). Vineyard nutrition management remains crucial since it impacts vine growth, crop yield, berry composition and ultimately, must and wine quality (Proffitt & Campbell-Clause, 2012). The nutrient requirements of annual crops are dependent on the biological stage of growth and vary from seed to harvest (Kafkafi & Tarchitzky, 2011). Vineyard fertilisation practices aim to ameliorate the supply of available macro-nutrients in the soil to levels required for optimum grapevine growth and yield (Kafkafi & Tarchitzky, 2011). Fertigation entails the application of essential mineral nutrients though irrigation water (Conradie & Myburgh, 2000; Treeby *et al*., 2004; Alva *et al*., 2008), an increasingly common practice in the SA viticulture industry (Conradie & Myburgh, 2000). The practice of fertigation is a contemporary agro-technique, which provides an excellent opportunity to maximise yield and minimise environmental pollution (Hagin *et al*., 2002) through increasing fertiliser use efficiency.

The chemical compositions of soluble straight fertilisers (contributing single nutrient) and compound fertilisers produced by the fertiliser industry are generally the same throughout the world. However, their application is highly site specific and dependent on soil type, climatic conditions and water quality (Kafkafi & Tarchitzky, 2011). Grapevines require a number of macro-nutrients, while micronutrients are also required, but in lesser amounts. The major macro-nutrients that play an essential role in vegetative and fruit developments for grapevines include nitrogen (N), phosphorous (P), potassium (K), magnesium (Mg), calcium (Ca) and sulfur (S) (Goldammer, 2015).

2.3.7.4. Nitrogen (N) in fertigation

Nitrogen (N) is usually the most limiting element for grapevine growth and yield. The application of N to the soil is dependent on the inherent N supply (Proffitt & Campbell-Clause, 2012; Goldammer, 2015). N is customarily applied each growing season. N requirements are based on the crop to be grown and the soil type, which influences yield goals (Maguire, 2009). Recommendations for application are generally made in conjunction with soil test reports. A number of studies have been conducted on the impact of various rates and timing in the application of N in vineyards. The supply of N affects the amount of N in the berries: too much N results in rapid fermentation and undesirable compounds potentially forming in the final wine, while too little N results in stalled fermentation and the production of hydrogen sulphide (H_2S) (Proffitt & Campbell-Clause, 2012).

2.3.7.5. Phosphorus (P) in fertigation

Generally, adequate amounts of phosphorous (P) are found in vineyard soils. However, if P is found to be deficient this needs to be corrected during site preparation. Vines growing in soils deficient in P can result in poor vegetative and reproductive growth. This will, in turn, result in negative effects on berry composition and subsequent must and wine quality (Proffitt & Campbell-Clause, 2012).

2.3.7.6. Potassium (K) in fertigation

Potassium (K) is one of the more important fertiliser elements required for grapevine production (Mpelasoka *et al*., 2003). Grapes appear to be not very efficient at obtaining K from the soil, and K is required in large amounts for grapevine production. Significant amounts of K are removed from the vineyards in the form of grapes during the harvest dormancy. The amount of fertiliser applied, timing, frequency of application and soil

characteristics are the various factors which influence the impact of K fertiliser on the level of available K in the soil and uptake (Raath, 2012). Grapevines tend to exhibit a deficiency in K when they have been heavily cropped and maintenance applications of K have not been made to the vineyard. A deficiency in K could result in the bronzing of leaves; some leaves may even develop dark spots or blotches (Proffitt & Campbell-Clause, 2012). Marginal chlorosis, the browning and dying of vine leaves may occur as the deficiency becomes more marked. In severe cases, more than half of the leaves on a vine may display these symptoms (Proffitt & Campbell-Clause, 2012).

2.4. Membrane technology in water desalination and reclamation

A growing population, diminishing water supply and elevated energy usage have led to increased research into alternative water and energy resources (Fang *et al*., 2012; Klaysom *et al.,* 2013; Low *et al.,* 2015). Membrane separation technology is currently in a state of rapid growth and innovation (Qasim *et al*., 2015). A growing number of academic, industrial and government research groups around the world are conducting work on water treatment and reuse, particularly in the area of membrane-based water treatment (Klaysom *et al.,* 2013; Korenak *et al*., 2017). This has sparked significant interest as a potential solution to the ongoing formidable global challenges of water and energy scarcity (Klaysom *et al*., 2013; Qasim *et al*., 2015).

Membrane separation processes compete directly with conventional water treatment technologies in water desalination and purification. Membrane separation technologies offer the advantage of simple operation yielding a higher quality product (Korenak *et al*., 2017). In addition, membrane processes are easy to up- and down-scale and have the advantage of operating at ambient temperatures, avoiding any change in or degradation of products (Korenak *et al*., 2017). The criteria used to distinguish the practical application of separation processes are that i) separation must be technically feasible, and ii) separation must be economically feasible.

High water quality can be produced via nanofiltration (NF) and reverse osmosis (RO). Today, about 63% of established desalination plant capacity around the world is based on membrane technology (Phuntsho *et al*., 2016). RO is the preferred membrane process for many desalination applications in SA, including the desalination of seawater (SW) (Turner *et al*., 2015). However, new emerging technologies are being investigated; forward osmosis (FO) is a promising candidate for low pressure, low energy and low cost desalination (Qasim *et al*., 2015; Phuntsho *et al*., 2016; Korenak *et al*., 2017).

2.4.1. Nanofiltration (NF)

Nanofiltration (NF) is a pressure-driven membrane bio-separation process. NF relies on the ability of the membrane acting as a selective barrier to allow the passage of solvents while impeding the passage of solutes. Separation and filtration in NF are attained though a combination of solubility diffusion, sieving and charge rejection though micropores (<2 nm) (Huei, 2005; Judd, 2011; Simate *et al*., 2011). NF is primarily used for water pre-treatment, treatment and purification (Rautenbach & Groeschl, 1990; Miyaki, *et al*., 2000; Atkinson, 2002; Van der Bruffen & Vandecasteele, 2003; Costa & de Pinho, 2006; Garcia *et al*., 2013; Naidu *et al*., 2015). Typical pressure requirements for NF are between 10 and 40 bars (Thorsen & Fløgstad, 2006).

2.4.2. Reverse osmosis (RO)

Reverse osmosis (RO) has become increasingly popular as a separation technique for the removal of undesired solutes from a solution (McCutcheon & Elimelech, 2006; Motsa *et al.,* 2014). RO is a pressure-driven membrane process (PDMP) in which significant hydraulic pressures are used to overcome the osmotic pressure (OP) of the feed water or feed solution (FS). As shown in Figure 2.3 (A), hydraulic pressure (P) is the driving force that permits the transport of water across the semi-permeable membrane, thus separating solutes from the solution (Gray *et al*., 2006; McCutcheon & Elimelech, 2006; Phuntsho *et al.,* 2011). The typical pore size and pressure requirements for RO are <0.6 nm and 30 to 70 bars, respectively (Thorsen & Fløgstad, 2006). RO has been employed heavily in the field of desalination and wastewater for water reuse (Fritzmann *et al*., 2007; Greenlee *et al*., 2009; Tu *et al*., 2010; Turner *et al*., 2015). However, its major drawback is its operational cost, deriving from its elevated hydraulic pressure requirement (Gray *et al*., 2006; McCutcheon & Elimelech, 2006; Phuntsho *et al.,* 2011; Fang *et al*., 2012; Klaysom *et al.,* 2013; Qasim *et* al., 2015; Phuntsho *et al*., 2016).

2.4.3. Forward osmosis (FO)

Forward osmosis (FO) is a developing technology that has gained much interest due to its relative simplicity and lower energy consumption: the actual osmosis process powers itself. As shown in Figure 2.3 (B), FO utilizes the OP difference ($\Delta\pi$), where a draw solution (DS) having a significantly higher OP than that of the saline FS, prompts water to be transported across the semi-permeable membrane due to the natural OP gradient (Gray *et al*., 2006; McCutcheon & Elimelech, 2006; Klaysom *et al.,* 2013; Motsa *et al.,* 2014; Akther *et al.,* 2015; Low *et al.,* 2015; Phuntsho *et al.,* 2016; Korenak *et al*., 2017).

The osmotic driving forces in FO may prove to be significantly greater than the hydraulic driving forces in RO, potentially leading to larger water flux and recovery rates (Al-Hemiri *et al*., 2009). The absence of hydraulic pressure may result in a substantially less expensive process. However, the draw-regeneration step in the FO process can be energy-intensive (Fang *et al*., 2012; Alsvik & Hägg, 2013; Klaysom *et al.,* 2013; Lutchmiah *et al.,* 2014). Figure 2.4 illustrates the FO process schematic with the energy-intensive draw regeneration process. Since FO technology is the focus of this study it will be explained in more detail in the following sections.

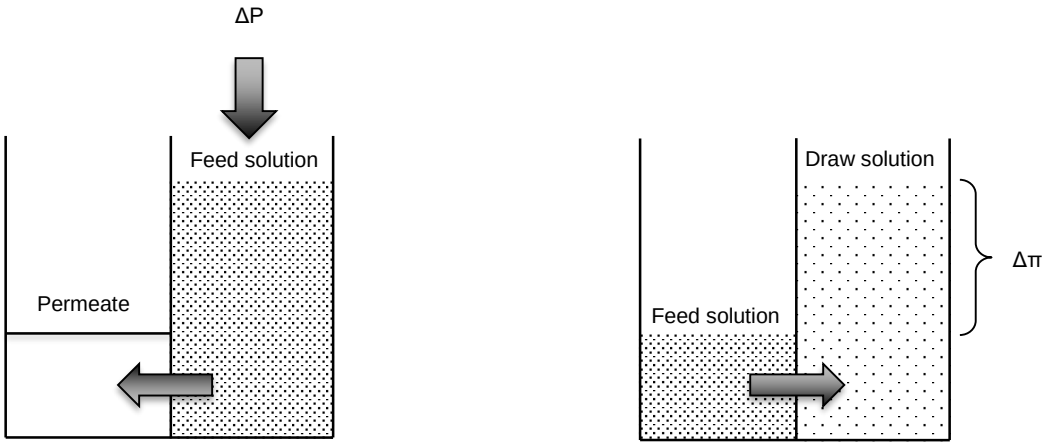

Figure 2.3: Schematic of the (A) RO and (B) FO process (adapted from Alsvik & Hägg, 2013)

2.5. Basic principles of forward osmosis (FO) technology

FO operation is similar to that of RO in that water is transported across a semi-permeable membrane, which impedes the transport of solutes. However, the distinguishing feature which sets FO apart from RO is its ability to generate a natural OP gradient which is the result of a highly concentrated DS (Gray *et al*., 2006; Motsa *et al.,* 2014; Akther *et al.,* 2015; Low *et al.,* 2015; Phuntsho *et al.,* 2016). A semi-permeable membrane separates two aqueous solutions (i.e. FS and DS) each possessing different OPs. The Δπ between the low solute concentrated FS and highly concentrated DS is the driving force for the movement of water across the semi-permeable membrane (Gray *et al*., 2006; McCutcheon & Elimelech, 2006; Klaysom *et al.,* 2013; Motsa *et al.*, 2014; Akther *et al.,* 2015; Low *et al.,* 2015; Phuntsho *et al.,* 2016).

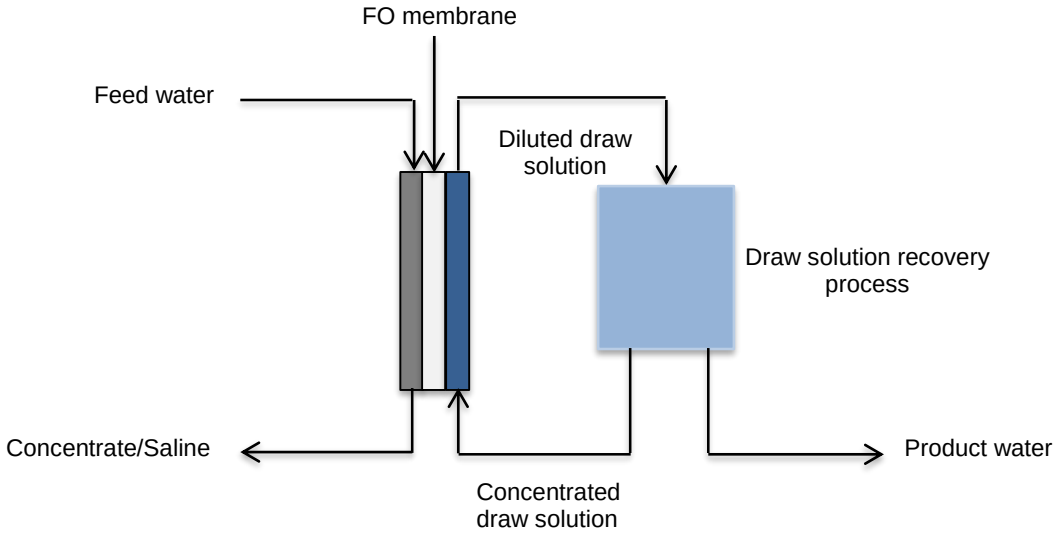

Figure 2.4: Forward osmosis process schematic with energy-intensive draw regeneration process (adapted from Raphael *et al*., 2010)

2.5.1. Forward osmosis (FO): Feed solution (FS)

The FS is a concentrated solution that exhibits a lower OP than that of the DS. A lower OP is imperative for the natural OP gradient, the driving force of the FO operation (McCutcheon & Elimelech, 2006). FO can be engineered and adapted to treat a variety of intricate feed types, including complex industrial streams (e.g. from textile industries, as well as oil and gas well fracturing) (Said, 2011; Coday *et al.,* 2014; Zhao *et al*., 2015; Han *et al*., 2016).

The use of deionised (DI) water has been prominent in much research as a controlled FS for comparative study (Achili *et al.,* 2010; Phunthso *et al.,* 2011; Phuntsho, 2012; Phunthso *et al.,* 2012; Boo *et al.,* 2013; Zaviska & Zou, 2014; Zhang *et al.,* 2014b). Alternative FSs for comparative studies of suitable DS have included model brackish water (BW) in various concentrations ranging from 5 000 to 20 000 $mg.L^{-1}$ sodium chloride (NaCl); model brackish ground water (BGW) ranging from 3 912 to 27 382 $mg.L^{-1}$ NaCl; model seawater of 35 000 $mg.L^{-1}$; and real seawater (SW) (Gray *et al.,* 2006; Phunthso *et al.,* 2011; Phuntsho, 2012).

2.5.2. Forward osmosis (FO): Draw solution (DS)

The driving force in FO operation is generated by passing a concentrated solution across the permeate side of the semi-permeable membrane. The concentrated solution is commonly referred to as the DS (McCutcheon & Elimelech, 2006; Fang *et al*., 2012).

The selection of an appropriate DS is imperative for process efficiency and performance. An ideal DS should exhibit a higher OP than the FS. The reverse transport (reverse solute flux) from the DS side to the FS side should be minimal, and the DS should be readily available when regeneration is not required. Aside from these characteristics the DS should be non-toxic, highly soluble, have a neutral pH, be inert and have a minimal chemical or physical impact on the physical membrane (McCutcheon & Elimelech, 2006; Fang *et al*., 2012; Wicaksana *et al.,* 2012; Klaysom *et al.,* 2013; Shaffer *et al.,* 2015).

Simple dissolved inorganic and thermolytic solutions (i.e. NaCl, magnesium chloride ($MgCl_2$), and ammonia carbonate ($(NH_4)_2CO_3$)) remain the most commonly used, and arguably most effective DSs (Shaffer *et al.,* 2015). NaCl solutions appear to be the most employed DS in FO experiments (accounting for approximately 40% of all experiments), due to its high solubility (Cath *et al*., 2006; Shaffer *et* al., 2015; Qasim *et al*., 2015); low costs (Achilli *et al*., 2010); and relatively high OP. NaCl has been used as a DS in molar concentrations between 0.3 and 6 M but is often used at 0.5 M, stimulating the osmotic power of SW and promoting the use of real SW as a DS (Lutchmiah *et al*., 2014). The use of specialized DSs for niche applications may prove beneficial. Alternative DSs can be strategically chosen to serve as a final product, most notably nutrient-rich substances such as fertilisers (Phunthso *et al.,* 2011; Phuntsho, 2012; Phuntsho *et al*., 2014; Shaffer *et al.,* 2015; Phunthso *et al.,* 2016) and inorganic substances such as KCl (potassium chloride) and $MgCl_2$ (Achilli *et al.,* 2010; Motsa *et al.*, 2014; Zaviska & Zou, 2014). This eliminates the energy-intensive draw regeneration process.

2.5.2.1. Types of draw solutions (DS)

Several types of solutions have been tested as DSs in FO application. The advantages and disadvantages of these types of DSs are listed in Table 2.5. Draw solutes can be categorized as follows (Wicaksana *et al.,* 2012):

i. Inorganic salts.
ii. Organic microsolutes.
iii. Organic macrosolutes.
iv. Dissolved gases.
v. Magnetic particles.

Table 2.5: An overview of DSs considered in wastewater application

Draw solution type	Example	Advantages	Disadvantages	References
Inorganic substances	Salts	• High solubility • Low cost • High osmotic potential	• Salt leakage may inhibit anaerobic digestion • Clogging/scaling/fouling • ICP • Recovery is not often feasible • Limited storage time due to biodegradation	Chung *et al*., 2012
Nutrient rich substances	Fertilisers	• Direct fertigation • No recovery necessary	• Osmotic equilibrium limits • Dilution of nutrients	Phuntsho *et al*., 2011; Phuntsho *et al*., 2012
Readily available resources	Seawater, RO brine	• Abundant source	• TEP fouling • Seawater only cost efficient if applied near coastal areas	Cath *et al*., 2005; Cath *et al*., 2010; Logan & Elimelech, 2012

* Note: TEP: Transparent exopolymer particles

Inorganic-based compounds remain the most extensively utilised DSs. Their high water solubility, high OP, lower specific cost and toxicity, all of which are imperative criteria for an optimal DS, greatly impacts FO technology. Table 2.6 illustrates the physiochemical properties of DSs commonly utilised in FO technology.

Table 2.6: Physiochemical properties and experimental water fluxes for inorganic salts and nutrient-rich substances tested as DSs

Draw solutions tested	Molecular weight (M_w) in g.mol^{-1}	Osmotic pressure at 2 M (kPa)	Experimental water flux (J_w) in µm.s^{-1}	References
CaCl	111	217.6	2.64	Achilli *et al*., 2010; Tan & Ng, 2010
KCl	74.55	89.3	6.337	Achilli *et al*., 2010; Tan & Ng, 2010
K_2SO_4	174.26	32.4	2.52	Achilli *et al*., 2009
$MgCl_2$	95.2	256.5	2.33	Achilli *et al*., 2009; Martinetti *et al*, 2009
$MgSO_4$	120.4	54.8	1.54	Achilli *et al*., 2009; Martinetti *et al*, 2009
NaCl	58.4	100.4	2.68	Achilli *et al*., 2009; Martinetti *et al*, 2009
$(NH_4)_2SO_4$	132.1	92.1	5.391	Achilli *et al*., 2010

2.6. Osmotic pressure (OP)

The OP of a solution is the pressure difference required to prevent the passage of a solvent across a semi-permeable membrane. The OP of structurally different solutions can be determined by both theoretical and experimental methods.

2.6.1. Methods for determining osmotic pressure (OP)

2.6.1.1. Van't Hoff's equation

The most common OP theory applicable for ideal dilute mixtures where ions behave independently of one another is Van't Hoff's equation (Phuntsho *et al.,* 2012). Van't Hoff's theory maintains that substances in a dilute solution obey the ideal gas laws, resulting in the OP formula (Phuntsho *et al.,* 2012):

$$\pi = i\left(\frac{n}{V}\right)RT = i[C_i]RT \quad (2.1)$$

Where R is the universal gas constant (R=8.31447 J.g.mol^{-1}.K^{-1}), T the absolute temperature (K), C_i corresponds to the molarity of a solution of a non-dissociating solute and i, the Van't Hoff's index, which accounts for solute dissociation (Wilson & Stewart

2013). Van't Hoff's equation has been known to fail for very dilute solutions, but when the concentrations of these molecules are sufficiently low, their solutions behave ideally (Grattoni & Merlo, 2007).

2.6.1.2. OLI Stream Analyser (OLI System)

In literature the bulk OPs of DSs have been predominately calculated using software from OLI Systems Inc. The prediction of properties of solutions over a wide range of concentrations and temperatures is executed though the utilization of thermodynamic modelling based on published experimental data (Phuntsho *et al.,* 2011; Wilson & Stewart, 2013). However, as a software package, the individual researcher has limited access to the assumptions underlying the software, thus potentially limiting its usefulness (Wilson & Stewart, 2013). Table 2.7 illustrates the OP of FSs and DSs assessed in previous studies, OP was determined by the OLI Stream Analyser 3.2.

Table 2.7: Compositions of FSs and DSs used in previous studies. OP determined by OLI Stream Analyser 3.2

Test solutions	**Concentration ($mg.L^{-1}$)**	**Osmotic potential (atm)**	**Osmotic potential (kPa)**	**Reference**
Feed solutions (FSs)				
Deionised (DI) water	Pure water	0	0	(Phuntsho, 2012)
Synthetic brackish water (BW5)	5 000	3.9	395	(Phuntsho, 2012)
Synthetic seawater (SSW)	35 000	28	2837	(Phuntsho, 2012)
Draw solutions (DSs)				
NaCl	17 900	13.8	1 400	(Achilli *et al*., 2010)
	35 200	27.6	2 800	
	51 800	41.5	4 200	
$MgCl_2$	20 000	13.8	1 400	(Achilli *et al*., 2010)
	34 200	27.6	2 800	
	47 600	41.5	4 200	
KCl	23 400	13.8	1 400	(Achilli *et al*., 2010)
	47 000	27.6	2 800	
	70 300	41.5	4 200	

*Note: Conversion factor, 1 atm = 101.325 kPa

2.6.1.3. Osmometer

The alternative way of determining the OP of a solution is by measuring the osmolality of the solution using an osmometer. An osmometer measures the osmolarity in $mOsmoles.kg^{-1}$ of a solution, based on the freezing point depression method. The

application of the osmometer is limited to solutions with infinite dilutions and therefore not suitable at higher concentrations (Phuntsho, 2012).

2.7. Advantages of forward osmosis (FO)

FO is claimed to possess a high potential for alternative applications in wastewater treatment, water purification and SW desalination (Fang *et al*., 2012; Motsa *et al.,* 2014). When compared with conventional PDMPs such as RO, the FO process offers the advantages of no hydraulic pressures for operation, nearly complete rejection of a wide range of contaminants and possibly low membrane fouling (Fang *et al*., 2012; Akther *et al.,* 2015; Shaffer *et al.,* 2015). Other advantages of FO over PDMPs include minimal pre-treatment of the feed; reduced cake layer formation, which in turn simplifies membrane cleaning; and the use of versatile water resources for FSs as long as their OP is lower than that of the DS. This allows for the application of FO technology in areas where the fresh water supply is limited (Phuntsho *et al.,* 2012; Klaysom *et al.,* 2013; Motsa *et al.,* 2014; Akther *et al.,* 2015; Shaffer *et al.,* 2015). The challenges relating to FO technology will be covered below, in Section 2.9.

2.8. Forward osmosis (FO) applications

FO is an alternative membrane process, which has gained interest though the commercialisation of membranes specifically tailored for the FO process (Lutchmiah *et al.,* 2014). Since then FO has attracted growing attention in the processing of municipal wastewater, BGW and SW desalination, food and pharmaceutical processing, as well as energy production (Klaysom *et al.,* 2013; Zhang *et al.,* 2014b; Zaviska & Zou, 2014). FO can also be employed in conjunction with biological processes for wastewater reuse in osmotic membrane bioreactors (OMBRs) (Achilli *et al*., 2010). The attractive characteristics exhibited by FO have attracted significant interest in novel areas where the separation and recovery of the DS are not necessary (Phunthso, 2011; Phuntsho, 2012; Phuntsho *et al.,* 2012; McGovern, 2014; Phuntsho *et al*., 2014; Phuntsho *et al*., 2016). Table 2.8 highlights the benefits and challenges associated with alternative FO applications.

Table 2.8: Benefits and challenges of different FO applications (adapted from Chung *et al*., 2012)

Applications of FO	Benefits	Challenges
Desalination	Lower energy consumption for water transport across the semipermeable membrane	Ineffective membranes; lack of cost effective draw solutes
Direct fertigation	Fertilisers are natural draw solutes; diluted DSs are useful for irrigation	Limited application sites
Osmotic power generation	Seawater is a natural draw solute	Pre-treatment of seawater and river water; complicated fouling phenomenon owing to the high pressure of seawater
Osmotic membrane bioreactor	Low fouling and low energy consumption	Need to obtain low cost and easily recyclable draw solutes

2.8.1. Osmotic dilution applications

Osmotic dilution is the concept of utilizing the concentration difference between two solutions (FS and DS) to drive water permeation across the semi-permeable membrane in FO (Shaffer *et al*., 2015). In osmotic dilution, the less concentrated FS becomes concentrated and the highly concentrated DS is diluted as permeation occurs across the semi-permeable membrane (Shaffer *et al*., 2015). Both the concentrated FS and diluted DS serve as the final product water of osmotic dilution, eliminating the energy-intensive draw recovery stage (Cath *et al*., 2010; Shaffer *et al*., 2015). By eliminating the energy-intensive draw recovery stage, osmotic dilution is truly a low-energy FO process (Shaffer *et al*., 2015; Qasim *et al*., 2015).

Osmotic dilution can potentially be adapted at two stages in a conventional SW desalination facility by i) diluting the DS to a lower salinity for RO treatment, resulting in reduced energy requirements; and ii) diluting the concentrated brine prior to discharge, mitigating the detrimental impacts on the surrounding environment (Cath *et al*., 2010; Shaffer *et al*., 2015). Osmotic dilution offers the potential for energy and cost saving in RO facilities by lowering operating hydraulic pressures, which in turn reduces energy requirements (Shaffer *et al*., 2015).

2.8.2. The concept of the fertiliser drawn forward osmosis (FDFO) process for direct fertigation

Desalination utilising a natural osmotic process is a novel concept, and its application for the production of potable water from BW and SW remains a significant challenge.

The separation of the diluted draw solutes from desalted water for recovery is a complex task, requiring an additional processing unit and therefore consuming extra energy (Chung *et al*., 2012; Phuntsho, 2012; Phuntsho *et al*., 2012; Chekli *et al*., 2016). The success of FO for the production of potable water greatly depends on the efficiency of the draw recovery stage (Phuntsho *et al*., 2012; Chekli *et al*., 2016). It is essential that the DS recovery stage has low capital and operational costs, as well as low energy consumption. The recovery stage is determined primarily by the choice of DS. However, finding an optimal DS remains a major challenge (Achilli *et al*., 2010; Akther *et al.,* 2015, Low *et al.,* 2015; Shaffer *et al.,* 2015; Chekli *et al*., 2016). While inorganic and thermolytic salts should adequately serve most FO applications, marginal benefits may be obtained from the use of specialized DSs for niche applications (Shaffer *et al.,* 2015). The use of specialized DSs chosen to serve as the final product could eliminate the energy-intensive draw recovery stage (Phuntsho, 2012; Phuntsho *et al*., 2012; Shaffer *et al.,* 2015; Chekli *et al*., 2016).

The concept of a fertiliser drawn forward osmosis (FDFO) has received increased attention. The novelty of the FDFO encompasses the use of fertilisers as DSs (Phuntsho, 2012; Phuntsho *et al*., 2012; Chekli *et al*., 2016), where the final product water (the diluted fertiliser) DS can be used directly for irrigation or fertigation as it contains the essential macro-nutrients required for plant growth (Phuntsho, 2012; Phuntsho *et al*., 2012; Chekli *et al*., 2016). Figure 2.5 illustrates the conceptual layout for the FDFO desalination process for direct fertigation. The process does not differ significantly from conventional FO desalination processes (see Figure 2.4), apart from the exclusion of the energy-intensive draw recovery stage. The process consists of the FO membrane cell connected to two channels; the FS and DS. Permeation is accomplished by the natural OP gradient, where water flows from the FS with a lower concentration towards the highly concentrated fertiliser DS (Phuntsho, 2012; Phuntsho *et al*., 2012; Chekli *et al*., 2016).

2.8.2.1. Advantages of the fertiliser drawn forward osmosis (FDFO) process

The use of fertiliser DSs for FO desalination is not intended to encourage the use of fertilisers as DSs (Phuntsho *et al*., 2011). The concept of the FDFO process is based on the use of inorganic fertilisers for the production of crops (Phuntsho *et al*., 2011). The concept offers several advantages: the cost of desalinated water remains relatively low, and the DS need not undergo the energy-intensive draw recovery stage (Phuntsho *et al*., 2011). Besides producing readily available irrigation water at a lower energy cost, the concept of a FDFO process may prove to be advantageous for farms adopting

fertigation as a means of supplying water and the required macro-nutrients to crops in an effective and cost-efficient manner (Phuntsho *et al*., 2011; Phuntsho *et al*., 2012).

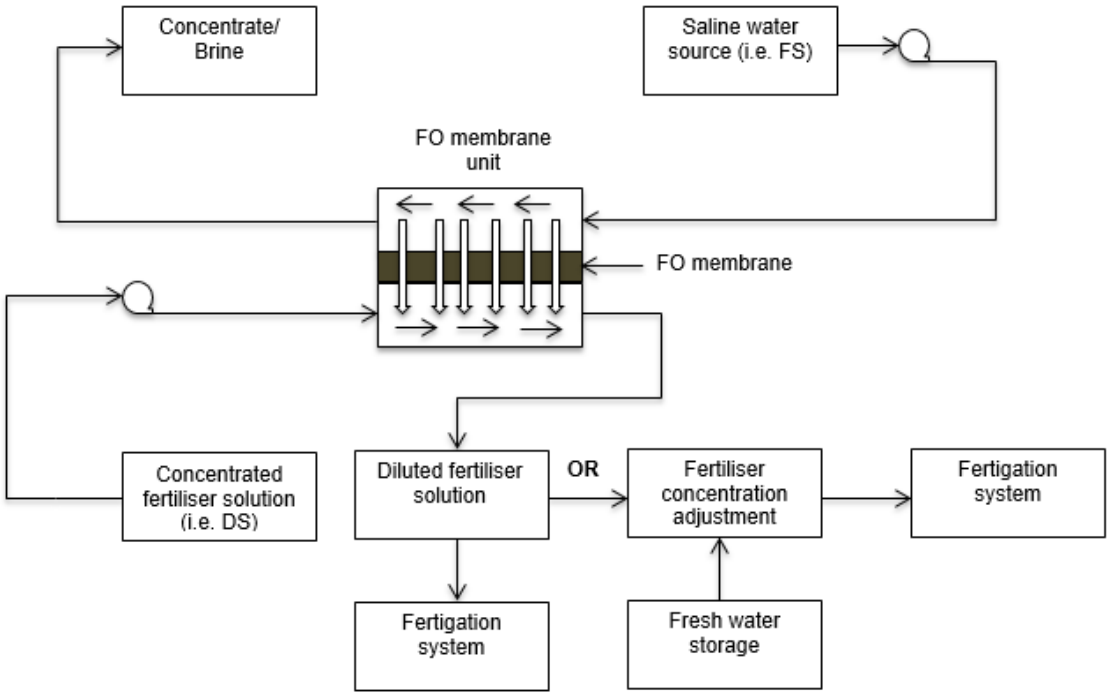

Figure 2.5: Initial design concept for FDFO desalination for direct fertigation (adapted from Phuntsho *et al*., 2012)

2.9. Challenges in forward osmosis (FO) operation

Despite the high potential of FO technology, several technological barriers hinder its practical application. A key component for the successful development of FO technology is the selection of an optimal DS (Achilli *et al*., 2010; Akther *et al.,* 2015, Low *et al.,* 2015; Shaffer *et al.,* 2015). There are several criteria for an ideal DS (McCutcheon & Elimelech, 2006; Fang *et al*., 2012; Klaysom *et al.*, 2013; Shaffer *et al.,* 2015):

i. DS should have a significantly higher OP than that of the FS to obtain a greater water flux.
ii. Separation of water from DS should be easy.
iii. DS should be easily regenerated, reused and economical.
iv. DS should be non-toxic and chemically compatible with the FO membrane.
v. Solutes in the DS should have a high diffusivity in liquid and low permeability through the selective layer of the membrane.

These ideal properties of the DS will promote enhanced water flux, minimal draw solute loss and minimal membrane fouling (Fang *et al*., 2012). In this study fertilisers used within the SA wine industry will be assessed for their suitability as DSs.

Another challenge in FO technology is the design and preparation of adequate membranes, which are capable of reducing the effect of concentration polarization (CP), fouling and reverse solute diffusion (Fang *et al*., 2012; Alsvik & Hägg, 2013; Akther *et al.,* 2015; Shaffer *et al.,* 2015). To promote FO feasibility, new commercial membranes must be developed and existing ones improved upon. Several recent reviews have focused on FO membrane development (Fang *et al*., 2012; Zhao *et al*., 2012; Alsvik & Hägg, 2013; Klaysom *et al.*, 2013; Lutchmiah *et al.,* 2014; Akther *et al.,* 2015; Shaffer *et al.,* 2015). In general, any dense, non-porous, and semi-permeable material can be employed as a membrane in the FO process. Membrane properties for the support and active layers are critical in the design of an ideal FO membrane (Lutchmiah *et al.,* 2014; Shaffer *et al.,* 2015; Qasim *et al.,* 2015). Membrane design should aim for:

i. Minimization of the membrane structural parameter (S) in the membrane support layer to mitigate mass transfer and thus increase water flux (Shaffer *et al.,* 2015; Qasim *et al.,* 2015).
ii. Maximization of the reverse solute flux selectivity (RSFS) of the membrane active layer to limit the loss of the draw solute (Shaffer *et al.,* 2015).

In this study, biomimetic membranes will be evaluated and compared to conventional well-known cellulose triacetate (CTA) membranes in a FDFO process. FO membranes and modules will be discussed in more detail in the following sections.

2.9.1. Concentration polarization (CP) in forward osmosis (FO)

CP is a common phenomenon in membrane processes (Klaysom *et al.,* 2013). However, more severe in ODMPs than in other membrane processes. CP arises from an increased OP at the membrane active layer which inhibits permeate flow (McCutcheon & Elimelech, 2006; Zhang *et al*., 2014a; Akther *et al.,* 2015; Qasim *et al.,* 2015). The effects of CP remain one of the most challenging problems in the practical realization of FO technology (McCutcheon & Elimelech, 2006; Akther *et al.,* 2015; Shaffer *et al.,* 2015; Qasim *et al.,* 2015). Two types of CP effects tend to reduce the effective $\Delta\pi$ in the FO desalination processes, namely external concentration polarization (ECP) and internal concentration polarization (ICP) (McCutcheon & Elimelech, 2006; Lutchmiah *et al.,* 2014; Akther *et al.,* 2015; Qasim *et al.,* 2015). ICP occurs exclusively in ODMPs (FO

and PRO) (McCutcheon & Elimelech, 2006; Alsvik & Hagg, 2013; Qasim *et al.,* 2015). The nature of ICP is dependent on membrane orientation: it may be concentrative or dilutive. When the feed is placed against the support layer of an asymmetric membrane (PRO mode), water enters the porous support layer and diffuses across the active layer into the DS. The salt in the FS freely enters the porous support layer by convective water flow; however, salt cannot penetrate the active layer from the support layer, which causes an increase in the concentration within the porous support layer. Hence this is referred to as concentrative ICP (McCutcheon & Elimelech, 2006; Alsvik & Hagg, 2013; Qasim *et al.,* 2015). In dilutive ICP, the FS is against the active layer and the DS is against the support layer (FO mode). The ICP phenomenon occurs on the permeate side, as the DS is diluted by the permeate water within the porous support layer (McCutcheon & Elimelech, 2006; Alsvik & Hagg, 2013; Qasim *et al.,* 2015). Research has indicated that the major factor contributing to the decline in water permeation rate in FO technology is ICP (McCutcheon & Elimelech, 2006; Alsvik & Hagg, 2013; Akther *et al.,* 2015; Qasim *et al.,* 2015).

2.10. Forward osmosis (FO) membranes and modules

2.10.1. Membrane development

A membrane is a thin film separating two phases, acting as a selective barrier permitting the transportation of specific entities while restricting the passage of others. Membranes are an integral part of the osmotic process, and the selection of an optimal membrane is crucial for effective FO operation (Phuntsho *et al.,* 2011).

2.10.2. Desired characteristics for forward osmosis (FO) membranes

Desired FO membrane characteristics for use in wastewater reclamation entail (Lutchmiah *et al.,* 2014):

i. A dense, ultra-thin, active-separating layer capable of high solute rejection.
ii. Mechanical stability for sustainable operation and reduced ICP.
iii. A high affinity for water (i.e. hydrophilicity) for enhanced water flux and reduced fouling.
iv. Low costs.
v. An open, thin, hydrophilic support layer.

2.10.3. Forward osmosis (FO) membrane material

Various materials are used for the synthesis of FO membranes.

2.10.3.1. Cellulose triacetate (CTA)

The widely-used CTA membrane is a typical high-performance membrane (Sunohara & Masuda, 2011). CTA is a plastic-like material manufactured from cellulose, which exhibits characteristics quite different from those of cellulose due to the substitution of a carboxyl group for the cellulose hydroxyl group. The CTA membrane has a homogenous membrane structure and can be produced with a wide range of permeability, from low-flux performance to high-flux performance. Hydrophilic CTA membranes offer special advantages such as excellent chlorine tolerance and higher solute rejection (Chen *et al*., 2017). The CTA membrane is less prone to absorptive fouling, making it suitable for the treatment of heavy-duty wastewaters (Gray *et al.,* 2006; Sunohara & Masuda, 2011; Fang *et al*., 2012; Lutchmiah *et al.,* 2014; Chen *et al*., 2017).

2.10.3.2. Polybenzimidazole (PBI)

Polybenzimidazole (PBI) is a glassy thermoplastic. PBI is known for its ability to maintain its physical properties at elevated temperatures. PBI is broadly chemical resistant and has high strength and structural stability. Collectively these attributes make for a thermo-mechanically stable water-selective layer (Alsvik & Hägg, 2013).

2.10.3.3. Polysulfone (PSF) and Polyethersulfone (PES)

Polysulfone (PSF) membrane filters are employed as a thermoplastic material in fabricating membranes (Huang & Yang, 2006). PSF is known for its good chemical resistance and mechanical properties. It displays excellent thermal oxidative resistance, resistance to hydrolysis and industrial solvents. Polyethersulfone (PES) and PSF exhibit similar properties, however despite their regular structure, they cannot be crystalized. The hydrophilic nature of both PSF and PES means that no added surfactants are used to increase wettability, resulting in an increase in ICP and reduction in water flux (Huang & Yang, 2006; Zhao, 2013).

2.10.3.4. New membrane development for forward osmosis (FO) technology: Biomimetic membranes

Membrane technology has become one of the most important technologies in chemical and biological separation processes (Zhao *et al.,* 2014). Synthetic membranes have come a long way over the past years with the invention of the cellulose acetate (CA) RO desalination membranes (Tang *et al*., 2013). Modern synthetic membranes at optimum conditions can desalinate SW at an energy demand 15 to 20% of that used for earlier RO membranes (Tang *et al*., 2013) However, there are ongoing efforts to produce membranes with improved performance to provide better separations at reduced energy demand. This has led to a better understanding of molecular structure and the function of biological membranes. Simultaneously, rapid advancements in molecular engineering have increased the ability to replicate biological structures with near-molecular precision (Shen *et al.,* 2014). These advances have sparked interest in the area of biomimetic membranes.

Biomimetic membranes are membranes that are fabricated with natural or natural-like materials via biomimetic and bio-inspired approaches (Hélix-Nielsen, 2009; Zhao *et al.,* 2014). Cell membranes conduct substrate and solvent transport with exceptional selectivity and high transport rates unprecedented in synthetic systems (Shen *et al.,* 2014). These efficient membranes are of interest because of their antifouling characteristics both at a cellular level and higher levels of organization (e.g. lotus leaves) (Blossey, 2003). Research pertaining to biomimetic and bio-inspired membranes has seen significant developments in the last decade, with enhanced knowledge of mechanisms, models, and functions being implemented in many scientific disciplines. Biomimetic and bio-inspired membranes should possess the following features (Zhao *et al.,* 2014):

i. Membrane fabrication is often conducted though self-assembly under mild conditions close to the natural environment, such as atmospheric pressure, room temperature, and aqueous environment.
ii. Membrane materials are usually common materials with excellent hydrodynamic, mechanical, wetting, and adhesive properties.
iii. Membrane properties are often highly dependent on the content and state of water in the structure, and membrane processes can be intensified by rationally manipulating the multiple selectivity mechanisms in a simple way.

The idea of incorporating aquaporin (AQP) properties into desalination membranes was first proposed by Kumar et al., 2007. AQPs are specialised pore-forming proteins in living

cells; under the right conditions these proteins form ‘water channels’ able to exclude ionic species (Tang *et al*., 2013; Tang *et al*., 2015). In this context, AQPs may represent a new membrane material that may provide selective conduits for water with a high osmotic permeability (Tang *et al*., 2015). The past half-decade has seen a surge of activity aimed at developing biomimetic desalination membranes incorporating AQPs (Tang *et al*., 2013; Zhao *et al*., 2012; Tang *et al*., 2015; Qi *et al*., 2016). The incorporation of AQPs into biomimetic desalination membranes may be the new direction in desalination.

2.10.4. Membrane orientation

Most FO membranes have an asymmetric structure with two different layers, an active layer and a support layer. The active layer is generally a dense highly selective layer, while the porous support layer provides the mechanical support (Lutchmiah *et al*., 2014). The asymmetric structure of the FO membrane allows for two modes of operation, namely: i) the FO mode in which the active layer faces the feed side (AL-FS); and ii) the pressure retarded (PRO) mode in which the active layer faces the draw side (AL-DS) (Phunthso, 2012; Lutchmiah *et al*., 2014). Membrane asymmetry has a significant impact on FO performance, such as flux and fouling. Extensive research has reported comparatively higher water fluxes in the PRO mode than in the FO mode (Gray *et al*., 2006; Lutchmiah *et al*., 2014). The difference in water flux between the FO and PRO modes is attributed to the difference in the membrane structural resistance (Phunthso, 2012).

2.10.5. Forward osmosis (FO) membrane performance and applications

FO studies and applications have predominantly utilised the commercial CTA FO membrane or polyamide based thin film composite (TFC) RO membranes. TFC membranes remain the standard for RO application due to their high water permeability, high solute selectivity and chemical and physical stability (Shaffer *et al*., 2015). However, the use of TFC RO membranes in FO applications has resulted in comparatively lower water fluxes. The unsuccessful application of TFC RO membranes is due to their thick support layers. The thick support layer in TFC RO membranes is necessary for mechanically stability under high hydraulic pressures. The same mechanical support is not necessary for FO application since water permeation is a result of the natural osmosis process. The influence of CTA and TFC FO membranes and their orientation on the performance in a FDFO process was compared in terms of water flux and reverse

solute flux. The findings are presented in Table 2.9. Table 2.10 illustrates the physical and chemical properties of the CTA and TFC FO membranes.

Table 2.9: Influence of membrane type and orientation on the performance of FO processes (adapted from Phuntsho, 2012)

Membrane properties	**CTA FO**	**TFC FO**
Materials	Cellulose triacetate	Polyamide on PSF
Supplier	HTI Inc., USA	WJ (TFC2)
Water permeability or A ($L.m^{-2}.h^{-1}.atm^{-1}$)	1.015±0.029	5.215
FO mode water flux 1 M KCl: DI FS ($L.m^{-2}.h^{-1}$)	9.832	27.976
Reverse solute flux ($g.m^{-2}.h^{-1}$)	11.968	9.382
Specific reverse solute flux ($g.L^{-1}$)	1.217	0.351
FO mode water flux 1 M KCl: 5gL^{-1}NaCl FS ($L.m^{-2}.h^{-1}$)	8.734	18.948
Reverse solute flux ($g.m^{-2}.h^{-1}$)	10.10	58.74
Specific reverse solute flux ($g.L^{-1}$)	1.156	0.310

Table 2.10: Comparison of physical and chemical properties of CTA and TFC FO membranes (adapted from Jin *et al*., 2012)

Sample	**Active layer material**	**Contact angle (°)**		**Zeta potential at pH 6 (mV) active layer**	**Operating pH**	**Membrane thickness (μm)**
		Active layer	**Support layer**			
CTA	Cellulose triacetate	76.6	81.1	-2.1	3-8	93
TFC	Polyamide	45	45	86	2-12	116±1

2.11. Membrane transport in osmotically driven membrane processes (ODMPs)

While ODMPs are relatively simple in operation, mass transport though ODMP membranes is complex and limited (Klaysom *et al*., 2013; Lutchmiah *et al*., 2014). Mass transport is dependent on various parameters, which include membrane type, structure, orientation, temperature, and composition of the FS and DS (Klaysom *et al*., 2013).

2.11.1. Modelling water flux (J_w)

The general equation describing water transport though any membrane process is given by Equation 2.2 (Cath *et al*., 2006; Phuntsho, 2012; Klaysom *et al*., 2013; Qasim *et al*., 2015):

$$J_w = A(\sigma\Delta\pi - \Delta P) \quad (2.2)$$

Where J_w is the water flux ($L.m^{-2}.h^{-1}$), A is the pure water permeability coefficient ($L.m^{-2}.h^{-1}.bar^{-}$), which is an intrinsic characteristic of the membrane, σ is the reflection coefficient, Δπ is the OP difference, and ΔP is the applied hydrostatic pressure difference (Phuntsho, 2012; Qasim *et al*., 2015). In Equation 2.2, the term (σΔπ - ΔP) represents the effective driving force of the transport of water molecules across the membrane. Since no hydraulic pressure is applied in FO desalination, the sole driving force is the difference in OPs. Equation 2.2 for FO desalination can be expressed by (Qasim *et al*., 2015):

$$J_w = A(\sigma\Delta\pi_{bulk}) = A\sigma(\pi_{d,b} - \pi_{f,b}) \quad (2.3)$$

Where, $\pi_{d,b}$ is the bulk OP of the DS and $\pi_{f,b}$ is the bulk OP of the FS (Phuntsho, 2012; Qasim *et al*., 2015). Equation 2.3 predicts flux as a function of the effective driving force only in the absence of concentrative or dilutive ECP (McCutcheon & Elimelech, 2006; Phuntsho, 2012), which may be valid only when the permeate flux is very low.

CHAPTER THREE
MATERIALS AND METHODS

3.1. Introduction

This chapter describes in detail the procedures for all the bench-scale experiments carried out. It includes preliminary assessments of the alternative feed solutions (FSs), six straight fertiliser draw solutions (DSs) and blended fertiliser DSs used in the fertiliser drawn forward osmosis (FDFO) desalination study.

3.2. Alternative feed solutions (FSs) for the fertiliser drawn forward osmosis (FDFO) desalination study

Different types of FSs were identified and evaluated for their potential in the application of the FDFO desalination study. These are listed in Table 3.1. Deionised (DI) water was used as an initial controlled FS against alternative FSs. Other FSs comprised of synthetic brackish water (BW5) (5 000 $mg.L^{-1}$ NaCl), synthetic seawater (SSW) (35 000 $mg.L^{-1}$ NaCl), collected seawater (SW) samples from the Atlantic Ocean seaboard (AOSB) and Indian Ocean seaboard (IOSB), actual winery wastewater and synthetic winery wastewater (SWW). Table 3.1 illustrates the various total dissolved solids (TDS) of the alternative FSs, analysed at an external independent South African National Accreditation System (SANAS) accredited laboratory (Bemlab, SA).

3.2.1. Preparation of synthetic brackish water (BW5) and synthetic seawater (SSW)

All the sodium chloride (NaCl) used in the preparation of the BW5 and SSW was of reagent grade, obtained from Merck (Pty) Ltd, South Africa (SA). The FS samples were prepared by dissolving a specific amount of reagent grade NaCl into DI water to obtain the various NaCl concentrations. The concentrations of the BW5 and SSW were 5 000 $mg.L^{-1}$ NaCl and 35 000 $mg.L^{-1}$ NaCl, respectively. FS samples were prepared in duplicate for analysis. Basic properties of the FSs, such as electrical conductivity (EC) and pH were determined using a multi-meter probe (Lovibond SD150, SA) supplied by Selectech (Pty) Ltd, SA.

Table 3.1: Alternative FSs with their respective TDS

Type of FSs	Total dissolved solids (TDS)
Deionised (DI) water	Pure water
Synthetic brackish water (BW5)	6 823 mg.L^{-1}
Synthetic seawater (SSW)	36 267 mg.L^{-1}
Seawater: Atlantic seaboard (AOSB)	
Clifton 4th	30 000 mg.L^{-1}
Sea Point	30 850 mg.L^{-1}
Camps Bay	31 000 mg.L^{-1}
Seawater: Indian Ocean seaboard (IOSB)	
Strand B	28 300 mg.L^{-1}
Gordon's Bay	30 650 mg.L^{-1}
Strand A	30 850 mg.L^{-1}
Winery wastewater	
Winery wastewater before biological sand filters (BBSF)	892 mg.L^{-1}
Winery wastewater after biological sand filters (ABSF)	925 mg.L^{-1}
Synthetic winery wastewater (SWW)	120 mg.L^{-1}

*Note: TDS for actual winery wastewater and SWW were analysed using a calibrated PCSTestr 35 multiparameter (Wirsam Scientific and Precision Equipment (Pty) Ltd, SA)

3.2.2. Collected seawater (SW) samples

Duplicate SW samples were collected from the AOSB (Camps Bay, Clifton 4th, and Sea Point), at GPS coordinates -33.951,18.377; -33.940,18.375 and -33.906,18.398, respectively. SW samples were also collected from the IOSB (Gordon's Bay, Strand A, and Strand B), at GPS coordinates, -34.159,18.867; -34.126,18.834 and -34.119,18.827, respectively. The collected SW samples were filtered with the use of a Buchner funnel (50 cm). Filter paper (50mm Munkfell filter paper) was placed within the Buchner funnel where DI water (water being the predominant solvent in the solution) was used to moisten the filter paper. SW samples were filtered to remove any suspended particles and contaminants that might affect the osmotic potential (OP) of the sample analysed. NaCl concentrations of the SW samples were determined though a full water analysis by an external independent SANAS accredited laboratory (Bemlab, SA). The full water analysis is presented in Appendix A.

3.2.3. Winery wastewater

Winery wastewater analysed as a potential alternative FS was collected from a winery in the Stellenbosch region of the Western Cape (WC), SA. Winery wastewater collected from the winery was passed though biological sand filters (BSFs) as a treatment process for bioremediation (Ramond *et al*., 2013; Welz & le Roes-Hill, 2014; Welz *et al*., 2014).

The OP of the winery wastewater collected was analysed before and after the treatment process. The TDS of the winery wastewater was analysed before and after BSF treatment using a calibrated PCSTestr 35 multiparameter, supplied by Wirsam Scientific and Precision Equipment (Pty) Ltd, SA.

3.2.4. Synthetic winery wastewater (SWW)

The unstable and unpredictable nature of winery wastewater rendered it inappropriate for comparative experiments. SWW was therefore prepared, based on the reported chemical composition of SWW (Welz & le Roes-Hill, 2014). Chemical analysis of winery wastewater was performed on actual winery wastewater samples collected from two storage dams shortly after the crush season at a Stellenbosch winery in the WC region of SA. SWW effluent compositions were formulated from the analysis of the sampled winery wastewater. The composition of the SWW in Table 3.2 is expressed in terms of chemical oxygen demand (COD) contribution in $mg.L^{-1}$. TDS of the SWW was analysed using a calibrated PCSTestr 35 multiparameter (Wirsam Scientific and Precision Equipment (Pty) Ltd, SA).

Table 3.2: Composition of the SWW with the compositions expressed in terms of chemical oxygen demand (COD) $mg.L^{-1}$ (adapted from Welz & le Roes-Hill, 2014)

Gallic acid	Vanillin	Ethanol	Acetic acid	Final concentration[a]
25	25	250	200	527[1]
50	50	500	400	1 027[2]
100	100	1 000	800	2 027[3]

[a] Includes contribution from glucose (27 COD $mg.L^{-1}$) as a base nutrient solution. [1] SWW with low COD contribution. [2] SWW with a medium COD contribution. [3] SWW with high COD contribution (Welz & le Roes-Hill, 2014).

3.3. Draw solutions (DSs) for evaluation and suitability for the fertiliser drawn forward osmosis (FDFO) desalination study

3.3.1. Straight fertilisers

Six different types of straight fertilisers that are commonly utilised in grapevine production in SA vineyards were evaluated as DSs. The list comprised of only straight fertilisers (fertilisers that contribute only a single nutrient). Complete fertilisers (Nitrogen, Phosphorous, Potassium or N/P/K) are commercially available. However, their chemical compositions remain proprietary and they were therefore excluded from the list of

preliminary fertilisers evaluated as DSs. Fertiliser DSs of molar concentrations ranging from 0 to 10 M were prepared by dissolving their respective salts in DI water. Basic properties of the fertiliser DSs, such as EC and pH, were determined using a multi-meter probe (Lovibond SD150, Selectech (Pty) Ltd, SA). The fertilisers were of reagent grade and sourced from Merck and Sigma-Aldrich (SA). Table 3.3 lists all the straight fertiliser DSs evaluated for use in the FDFO desalination study. The list excludes single phosphorous (P) fertilisers since P is generally found in adequate amounts in vineyards. The use of single P fertilisers in the SA wine industry is less prominent than that of single nitrogen (N) and single potassium (K) fertilisers.

Table 3.3: Fertiliser DSs identified and evaluated as potential DSs for the bench-scale cross-flow FDFO desalination study

Fertilisers	**Chemical formula**	**Molecular weight (M_W) in g.mol^{-1}**	**Supplier**
Ammonium nitrate	NH_4NO_3	80.04	Merck
Ammonium sulphate (SOA)	$(NH_4)_2SO_4$	132.1	Merck
Potassium chloride	KCl	74.55	Merck
Potassium nitrate	KNO_3	101.01	Merck
Potassium sulphate	K_2SO_4	174.26	Merck
Urea	$CO(NH_2)_2$	60.06	Sigma-Aldrich

3.3.2. Blended fertilisers

Blended fertilisers are mixes of straight fertilisers that are made to vary the macro-nutrient (N/P/K) ratio to meet crop requirements. Fertiliser blends were also analysed as suitable DSs. The blends were prepared by mixing two straight fertilisers together in DI water, in molar concentrations ranging from 0 to 2 M at a 1:1 molar ratio, so as to provide a substantial ratio of the major nutrients required for grapevine production. Blended fertilisers were prepared in a similar way to the straight fertilisers listed under Section 3.3.1, using a mixture of different straight N and K fertilisers, as shown in Table 3.3. Table 3.4 lists the fertiliser blends analysed for OP and their respective average molecular weight ($\overline{M_w}$) as well as N/K ratio.

Table 3.4: Blended fertiliser DSs analysed for OP

Fertiliser blend	Average molecular weight ($\overline{M_w}$) in g.mol^{-1}	N/K ratio
Urea blended DSs		
$CO(NH_2)_2 + NH_4NO_3$	70.02	N/N
$CO(NH_2)_2 + (NH_4)_2SO_4$	95.46	N/N
$CO(NH_2)_2 + KCl$	67.1	N/K
$CO(NH_2)_2 + KNO_3$	80.7	N/K
$CO(NH_2)_2 + K_2SO_4$	116.61	N/K
Ammonium nitrate blended DSs		
$NH_4NO_3 + (NH_4)_2SO_4$	105.92	N/N
$NH_4NO_3 + KCl$	77.36	N/K
$NH_4NO_3 + KNO_3$	90.61	N/K
$NH_4NO_3 + K_2SO_4$	126.58	N/K
Ammonium sulphate blended DSs		
$(NH_4)_2SO_4 + KCl$	104	N/K
$(NH_4)_2SO_4 + KNO_3$	116.71	N/K
$(NH_4)_2SO_4 + K_2SO_4$	153.23	N/K
Potassium chloride blended DSs		
$KCl + KNO_3$	88.22	K/K
$KCl + K_2SO_4$	125.56	K/K
Potassium nitrate blended DSs		
$KNO_3 + K_2SO_4$	137.46	K/K

3.4. Forward osmosis (FO) membranes

The two types of membranes used in this FDFO desalination study were: (i) a commercial cellulose triacetate (CTA) FO membrane supplied by Fluid Technology Solutions, Inc., United States of America (USA); and (ii) a novel thin film composite (TFC) flat sheet aquaporin-based biomimetic membrane (ABM), obtained from Aquaporin A/S, Denmark.

The CTA FO membrane is an asymmetric membrane that comprises of a CTA active layer embedded with a polyester screen as support layer. Characteristics of the CTA FO membrane have been widely reported in many previous studies (Zhang *et al*., 2014a; Zhang *et al*., 2014b; Benavides & Phillip, 2016; Phuntsho *et al*., 2016). The second FO membrane, the ABM, was fabricated by the interfacial polymerization (IP) method, with aquaporin (AQP) protein vesicles embedded into a polyamide active layer, supported by a porous polysulfone (PSF) support layer (Zhao *et al*., 2012; Madsen *et al*., 2015). The performance of second- and third-generation ABM FO membranes was analysed in this FDFO desalination study. The FO membranes used in this study are referred to

throughout this thesis as CTA; second generation aquaporin biomimetic membrane (ABM_A01), and third generation aquaporin biomimetic membrane (ABM_A02). The physical and chemical properties of the FO membranes used in this study are presented in Table 3.5.

Table 3.5: Membrane properties of the CTA - FO membrane and ABM - FO membrane used in the FDFO desalination study (adapted from Phunthso, 2012; Zhao *et al*., 2012)

Membrane properties	**CTA FO** (Phunthso, 2012)	**ABM FO** (Zhao *et al*., 2012)	
Manufacturer	Fluid Technology Solutions, Inc	Aquaporin A/S	
Material of active layer	Cellulose triacetate	Polyamide	
Material of support layer	Polyester mesh embedded	Polysulfone	
Membrane thickness (µm)	93 $\pm$ 3	110 $\pm$ 15	
Operating pH	3 – 8	2 – 11	
		ABM_A01	**ABM_A02**
Shelf life	-	6 months	3 months
Water flux: H_2O vs. 1 M NaCl; FO mode ($L.m^{-2}.h^{-1}$)	-	> 7	> 10
Revers flux: H_2O vs. 1 M NaCl; FO mode ($g.m^{-2}.h^{-1}$)	-	< 2	-
Specific reverse salt flux: H_2O vs. 1 M NaCl; FO mode ($g.L^{-1}$)	-	-	< 0.3

The separation properties of both the CTA and ABM FO membranes have been reported in literature (Phunthso, 2012, Zhao *et al*., 2012). Before each experiment, both the CTA and ABM FO membranes were immersed in DI water for 30 minutes. After completion of the experiment, both the CTA and ABM FO membranes were cleaned by running DI water though the FO cell counter-currently for two h at an elevated flow rate of 450 $mL.min^{-1}$. Periodic rinses with DI water at an elevated flow rate of 450 $mL.min^{-1}$ was used to clean the FO membranes (CTA and ABM) surfaces for membrane flux recovery. After periodic rinses, both the CTA and ABM FO membranes were stored in a refrigerator immersed in DI water until the next use. Scanning electron microscope (SEM) images of the virgin CTA, AMB_A01 and ABM_A02 membranes can be seen in Figures 3.1 to 3.3. (See Appendix B regarding biomimetic membrane handling, storage, and cleaning)

Membrane integrity experiments were performed for the ABM FO membranes after initial control experiments. Membrane integrity experiments were conducted to assess the optimal flow rate at which the ABM FO membranes could operate. The experiments used DI water as a FS and BW5 as a DS. Experiments were run at 5 h intervals. A methyl violet solution was used to assess any failures on the TFC flat sheet ABM's surface. (See Appendix C for methyl violet solution for stain damaged TFC ABMs).

CTA

a) b) c)

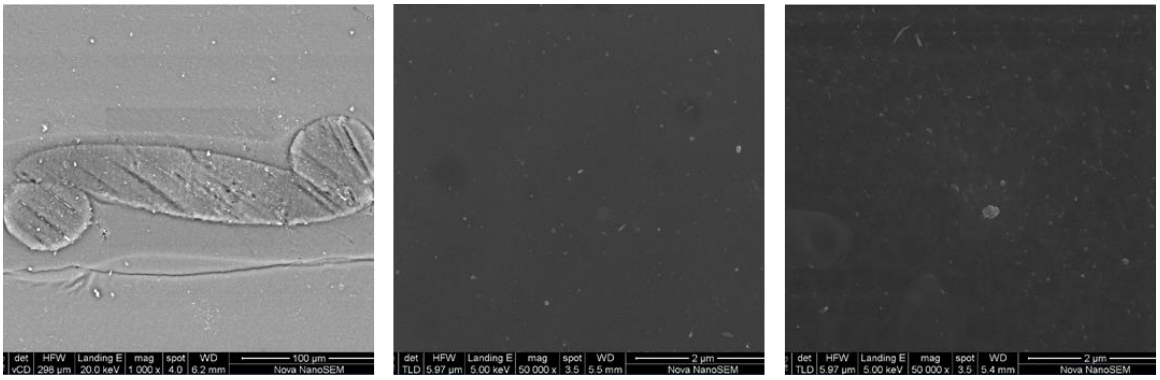

Figure 3.1: SEMs of the virgin CTA FO membrane (a) cross section, (b) active layer and (c) support layer [magnification (a) 100 µm x 1000 and (b and c) 2 µm x 50 000]

ABM_A01

a) b) c)

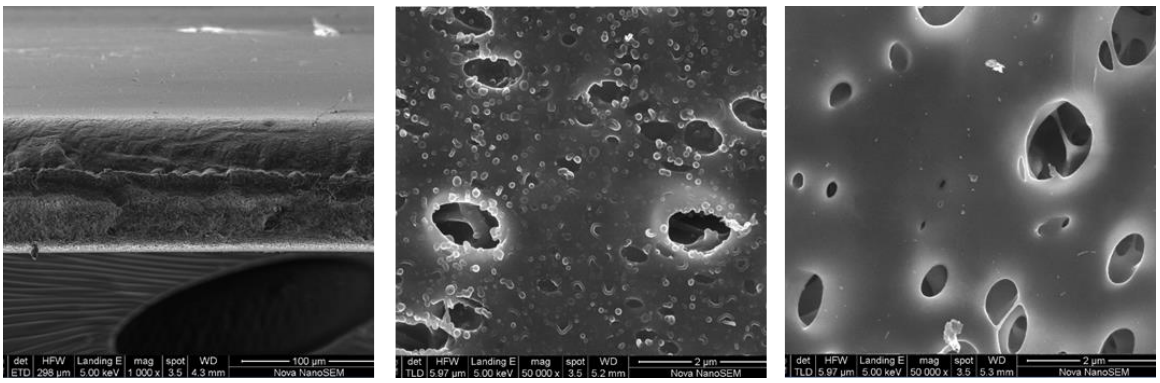

Figure 3.2: SEMs of the virgin ABM_A01 FO membrane (a) cross section, (b) active layer and (c) support layer [magnification (a) 100 µm x 1000 and (b and c) 2 µm x 50 000]

ABM_A02

a) b) c)

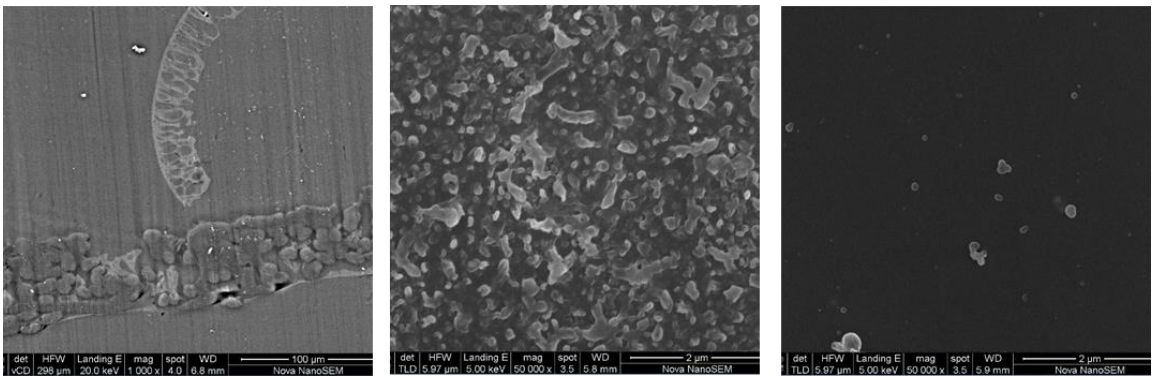

Figure 3.3: SEMs of the virgin ABM_A02 FO membrane (a) cross section, (b) active layer and (c) support layer [magnification (a) 100 µm x 1000 and (b and c) 2 µm x 50 000]

3.5. Forward osmosis (FO) cell

The CF042D-FO cell (Sterlitech, USA) is a laboratory-scale filtration unit with outer dimensions (12.7 x 10 x 8.3 cm) and an effective membrane area of 42 cm^2 designed for the evaluation of a variety of osmotically-driven membrane processes (ODMPs), including FO and pressure retarded osmosis (PRO) modes. It is able to simulate the flow dynamics of larger, commercially available membrane elements. The operating conditions and fluid dynamics of the CF042D-FO cell can be varied over broad ranges. Table 3.6 outlines the features and technical specifications of the CF042D-FO cell.

Table 3.6: CF042D-FO cell features and technical specifications (adapted from Sterlitech Corporation, 2016)

Parameter	Description
Membrane active area	42 cm^2
Hold up volume	17 mL
Maximum pressure	69 bar
Maximum temperature	82 ºC
O-rings	Buna
pH range	Membrane dependent
Cross flow velocity	Variable
Dimensions	
Slot depth	2.3 mm
Slot width	39.2 mm

3.6. Experimental set-up for fertiliser drawn forward osmosis (FDFO) system

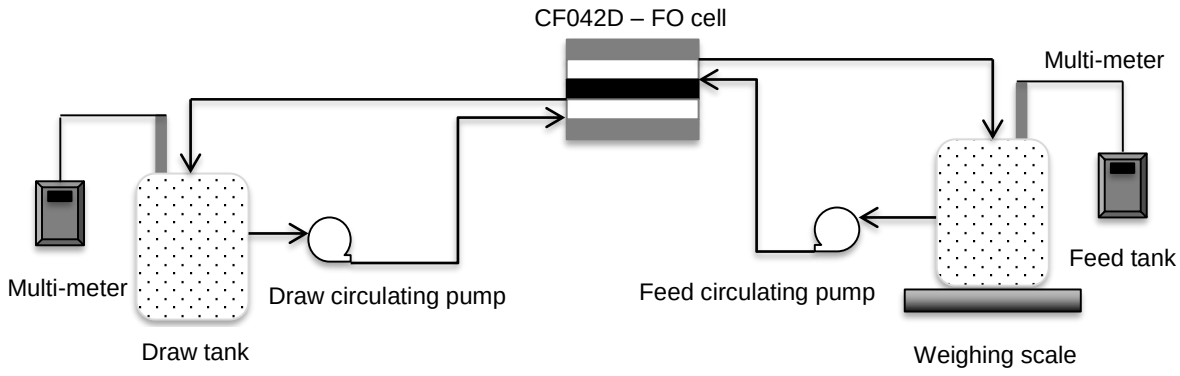

Figure 3.4: Process flow diagram (PFD) of the bench-scale FDFO set-up

All experiments for the application of the FDFO desalination study were performed using a bench-scale cross-flow filtration unit. The FO set-up adapted in this study was derived from similar previous studies (Phuntsho, 2012; Phuntsho *et al*., 2012; Zhao *et al*., 2012;

Phuntsho *et al*., 2014; Zhao *et al*., 2016). The FO unit illustrated in Figure 3.4 consisted of a FO membrane cell (CF042D – FO Membrane cell, Sterlitech, USA), with two channels located on either end in order to allow feed water to flow on one side of the membrane and the DS to flow on the other side of the membrane. Cross-flows of the FS and DS were circulated in a counter-current flow direction using two peristaltic pumps (323 Watson Marlow and 520S Watson Marlow) adopting a FO mode orientation (FS-AL). Initial volumes of the FS and DS were 2 and 0.5 L, respectively. Feed and DSs were re-circulated back to their respective reservoirs, which resulted in continuous dilution of the DS and concentration of the FS. The cross-flow volumetric flow rate of both the FS and DS were fixed at 400 $mL.min^{-1}$, similar to previous studies (Phuntsho *et al*., 2011; Phuntsho *et al*., 2012; Phuntsho, 2012). All performance experiments for the application of the FDFO desalination study were maintained at ambient temperatures of $25\pm1^{o}C$.

3.7. Forward osmosis (FO) experiments

3.7.1. Determining osmotic equilibrium (OE) of the fertiliser draw solutions (DSs)

These experiments were performed in order to determine the osmotic equilibrium (OE) in the FDFO desalination study. Literature states that any DS should be able to extract water from the FS until OE occurs. OE occurs when the OP of the DS reaches OE with the OP of the FS. Under counter-current cross-flow conditions in the FO process, the osmotic process will occur until the system has reached OE (Phunthso, 2012). Control experiments for the FDFO system were performed for the determination of OE in order to establish the bulk OP at which the water flux (J_w) reaches zero, using DI water as a controlled FS and a 1 M KCl fertiliser solution as the DS. The experiment for the determination of the OE was performed in duplicate only using the ABM_A01 FO membrane. Multi-meter probes were used to measure pH and EC. A weight balance was also used to measure weight changes in the FS for the determination of forward (J_w) and reverse solute flux (J_s).

3.7.2. Fertiliser drawn forward osmosis (FDFO) experiments

Experiments for the FDFO desalination study comprised of three FSs (one FS as the control) and two DSs. The FSs consisted of DI water as the control and BW5 and SWW as the alternative FSs. The DSs comprised of a 1 M KCl fertiliser solution and an N/P/K blended fertiliser solution, representative of similar N/P/K blended fertilisers used in the SA wine industry. KCl was selected as a DS because of its use within SA vineyards; KCl is the most commonly employed K fertiliser used to overcome plant deficiencies and

necessary for supplementing potash, an essential plant nutrient. The use of KCl as a suitable DS has also been widely reported in previous studies (Achilli *et al*., 2010; Phuntsho, 2012). Matching fertigation application rates and crop nutrient requirements is essential for optimizing crop production. Blending various types of fertilisers creates a means of meeting crop nutrient requirements and providing the correct N/P/K ratio. The N/P/K blended fertiliser was selected as DS so as to replicate typical N/P/K fertiliser blends used in the Boland (Cape Winelands) region of SA, consisting of the Stellenbosch, Paarl, and Worcester regions.

Targeted N/P/K ratios for the FDFO desalination study were deduced from typical N/P/K fertiliser blends employed (i) at various wine farms in the Boland area, and (ii) by an agricultural products distributor, supplying N/P/K blended fertilisers to the surrounding vineyards in the Boland area. The N/P/K blended fertiliser mass ratios along with their sources of plant nutrients were supplied. Table 3.7 illustrates the straight fertilisers used to make up the N/P/K blended fertiliser solution and their respective single nutrient content in weight percent. The single nutrient content of the fertilisers presented in Table 3.7 was necessary for determining the amount of fertiliser needed in grams for the concentration of N/P/K fertilisers. The N/P/K blended fertiliser DS was made up of straight fertilisers; $CO(NH_2)_2$, phosphoric acid (H_3PO_4) and KCl at molar concentrations of 2/0.15/1 M (N/P/K). Fertiliser DSs, 1 M KCl and blended N/P/K were prepared at elevated molar concentrations with the objective of producing a final fertiliser solution for direct fertigation with a reduced target nutrient concentration of 0.69 M and 1.57/0.1/0.69 M, respectively. The corresponding OP of the targeted concentrations for the straight (1 M KCl) and blended (N/P/K) fertiliser DSs was 3 323 and 6 944 kPa, respectively.

Table 3.7: Fertiliser DSs with their respective nutrient content in weight percent (adapted from Maguire, 2009)

		Nutrient wt. %		
Fertiliser (Source of nutrient)	**Chemical formula**	**N**	**P**	**K**
Urea	$CO(NH_2)$	46		
Phosphoric acid	H_3PO_4		26.9	
Potassium chloride	KCl			60

A commercial CTA FO membrane and novel ABM (ABM_A01 and ABM_A02) FO membranes (See Section 3.4) were used to compare and assess the suitability of commercially available FO membranes for use with frequently used fertilisers within the SA wine industry. FDFO experiments were run for 24 h. Multi-meter probes were immersed in both the FS and DS; pH, EC and mass increments (on the feed side only)

were recorded at one h intervals. These measurements were used to determine the experimental J_w and J_s of draw solutes across the membrane. OP analysis of the FS and DS were performed at two h intervals to determine the bulk OP difference of the FDFO system, and the targeted OP for fertiliser solutions relating to the target DS product concentration for direct fertigation.

3.8. Analyses and calculations

3.8.1. Determining the osmotic pressure (OP) of the solution samples

The OPs of the alternative FSs were determined using three methods: (i) analysis at an external SANAS accredited laboratory (Bemlab, SA). Methods used for determining the OP of the alternative FSs at Bemlab, SA are proprietary and were therefore not disclosed; (ii) Lenntech, an electronic calculator that determined the OP based on the van't Hoff's equation (See Chapter 2, Section 2.6.1.1, Eq. 2.1); and (iii) a cryoscopic osmometer. OP was measured in mOsmoles.kg^{-1}. The osmolal concentrations of the alternative FSs, straight fertiliser DSs and blended fertiliser DSs were measured using a cryoscopic osmometer (OSMOMAT 3000, Gonotec, Germany). Osmolal concentrations were predicted based on the freezing point depression method and had a measurement range of 0 to 3 000 mOsmoles.kg^{-1}. The osmometer calibration was performed by using NaCl standards of 290, 300 and 850 mOsmoles.kg^{-1} received from the supplier. Appendix D describes in detail the operating procedure and calibration of the Osmomat 3000 osmometer. The specifications of the Osmomat can be seen in Table 3.8.

Literature states that at 25°C the relationship between concentration and pressure is (Alexander, 1981; Larcher, 2003):

$$\frac{1\ Osmole}{kg} H_2O = 2.48MPa$$

$$\frac{1\ mOsmole}{kg} H_2O = \frac{0.001\ Osmole}{kg} H_2O$$

$$\frac{1\ mOsmole}{kg} H_2O = 2.48kPa \quad (3.1)$$

Table 3.8: Specifications of the Osmomat 3000 (Gonotec User Guide, 2014)

Specification	Osmomat 3000D
Measurement display	4.5 digits
Measurement range	0 to approximately 3 000 mOsmoles.kg^{-1}
Temperature range	10 - 35°C
Resolution	1 mOsmoles.kg^{-1} or 1 mOsmole digit across the entire measuring range
Sample volume of 50µl	<±0.5%

3.8.2. Determining the experimental water flux (J_w)

The experimental J_w across the FO membrane was calculated based on the changes in weight increments of the FS. Mass changes in the FS were recorded at one h intervals by placing the FS on a digital mass scale. Experimental J_w (L.m^{-2}.h^{-1}) was calculated using Equation 3.2 (Zhang *et al*., 2014a; Zhang *et al*., 2014b).

$$J_w = \frac{m_{f,t} - m_{f,0}}{\rho \times A_m \times \Delta t} \quad (3.2)$$

Where J_w (L.m^{-2}.h^{-1}) is the experimental water flux, $\Delta m_{f,t}$ and $\Delta m_{f,0}$ (g) are the mass of the FS at time = 0 and time = t, respectively. Δt (h) is the time interval, A_m (m^2) is the effective membrane area and ρ (g.L^{-1}) the density of pure water used for the conversion of mass to volume. To ensure the accuracy of the data, each J_w point in the J_w-time curve was obtained by repeating the experimental procedure under the same operational conditions and averaging the two data sets.

3.8.3. Determining the reverse solute diffusion (J_s) of the draw solutes

The J_s across the FO membrane was calculated according to the changes in mass increments and EC variation of the FS. Mass changes and EC variation in the FS were recorded at one h intervals. J_s (g.m^{-2}.h^{-1}) was calculated by using Equation 3.3 (Ge *et al*., 2013; Low *et al*., 2015).

$$J_s = \frac{(C_{f,t} V_{f,t} - C_{f,0} V_{f,0})}{A_m \times \Delta t} \quad (3.3)$$

Where J_s (g.m^{-2}.h^{-1}) is the reverse solute flux and $C_{f,0}$ and $C_{f,t}$ (g.L^{-1}) are the change in the FS salt concentration at time = 0 and time = t, respectively. $V_{f,0}$ and $V_{f,t}$ (L) are the change in FS volume at time = 0 and time = t, respectively. Changes in the salt

concentration for the FS were determined from a standard curve between the mass concentration ($g.L^{-1}$) and conductivity ($mS.cm^{-1}$).

3.8.4. Determining the percentage water recovery for the fertiliser drawn forward osmosis (FDFO) system

The percentage water recovery for the FDFO system was calculated after a 24 h filtration period using Equation 3.4.

$$\%Recovery = \frac{V_{DS}}{V_{FS,i}} \times 100 \quad (3.4)$$

Where ΔV_{DS} is the change in the draw solution volume (L) over a specific time interval and $V_{FS,i}$ is the initial volume of the feed solution (L).

3.8.5. Total nitrogen, phosphorous and potassium (N/P/K) determination

Total nitrogen, phosphorous and potassium (N/P/K) in $g.L^{-1}$ were determined though empirical and theoretical analyses of the FS and DS samples after each FDFO experiment in duplicate. Total N and P were determined empirically using the following standards:

(i) Phosphate (PO_4) (Merck Spectroquant Phosphate Test for the determination of orthophosphate, Cat. No. 1.4848.0001) (Appendix E).
(ii) Nitrogen (N) (Merck Spectroquant Nitrogen (total) cell test, Cat. No. 1.14763.0001) (Appendix F).

Theoretical determination of the total N/P/K was achieved through a dilution equation (See Appendix G for a sample calculation):

$$C_1V_1 = C_2V_2 \quad (3.5)$$

Where C_1 and C_2 ($mol.L^{-1}$) are the initial and final concentration of solutes in the solution and V_1 and V_2 (L) are the initial and final volumes of the solution.

CHAPTER FOUR
RESULTS AND DISCUSSION

4.1. Alternative feed solutions (FSs)

Table 4.1 shows the composition and osmotic pressure (OP) of the various feed solutions (FSs) evaluated for the fertiliser drawn forward osmosis (FDFO) desalination study. The FSs evaluated included synthetic brackish water (BW5); synthetic seawater (SSW); seawater (SW) samples collected from the Atlantic Ocean seaboard (AOSB) and Indian Ocean seaboard (IOSB); winery wastewater collected from a winery within the Stellenbosch region of South Africa (SA) prior and post biological sand filter (BSF) treatments; and synthetic winery wastewater (SWW). OPs of the alternative FSs were determined using three methods: (i) analysis at an external, independent South African National Accreditation System (SANAS) accredited laboratory (Bemlab, SA) - the methods used in determining OP at Bemlab are proprietary and are therefore not disclosed. See Appendix A for full water analysis); (ii) Lenntech, an electronic calculator that determined the OP based on van't Hoff's equation (See, Chapter 2, Section 2.6.1.1, Eq. 2.1); and (iii) a cryoscopic osmometer (OSMOMAT 3000, Gonotec, Germany) was used to measure the osmolal concentrations of the FSs in $mOsmol.kg^{-1}$.

From Table 4.1 it was evident that higher total dissolved solids (TDS) concentrations generated a higher OP. The saline waters used as alternative FSs contained significant concentrations of dissolved salt. Sodium chloride (NaCl), the most prevalent salt, is a strong electrolytic specie and when added to water will dissociate to form ions (Na^+ and Cl^-) which contribute to the overall OP of the solution. Two of the most prevalent ions in SW are chloride (Cl) and sodium (Na); together they make up over 90% of all dissolved ions in the ocean (NOAA, 2017). TDS for the AOSB comprised of 65% NaCl (20 021 $mg.L^{-1}$), while TDS for the IOSB comprised of 70% NaCl (20 986 $mg.L^{-1}$). SW samples collected from the AOSB, with an average TDS concentration of 30 617 $mg.L^{-1}$, produced an average OP of 2 574 kPa, while SW collected from the IOSB with an average TDS concentration of 29 933 $mg.L^{-1}$, produced an average OP of 2 510 kPa. It is thus postulated that the TDS concentration has a prominent effect on the OP generated for a solution. The TDS concentration of the AOSB and IOSB consisted of both NaCl and other dissolved salts. Therefore, other dissolved salts also contribute towards OP. The Lenntech measured and osmometer OP results for the alternative FSs compare well with previously reported studies in literature (Phuntsho, 2012). However, the results obtained from the SANAS accredited laboratory were lower and not comparable to the

reported, measured and calculated OP results. These discrepancies may be attributed to different methods used for OP analysis.

Table 4.1: Compositions of the alternative FSs with corresponding OPs using different methods (results are the average of duplicate samples)

Type of FS	**Total dissolved solids (TDS)**	**Bemlab OP analysis (kPa)**	**Lenntech OP calculator (kPa)**	**Measured OP Osmometer (kPa)**	**Literature references (kPa)**
Deionised water (DI)	Pure water	0	0	0	0 (Grey *et al*., 2006; Phuntsho *et al*., 2011; Phuntsho, 2012)
Brackish water (BW5)	6 823 $mg.L^{-1}$	384	387	414	390 (Phuntsho *et al*., 2011; Phuntsho, 2012)
Synthetic seawater (SSW)	36 267 $mg.L^{-1}$	2 057	2 710	2 761	2 800 (Phuntsho *et al*., 2011; Phuntsho, 2012)
Seawater: Atlantic Ocean seaboard (AOSB)					
Clifton 4^{th}	30 000 $mg.L^{-1}$	1 818	2 323	2 585	
Sea Point	30 850 $mg.L^{-1}$	1 856	2 389	2 566	2 800 (Phuntsho *et al*., 2011; Phuntsho, 2012)
Camps Bay	31 000 $mg.L^{-1}$	1 861	2 400	2 571	
Seawater: Indian Ocean seaboard (IOSB)					
Strand B	28 300 $mg.L^{-1}$	1 710	2 191	2 358	
Gordon's Bay	30 650 $mg.L^{-1}$	1 847	2 373	2 589	2 800 (Phuntsho *et al*., 2011; Phuntsho, 2012)
Strand A	30 850 $mg.L^{-1}$	1 858	2 389	2 583	
Winery wastewater before biological sand filters (BBSF)	892 $mg.L^{-1}$	NA	NA	136	No information in literature
Winery wastewater after biological sand filters (ABSF)	925 $mg.L^{-1}$	NA	NA	91	No information in literature
Synthetic winery wastewater (SWW)	120 $mg.L^{-1}$	NA	NA	61	No information in literature

*Note: NA – Not analysed using Bemlab and Lenntech methods.

4.2. Draw solutions: Straight fertiliser solutions evaluation

Six different straight fertilisers were evaluated as draw solutions (DSs) for the FDFO desalination study. The six fertilisers were selected because of their use within the SA wine industry. The physiochemical properties of the DS were considered, as the choice of DS is highly important in forward osmosis (FO) technology. DSs should ideally be inert, non-toxic and have a neutral or near-neutral pH. The measured OP of the straight fertiliser solutions evaluated as potential DSs were determined by a osmometer (OSMOMAT 3000, Gonotec, Germany). Figure 4.1 illustrates the OP of six different straight fertilisers at molar concentrations ranging from 0 to 10 M at ambient temperature (± 25 ºC). It was evident from Figure 4.1 that a linear correlation existed between OP generation and the concentration of draw solutes. K_2SO_4 generated the highest OP of 55 490 kPa at 10 M, while $CO(NH_2)_2$ generated the lowest OP of 2 530 kPa at 1 M.

Table 4.2 provides a comparison of the OP generated from the various fertilisers at a molar concentration of 2 M. At molar concentrations of 2 M $(NH_4)_2SO_4$ generated the highest OP of 11 408 kPa, K_2SO_4 generated the second highest OP of 11 135 kPa, and the next highest OP was observed for KCl at 9 027 kPa. At an elevated molar concentration of 10 M, K_2SO_4 generated the highest OP. However, at a lower molar concentration of 2 M, $(NH_4)_2SO_4$ generated the highest OP. At a molar concentration of 2 M, fertiliser solutions for K_2SO_4 and $(NH_4)_2SO_4$ were prepared with a dilution factor of 10 for OP analysis. K_2SO_4 has a significantly lower solubility than $(NH_4)_2SO_4$, which required a significant increase in the dilution factor for its OP analysis. The increased dilution factor of 50 is the result of increased OP at 10 M for fertiliser solution K_2SO_4.

OP is a colligative property and is therefore dependent on the ratio of solute particles to solvent particles in a solution, and not on the type or nature of the species present or formed. Different fertilisers resulted in different solution properties and therefore generate various OPs. A study by Phuntsho (2012) evaluated the performance of nine different fertilisers, which excluded K_2SO_4. In his study, Phuntsho (2012) illustrated the species formed from a 2 M fertiliser solution at ambient temperature and atmospheric pressure based on the OLI Stream Analyser 3.2. Table 4.2, adapted from Phuntsho (2012), illustrates the types of species formed for each straight fertiliser and their respective OP at 2 M. All six straight fertilisers (except K_2SO_4, which was excluded from Phuntsho's (2012) study) evaluated were electrolytes and generated charged species with the exception of $CO(NH_2)_2$. From Table 4.2 it was evident that the OP of fertilisers determined by the freezing point depression method was much higher than that determined by the OLI Stream Analyser 3.2. The prediction of OP using the OLI Stream

Analyser 3.2 is executed though the utilisation of thermodynamic modelling, based on published experimental data. The usefulness of the OLI Stream Analyser 3.2 may be potentially limiting since the individual researcher has limited access to the assumptions underlying the software. Discrepancies observed for the OP generated by fertiliser draw solutes are attributed to the different methods used in determining OP.

Figure 4.2 illustrates the OP of straight fertiliser DSs (read on the primary y-axis) as well as the OP of the alternative FSs (read on the secondary y-axis). The highest OP generated for the alternative FSs was 2 761 kPa for SSW. At a molar concentration of 1 M, all fertiliser DSs with the exception of $CO(NH_2)_2$ (2 530 kPa at 1 M) exhibited OPs greater than all the alternative FSs. This renders fertiliser solutions suitable as DSs for the FDFO process at molar concentrations of 1 M.

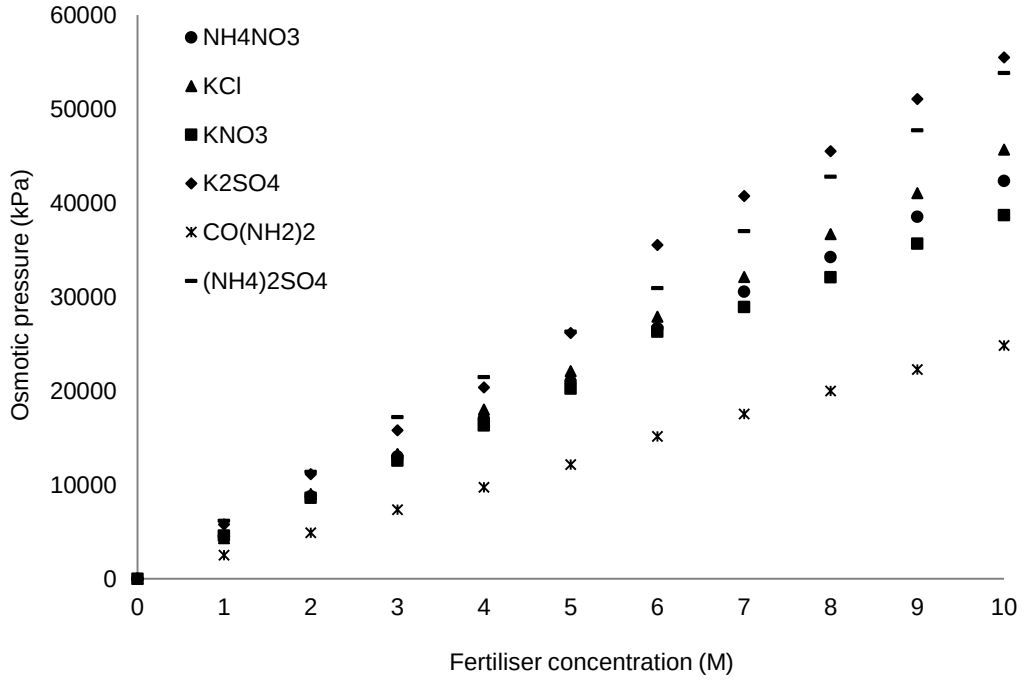

Figure 4.1: Measured OP of the six straight fertilisers evaluated as potential DSs. OP analysed using a cryoscopic osmometer at ambient temperature

Table 4.2: List of straight fertilisers evaluated as potential DSs at 2 M for the FDFO desalination study

Fertilisers	**Chemical formula**	**Molecular weight (M_W) in g.mol^{-1}**	**OP at 2 M (kPa) (this study)**	**OP at 2 M (atm) (Phuntsho, 2012)**	**OP at 2 M (kPa)**	**Species formed in 2 M solution**
Ammonium nitrate	NH_4NO_3	80.04	8 804	64.9	6 576	NH_4^+ : 0.85 M; NO_3^- : 0.85 M; NH_4NO_3 : aq 1.15 M
Ammonium sulphate (SOA)	$(NH_4)_2SO_4$	132.1	11 408	92.1	9 332	NH_4^+ : 3.07 M; SO_4^{2-} : 1.07 M; $NH_4SO_4^-$: 0.93 M
Potassium chloride	KCl	74.55	9 027	80.1	8 116	K^+ : 1.99 M; Cl^- : 1.99 M; KCl (aq.): 0.01 M
Potassium nitrate	KNO_3	101.01	8 606	59.9	6 069	K^+ : 2 M; NO_3^- : 2 M
Potassium sulphate	K_2SO_4	174.26	11 135	NA	NA	NA
Urea	$CO(NH_2)_2$	60.06	4 923	46.1	4 671	Urea does not dissociate in water

*Note: Conversion factor, 1 atm = 101.325 kPa. NA – Not analysed by Phuntsho (2012).

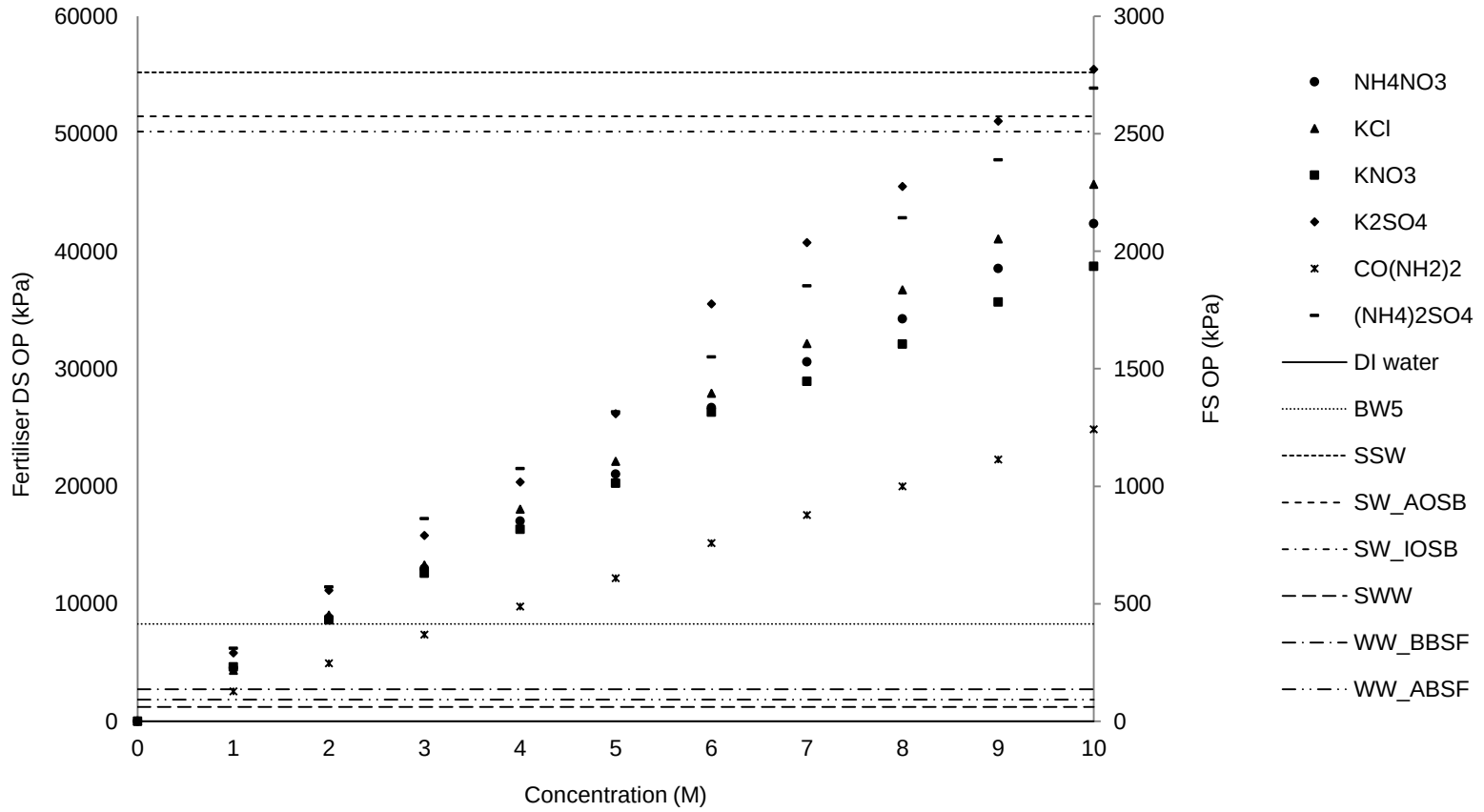

Figure 4.2: Measured OP of straight fertiliser DSs and alternative FSs evaluated for the FDFO desalination study

*Note: Winery wastewater before biological sand filter (WW_BBSF) and Winery wastewater after biological sand filter (WW_ABSF)

4.3. Draw solutions (DSs): Blended fertiliser evaluation

Fertiliser blending is a technical process that offers a customised balance by adjusting fertiliser inputs to meet crop requirements. The six straight fertilisers (Table 3.3) were blended together in equal molar concentrations ranging from 0 to 2 M at 1:1 molar ratio. As stated in the previous section, the physiochemical properties of the DS need to be considered as the selection of an optimum DS is imperative for FO technology. Solubility is amongst the most important physiochemical properties that directly affects the OP generated. In FO technology the thermodynamic driving force for forward flux is OP (Wilson & Stewart, 2013). Table 4.3 illustrates the solubility of the six straight fertilisers in 100 g of water at two temperatures, given in °C.

Table 4.3: Solubility of fertiliser DSs in water at various temperatures (adapted from Perry *et al*., 1997)

		Solubility	
		Temperature (°C)	
Fertiliser	**Chemical formula**	**20**	**30**
Ammonium nitrate	NH_4NO_3	192	241.8
Ammonium sulphate (SOA)	$(NH_4)_2SO_4$	75.4	78
Potassium chloride	KCl	31	34
Potassium nitrate	KNO_3	20.9	31.6
Potassium sulphate	K_2SO_4	9.22	11.11
Urea	$CO(NH_2)_2$	-	-

Table 4.4 displays both the measured OP of the various fertiliser blends and the calculated OP using the straight fertiliser OPs that make up the blend ratio. The differences between the measured OP of the fertiliser blended solutions and the calculated OP of straight fertilisers was not significant: in essence, the OP of the blended fertiliser should resemble the OP of the sum of the straight fertilisers' OPs. However, blending combinations of straight fertilisers may result in crystal growth or the formation of precipitate. As indicated in Table 4.4, it was observed that when KCl was blended with $(NH_4)_2SO_4$, the resultant measured OP of the blended fertiliser solution at a molar concentration of 1 M was lower than the sum of the individual straight fertiliser OPs. The same was observed when KCl was blended with $(NH_4)_2SO_4$ at a molar concentration of 2 M. Similarly, the resultant measured OP for the fertiliser blend of KCl and NH_4NO_3 was observed to be lower than the sum of the individual straight fertiliser OPs at higher molar concentrations of 2 M. When KCl is blended with $(NH_4)_2SO_4$, one of the products formed is K_2SO_4; similarly, when KCl is blended with NH_4NO_3, KNO_3 is a resultant product. These precipitates may be detrimental to the physical and chemical properties of the

final product. The solubility of precipitates K_2SO_4 and KNO_3 is much lower than the solubility of straight fertilisers KCl, $(NH_4)_2SO_4$ and NH_4NO_3 blended together, as seen in Table 4.3. The decrease in solubility was a result of the formation of K_2SO_4 and KNO_3 precipitates, which will, in turn, result in a decrease in OP, affecting recovery rates and overall performance of the FO process.

Table 4.4: Fertiliser blended DSs at 1 and 2 M with their respective measured and calculated OPs

Fertiliser blended DSs 1 M : 1 M	**Measured fertiliser blended DS OP (kPa) at 1 M : 1 M**	**Calculated OP from straight fertiliser DSs (DS_1+DS_2) (kPa) at 1 M : 1 M**	**Fertiliser blended DSs 2 M : 2 M**	**Measured fertiliser blended DS OP (kPa) at 2 M : 2 M**	**Calculated OP from straight fertiliser DSs (DS_1+DS_2) (kPa) at 2 M : 2 M**
			Urea blended DSs		
$CO(NH_2)_2 + NH_4NO_3$	7 626	7 068	$CO(NH_2)_2 + NH_4NO_3$	13 826	13 727
$CO(NH_2)_2 + (NH_4)_2SO_4$	7 713	8 730	$CO(NH_2)_2 + (NH_4)_2SO_4$	15 991	16 331
$CO(NH_2)_2 + KCl$	7 341	6 845	$CO(NH_2)_2 + KCl$	14 272	13 950
$CO(NH_2)_2 + KNO_3$	7 390	7 130	$CO(NH_2)_2 + KNO_3$	13 504	13 528
$CO(NH_2)_2 + K_2SO_4$	8 469	8 333	$CO(NH_2)_2 + K_2SO_4$	15 736	16 058
			Ammonium nitrate blended DSs		
$NH_4NO_3 + (NH_4)_2SO_4$	9 325	10 738	$NH_4NO_3 + (NH_4)_2SO_4$	18 005	20 212
$NH_4NO_3 + KCl$	9 610	8 854	$NH_4NO_3 + KCl$	17 620	17 831
$NH_4NO_3 + KNO_3$	9 238	9 139	$NH_4NO_3 + KNO_3$	16 641	17 410
$NH_4NO_3 + K_2SO_4$	9 746	10 342	$NH_4NO_3 + K_2SO_4$	18 687	19 939
			Ammonium sulphate blended DSs		
$(NH_4)_2SO_4 + KCl$	9 364	10 515	$(NH_4)_2SO_4 + KCl$	19 642	20 435
$(NH_4)_2SO_4 + KNO_3$	9 077	10 800	$(NH_4)_2SO_4 + KNO_3$	17 236	20 014
$(NH_4)_2SO_4 + K_2SO_4$	10 327	12 003	$(NH_4)_2SO_4 + K_2SO_4$	20 708	22 543
			Potassium chloride blended DSs		
$KCl + KNO_3$	8 903	8 916	$KCl + KNO_3$	17 038	17 633
$KCl + K_2SO_4$	10 032	10 118	$KCl + K_2SO_4$	19 369	20 162
			Potassium nitrate blended DSs		
$KNO_3 + K_2SO_4$	9 858	10 404	$KNO_3 + K_2SO_4$	18 054	19 741

4.4. Osmotic equilibrium determination for draw solution (DS) 1 M KCl

In theory, the osmotic process should occur until osmotic equilibrium (OE) occurs. OE occurs when the OP of the DS reaches equilibrium with the OP of the FS. A 1 M KCl fertiliser solution was used as a DS, with DI water as a controlled FS. The experiment for the determination of OE was performed in duplicate using an ABM (ABM_A01) FO membrane. An initial experiment was run for an operational time of 217 h (Experiment A), and a duplicate experiment for an operational time of 177 h (Experiment B). The initial experimental run of 217 h was stopped after it was observed that there was minimal experimental water flux (J_w) across the membrane. After the membrane was cleaned (periodic rinse with DI water at 450 $mL.min^{-1}$), a duplicate experimental run was commenced for 177 h. Figure 4.3 illustrates the bulk OP difference (Δπ) against filtration time, and indicates that after 125 h the bulk Δπ was 1 152 and 470 kPa for Experiments A and B, respectively. The variation in bulk Δπ for the two experiments (Experiments A and B) at an operational time of 125 h may be attributed to increased draw solute permeation across the ABM_A01 membrane after the initial experimental run of 217 h. Reverse permeation of draw solutes results in the increased concentration of the saline FS, which in turn increases the OP. Initial conductivity measurements for Experiments A and B were 0.0105 and 0.0097 $mS.cm^{-1}$, respectively. After 125 h, the increased conductivity measurement of 27.8 $mS.cm^{-1}$ for Experiment B was substantially greater than the conductivity measurement of 11.32 $mS.cm^{-1}$ for Experiment A. The increased conductivity experienced for Experiment B corroborated the observation that the reverse permeation of draw solutes (KCl) had a significant effect on the concentration of the feed solution and resulted in an increased OP, reducing the bulk Δπ of the FO system to achieve OE at a more elevated rate.

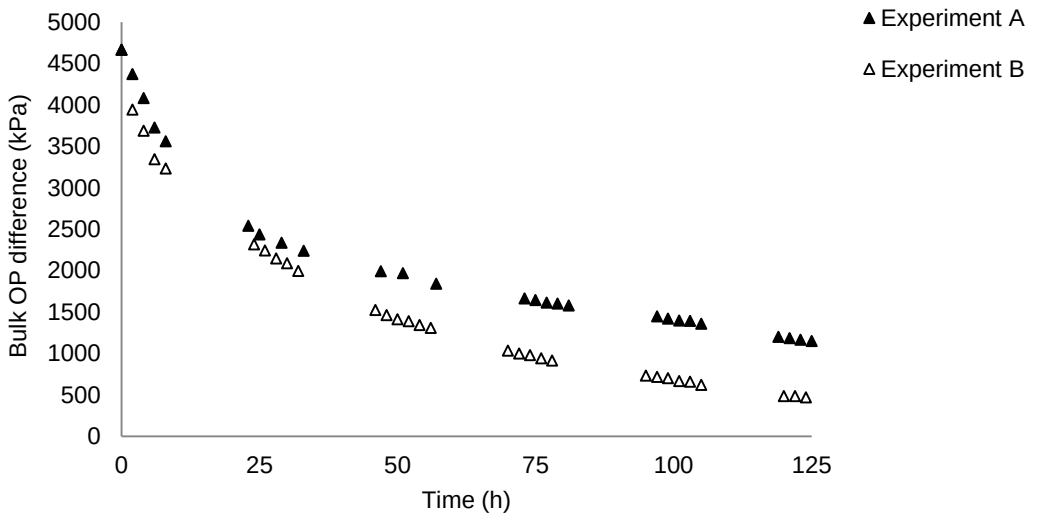

Figure 4.3: Bulk Δπ curve for DS 1 M KCl and FS DI water over a filtration period of 125 h

4.5. Performance evaluation of the fertiliser drawn forward osmosis (FDFO) desalination system comparing two different forward osmosis (FO) membranes

Two different FO membranes were used for comparative performance study: (i) a commercial cellulose triacetate (CTA) FO membrane (Fluid Solutions Inc., USA); and (ii) a novel aquaporin biomimetic membrane (ABM) (Aquaporin A/S, Denmark). Specifications of the CTA and ABM FO membranes were given earlier in Section 3.4 of Chapter 3. Two batches of ABMs were evaluated in the FDFO desalination study, here to referred to as second generation ABM (ABM_A01) and third generation ABM (ABM_A02).

Two selected fertiliser DSs (one straight and one blended) were tested using a bench-scale FDFO system, described earlier in Section 3.5 of Chapter 3. The straight fertiliser DS consisted of fertiliser solute KCl at a molar concentration of 1 M. The blended fertiliser solution was in an N/P/K ratio of 2/0.15/1 M, respectively; made up of straight fertilisers $CO(NH_2)_2$, phosphoric acid (H_3PO_4) and KCl. The straight fertiliser KCl was selected as a DS because of its use within SA vineyards. KCl is the most commonly employed potassium (K) fertiliser. The use of KCl as a suitable draw solute has also been widely reported in many previous studies (Achilli *et al*., 2010; Phuntsho, 2012). The N/P/K blended fertiliser was selected as a DS so as to replicate typical N/P/K blended fertilisers employed within the Boland (Cape Winelands) region of SA. Fertiliser blending offers a customised balance by adjusting fertiliser inputs to meet crop requirements. The selection of the blended fertiliser (N/P/K) ratio has been elaborated on in earlier sections (Chapter 3, Section 3.7.2). The straight (KCl) and blended (N/P/K) fertiliser DSs were

used at elevated molar concentrations of 1 M for single fertiliser DS KCl and 2/0.15/1 M for the blended N/P/K fertiliser DS, with the objective of reducing the final nutrient concentration to 0.69 M for single fertiliser DS KCl with corresponding OP of 3 323 kPa, and 1.57/0.1/0.69 M for the blended N/P/K fertiliser DS with a corresponding OP of 6 944 kPa of the final product water for direct fertigation. The ideal DS should generate a high OP, well above that of the saline FS. OPs generated for the fertiliser DSs KCl and N/P/K were 4 668 and 9 978 kPa, respectively, surpassing the OP generated for the alternative FSs, thus making them suitable DSs for the FDFO study. The performance of the two DSs was tested against a controlled FS (DI water) and two alternative FSs (BW5 and SWW). The preparation of FSs and DSs used in the FDFO desalination study was described earlier in Chapter 3, under Sections 3.2 and 3.3.

An operating time of 24 h was used for the bench-scale FDFO desalination study. The operational time of 24 h was selected after preliminary experiments to allow for the respective target concentrations to be reached and substantial data recorded to observe water permeation across the FO membrane. Data was recorded manually, continuously for 8 h (day time) and left running overnight. Data omitted from the figures in the following sections is the result of continual unmonitored running overnight. Tables 4.5 and 4.6 illustrate the experimental J_w and various times of the FDFO process for the 1 M KCl fertiliser DS and N/P/K blended fertiliser DS, respectiviely, with varying FSs (DI water, BW5 and SWW) using the CTA, ABM_A01 and ABM_A02 membranes. The experimental J_w after one hour (1 h) is provided in Tables 4.5 and 4.6 to account for the initial flux decline.

Table 4.5: Comparing the performance evaluation of FO membranes (CTA, ABM_A01, and ABM_A02) using 1 M KCl fertiliser DS and different FSs

Parameter	DS (KCl) : FS (DI water)			DS (KCl) : FS (BW5)			DS (KCl) : FS (SWW)		
	CTA	ABM_A01	ABM_A02	CTA	ABM_A01	ABM_A02	CTA	ABM_A01	ABM_A02
Δπ (kPa)		4 668			4 254			4 607	
Initial J_w ($L.m^{-2}.h^{-1}$)	8.38	9.25	14.25	7.23	7.88	4.33	6.77	3.09	12.97
J_w after 1 h ($L.m^{-2}.h^{-1}$)	5.13	5.43	10.77	4.25	3.68	2.4	5.41	3.24	8.56
J_w at target conc. (0.69 M) ($L.m^{-2}.h^{-1}$)	5	5.11	11	3.53	3.57	2.39	4.90	1.61	9.22
J_w after 24 h ($L.m^{-2}.h^{-1}$)	3.91	2.88	6.30	3.55	2.57	2.23	3.59	1.67	4.20

Table 4.6: Comparing the performance evaluation of FO membranes (CTA and ABM_A02) using an N/P/K fertiliser blended DS and different FSs

Parameter	DS (N/P/K blend) : FS (DI water)		DS (N/P/K blend) : FS (BW5)		DS (N/P/K blend) : FS (SWW)	
	CTA	ABM_A02	CTA	ABM_A02	CTA	ABM_A02
Δπ (kPa)		9 978		9 564		9 917
Initial J_w ($L.m^{-2}.h^{-1}$)	15.54	11.62	7.85	11.31	8.8	8.86
J_w after 1 h ($L.m^{-2}.h^{-1}$)	12.41	10.04	6.42	9.58	6.91	7.41
J_w at target conc. (1.57/0.1/0.69 M) ($L.m^{-2}.h^{-1}$)	11.78	8.57	5.41	11	5.10	6.32
J_w after 24 h ($L.m^{-2}.h^{-1}$)	7.36	4.89	3.83	6.35	4.98	4.20

4.5.1. Comparison of forward osmosis (FO) membrane performance: Water flux (J_w)

4.5.1.1. Draw solution (DS) KCl and feed solution (FS) deionised (DI) water

Targeted fertiliser solution concentrations for KCl fertigation in the Boland (Cape Winelands) region of SA varies from 0.49 to 0.73 M, depending on vineyard capacity and time of application. A targeted concentration of 0.69 M with a corresponding OP of 3 323 kPa was selected for this study. In theory, the DS should be able to extract water from the FS until OE occurs. As the FO process takes place and water is extracted from the FS, the KCl solution is diluted from 1 M to 0.69 M. Figure 4.4 illustrates the OP of the fertiliser DS (KCl) over 24 h using the CTA, ABM_A01 and ABM_A02 membranes. The targeted concentration with respective OP was achieved at approximately 14.68, 11.72 and 8.33 h for the CTA, ABM_A01 and ABM_A02 membranes, respectively.

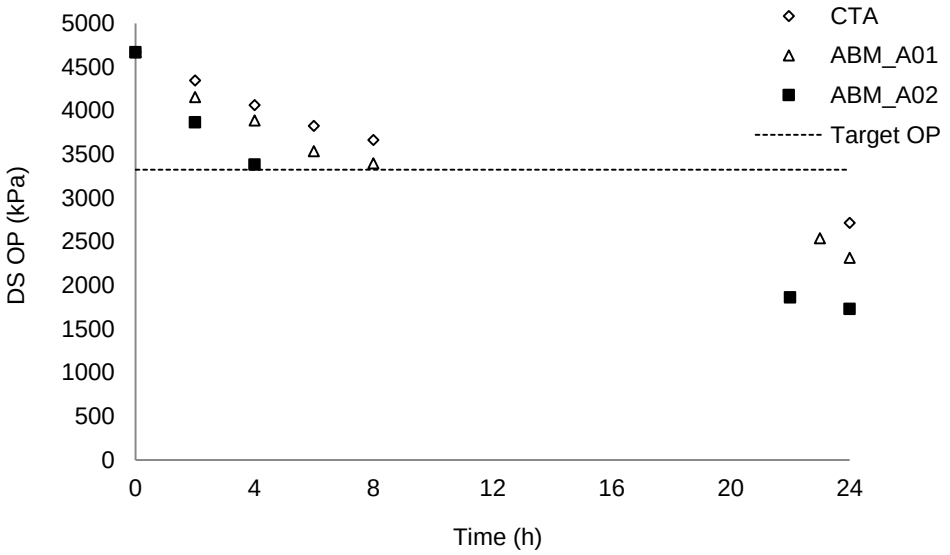

Figure 4.4: DS OP and targeted OP for KCl fertigation with FS DI water over 24 h

Table 4.5 illustrates the experimental J_w at various times for fertiliser DS 1 M KCl, with controlled FS, DI water. The highest experimental J_w was observed for the ABM_A02 membrane, well above fluxes obtained for both the CTA and ABM_A01 membranes. The ABM_A02 membrane achieved an initial experimental J_w of 14.25 $L.m^{-2}.h^{-1}$, 41 and 35% higher than that of the CTA and ABM_A01 membranes, respectively. The FDFO process with the CTA membrane, which generated the lowest experimental J_w, only achieved the target concentration after 14.68 h. The FDFO process with the ABM_A02 membrane, which generated an experimental J_w significantly higher than that of the CTA membrane, achieved the target concentration after 8.33 h, 43% faster than that of the CTA membrane.

As shown in Table 4.5 an initial experimental J_w decline of 39, 41 and 24% was experienced after a one h filtration period for the CTA, ABM_A01 and ABM_A02 membranes, respectively. After a 24 h filtration period, the experimental J_w had declined 53, 69 and 55% for the CTA, ABM_A01 and ABM_A02 membranes, respectively. Flux decline is inherent in membrane processes and is the result of changes in the bulk Δπ, concentration polarization (CP) and scaling phenomena. Fertiliser DS KCl contains monovalent ions (K^+ and Cl^{-1}). Phuntsho *et al.* (2014) concluded that fertilisers containing monovalent ions are less susceptible to scaling phenomena. Thus, flux decline experienced for the FDFO experiment with DS KCl and FS, DI water can be attributed to changes in the bulk Δπ and CP. Figure 4.5 illustrates the experimental J_w decline for the ABM_A02 membrane, with its corresponding bulk Δπ decline over a 24 h filtration period. As the bulk Δπ (the driving force for FO process) of the system decreased, so did the experimental J_w.

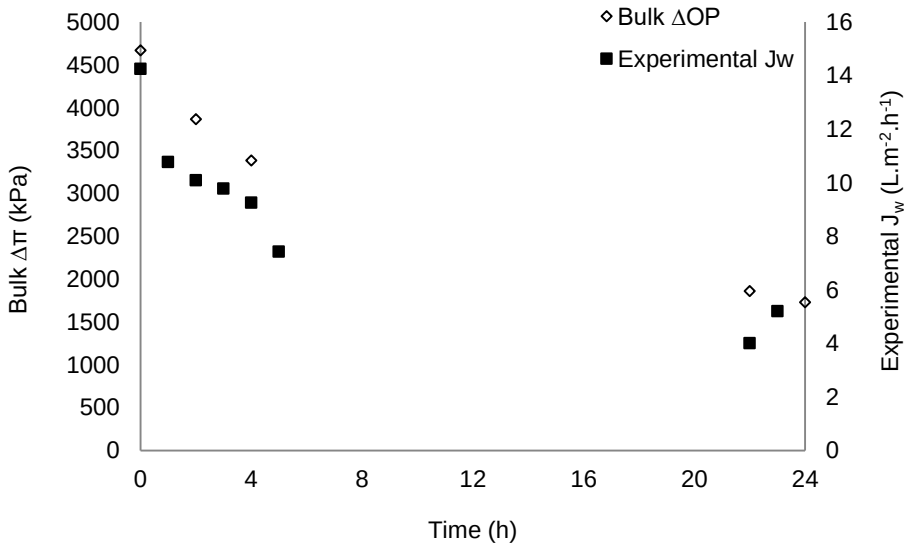

Figure 4.5: Experimental J_w decline with the corresponding decline in bulk Δπ for the ABM_A02 FO membrane over 24 h

The ABM_A02 membrane illustrated a gradual flux decline. However, despite having the lowest flux decline, the ABM_A02 membrane only achieved an experimental J_w recovery of 84% after simple membrane cleaning was employed. This was comparatively lower than that of the CTA and ABM_A01 membranes, which achieved recoveries of 94 and 97%, respectively. When water extraction capabilities for the CTA, ABM_A01 and ABM_A02 membranes were compared a significant water recovery of 65% was observed for the ABM_A02 membrane after a 24 h filtration period. Water recoveries after a 24 h filtration period were 43% and 35% for the CTA and ABM_A01 membranes. Not only did the ABM_A02 membrane perform well in terms of initial experimental J_w,

but its flux decline was gradual and its water extraction capacities proved superior to the conventional CTA membrane. Figure 4.6 illustrates the scanning electron microscopy (SEM) images of the used CTA, ABM_A01 and ABM_A02 membranes.

CTA

a) b) c)

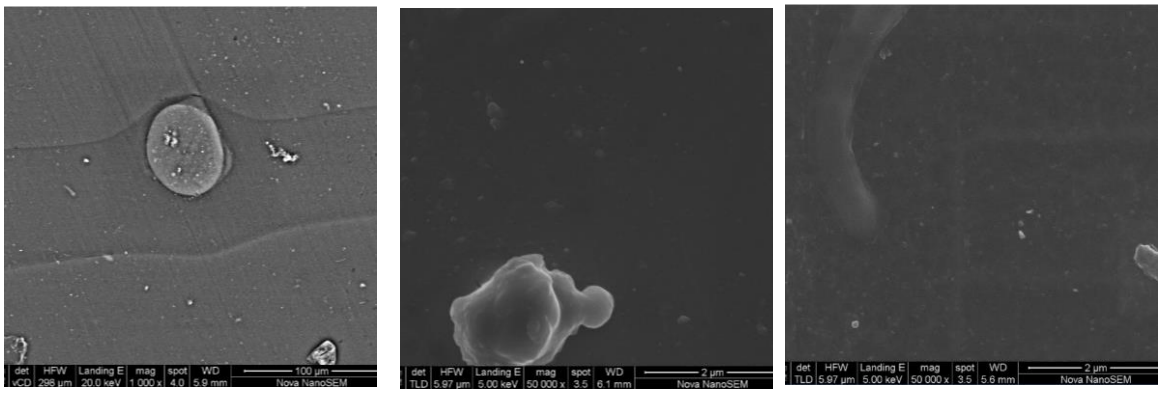

ABM_A01

a) b) c)

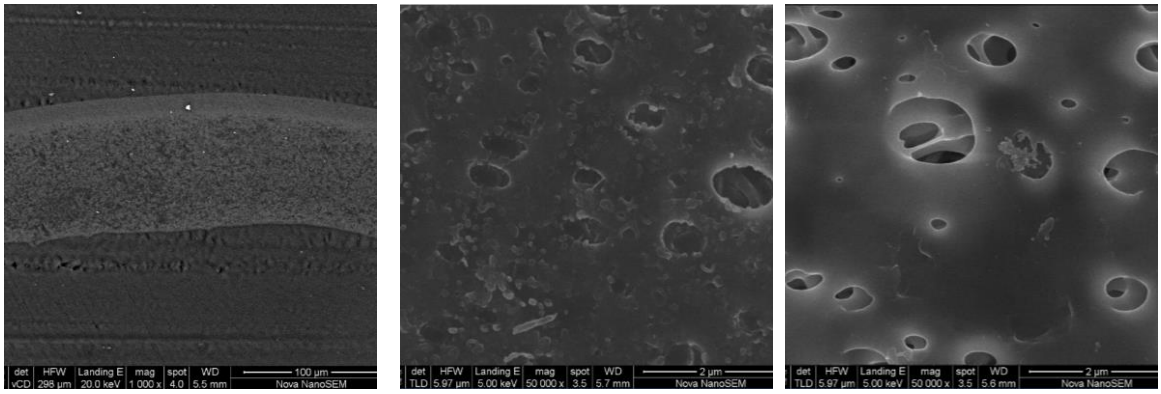

ABM_A02

a) b) c)

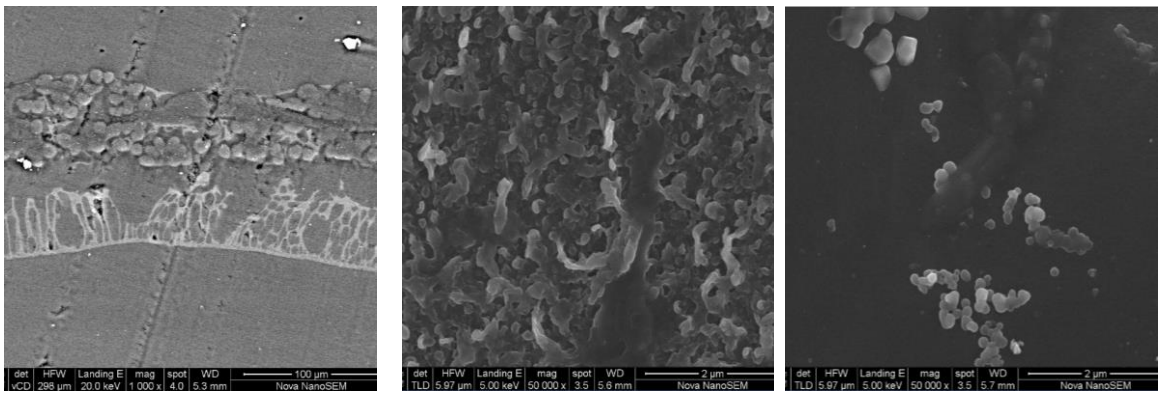

Figure 4.6: KCl & DI water: (a) cross section, (b) active layer and (c) support layer [magnification (a) 100 µm x 1000 and (b and c) 2 µm x 50 000]

There was little variation in the SEM images of the virgin CTA and ABM_A01 membranes and the used (KCl: DI water) CTA and ABM_A01 membranes. The active layer of the CTA membrane did, however, show salt concentration, which may be attributed to the reverse permeation of KCl draw solutes though the support and active layer of the CTA membrane. The SEM image of the used ABM_A02 support layer illustrated significant salt concentrations, which may be attributed to the reverse flux of draw solutes (KCl) though the support layer of the ABM_A02 membrane.

4.5.1.2. Draw solution (DS) KCl and feed solution (FS) synthetic brackish water (BW5)

As stated previously, a targeted fertiliser solution concentration for KCl fertigation was selected at 0.69 M with a corresponding OP of 3 323 kPa. Figure 4.7 illustrates the OP of fertiliser DS KCl over 24 h. The targeted concentration was achieved at 16.43 and 16.86 h for the CTA and ABM_A01 membranes, respectively. A filtration period of 24 h was not sufficient for the ABM_A02 membrane to achieve the targeted concentration. When an extrapolation of the fertiliser DS OP over a filtration period of 24 h was made, it was estimated that the targeted concentration would be achieved at 24.76 h for the ABM_A02 membrane.

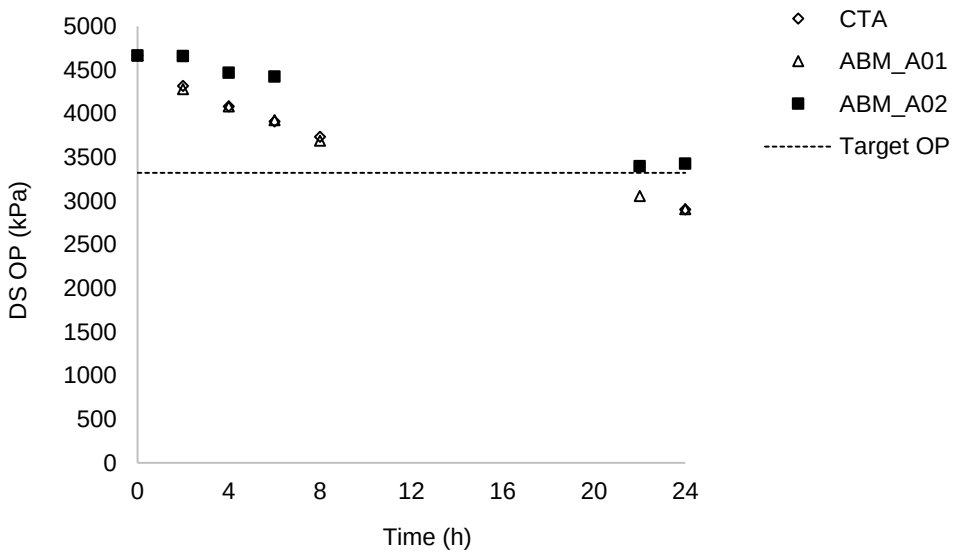

Figure 4.7: DS OP and targeted OP for KCl fertigation with FS BW5 over 24 h

Table 4.5, above, illustrates the experimental J_w at various times for the CTA, ABM_A01 and ABM_A02 membranes with a 1 M KCl DS and BW5 FS. The lower experimental J_w experienced when BW5 was used as an alternative FS was due to the lower initial bulk $\Delta\pi$ of 4 254 kPa, which was not significantly lower than the bulk $\Delta\pi$ of 4 668 kPa when DI water was used as a FS. Experimental J_w observed for the CTA and ABM_A01

membranes were comparable at 7.23 and 7.88 $L.m^{-2}.h^{-1}$, respectively. Thus a mere 8% variation in the experimental J_w was observed for the CTA and ABM_A01 membranes. The lower experimental J_w of 4.33 $L.m^{-2}.h^{-1}$ recorded for the ABM_A02 membrane was unusual since the membrane obtained an experimental J_w well above that of the CTA and ABM_A01 membranes when DI water was used as a controlled FS. The time taken to achieve the targeted concentration for KCl fertigation for the ABM_A02 membrane was substantiated by the low experimental J_w generated when BW5 was used as a FS. The low experimental J_w experienced for the ABM_A02 membrane may have been the result of severe external concentration polarization (ECP) effects. On the feed side (BW5), solutes may have concentrated at the membrane active layer surface. When water from the FS permeated though the active layer, the solutes (NaCl) were left behind in higher concentrations, ($C_{feed,m} > C_{feed,b}$) where $C_{feed,m}$, the feed concentration at the membrane boundary layer was greater than the feed concentration in the bulk solution ($C_{feed,b}$).

Initial declines in experimental J_w of 41, 53 and 44% after a one h of filtration period were observed for the CTA, ABM_A01 and ABM_A02 membranes, respectively. After a 24 h filtration period, the experimental J_w had declined 51, 67 and 78% for the CTA, ABM_A01 and ABM_A02 membranes. Flux declines for the CTA and ABM_A01 membranes when using BW5 as a FS showed little variation when compared to flux declines observed when using DI water as a controlled FS. However, the flux decline for the ABM_A02 membrane was significantly higher when BW5 was used as a FS. Initial experimental J_w decline after a one h filtration period for the ABM_A02 membrane was 46% higher when using BW5 than when using DI water as a FS. Figure 4.8 illustrates the experimental J_w decline, with the corresponding decline in bulk $\Delta\pi$ for the ABM_A02 membrane. Membrane flux recoveries of 72, 87 and 83% were achieved for the CTA, ABM_A01 and ABM_A02 membranes, respectively, after simple cleaning was employed. Despite generating the lowest experimental J_w, membrane flux recovery for the ABM_A02 membrane did not vary with changing FS. However, the membrane flux recovery for FO membranes CTA and ABM_A01 exhibited variations of 23 and 10%, respectively, when using BW5 as a FS.

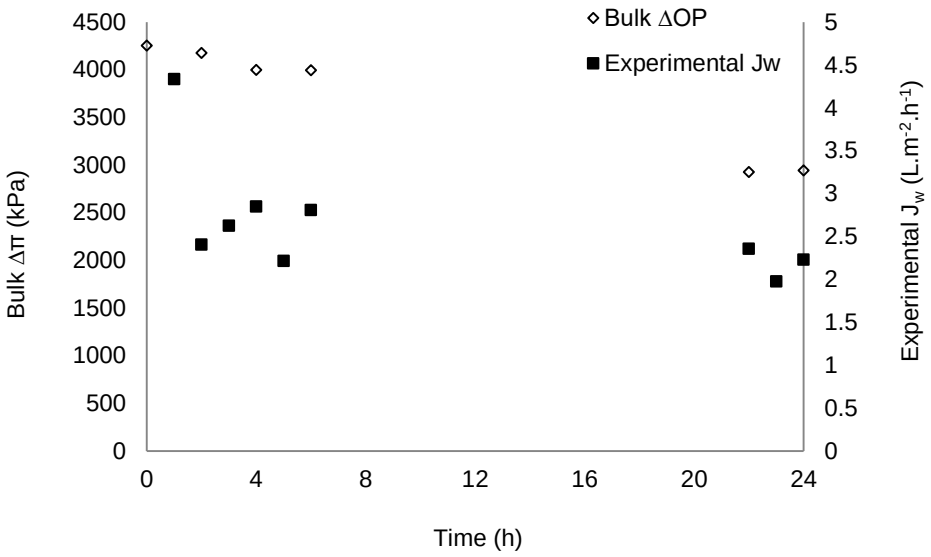

Figure 4.8: Experimental J_w decline with the corresponding decline in bulk Δπ for the ABM_A02 membrane with FS, BW5 over 24 h

When the water extraction capabilities of the CTA, ABM_A01, and ABM_A02 membranes were compared, it was observed that the CTA membrane achieved a water recovery rate of 41% over a 24 h filtration period, nearly double that of the ABM_A01 and ABM_A02 membranes, which only managed to achieve a water recovery rate of 34%. The ABM_A02 membrane, which exhibited such potential for reclamation using DI water, did not show the same potential for FSs containing strong electrolytic species. Figure 4.9 illustrates the SEM images of the used CTA, ABM_A01 and ABM_A02 membranes.

When comparisons are made between the virgin SEM images and the used SEM images (KCl: BW5), we observe little variation in the membrane surfaces for the CTA membrane. However, there seems to be minimal salt concentration (KCl) in the support layer of the ABM_A01 membrane. The ABM_A02 membrane, which experienced a significantly lower experimental J_w when BW5 was as a FS, illustrated severe salt concentration (KCl) in the support layer. The reverse diffusion of KCl draw solutes results in the decreased OP of the DS, which in turn reduces the bulk Δπ of the FO system.

CTA

a) b) c)

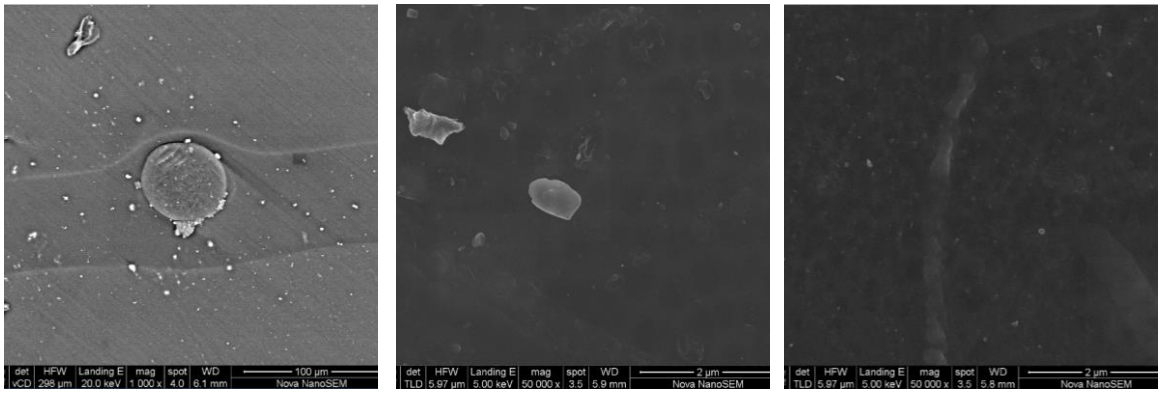

ABM_A01

a) b) c)

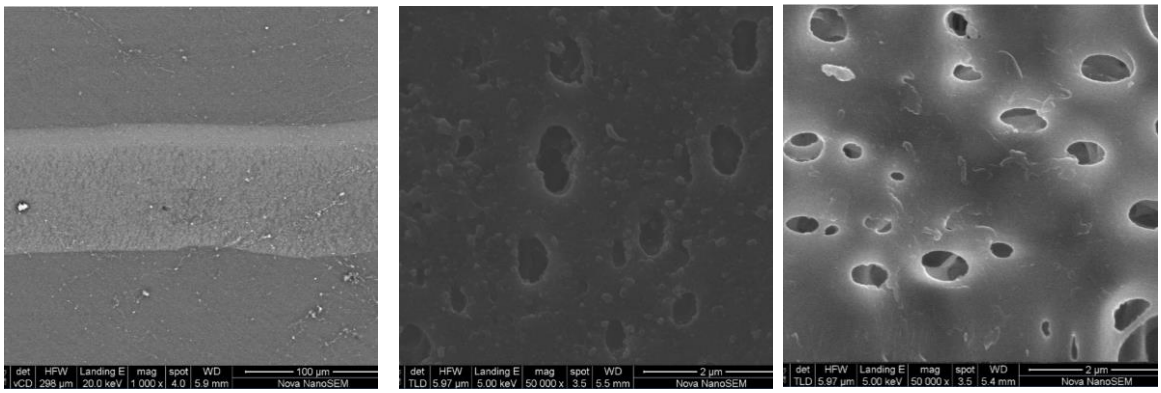

ABM_A02

a) b) c)

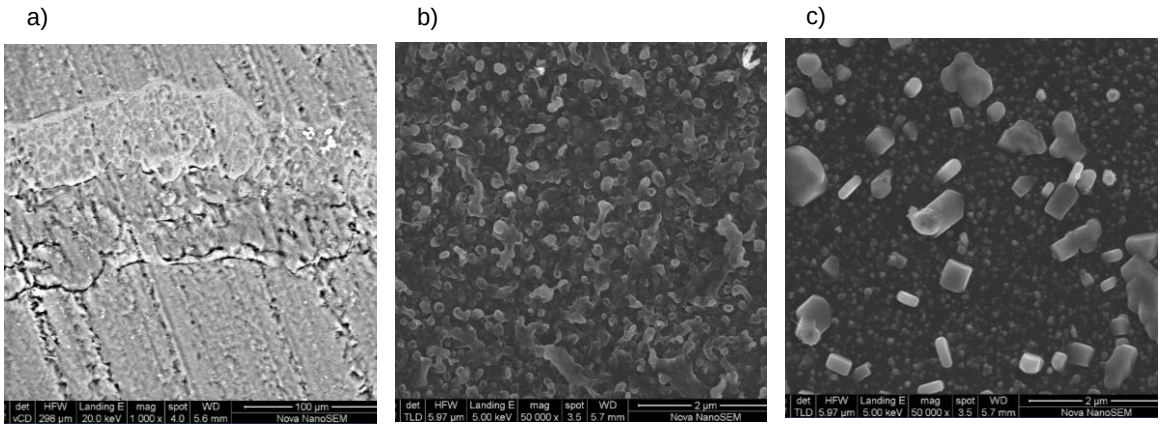

Figure 4.9: KCl & BW5: (a) cross section, (b) active layer and (c) support layer [magnification (a) 100 µm x 1000 and (b and c) 2 µm x 50 000]

4.5.1.3. Draw solution (DS) KCl and feed solution (FS) synthetic winery wastewater (SWW)

The target concentration for KCl fertigation of 0.69 M was selected with respective OP of 3 323 kPa. Figure 4.10 illustrates the time taken for the FDFO process using the CTA, ABM_A01 and ABM_A02 membranes to achieve the target concentration. A target concentration of 0.69 M for KCl fertigation was achieved at 14.64, 29.6 and 10.05 h for the CTA, ABM_A01 and ABM_A02 membranes, respectively.

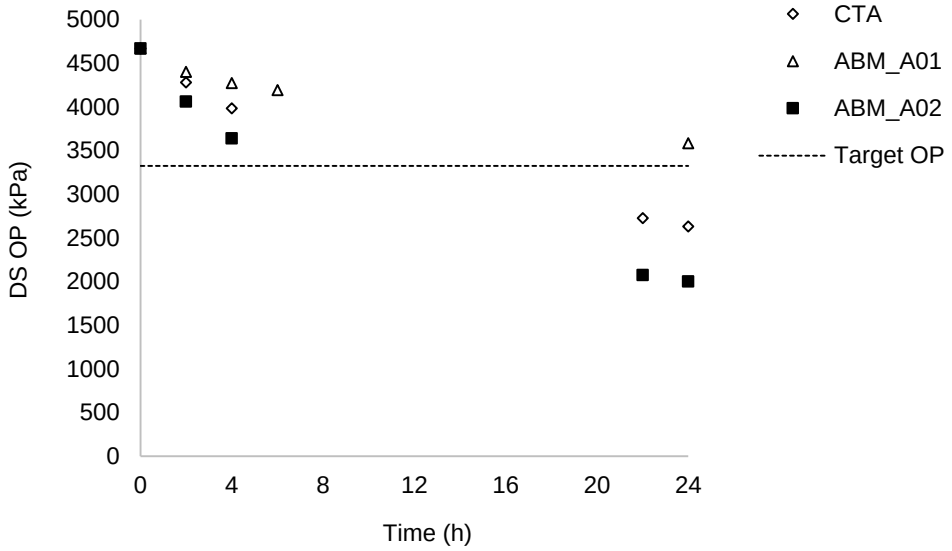

Figure 4.10: DS OP and targeted OP for KCl fertigation over 24 h with FS SWW

Table 4.5 illustrates the bulk Δπ with the respective experimental J_w generated at various times for the CTA, ABM_A01 and ABM_A02 membranes with a 1 M KCl fertiliser solution as DS and SWW as FS. Despite having a higher bulk Δπ of 4 607 kPa compared to a bulk Δπ of 4 254 kPa when BW5 was used as FS, the experimental J_w of 6.77 and 3.09 $L.m^{-2}.h^{-1}$ observed for the CTA and ABM_A01 membranes when using SWW as a FS was low. The exception was the ABM_A02 membrane, which produced an experimental J_w of 12.97 $L.m^{-2}.h^{-1}$, four times greater than that of the ABM_A01 membrane. The significantly lower experimental J_w experienced for the ABM_A01 membrane when SWW was used as a FS was unusual, since at a higher bulk Δπ a higher experimental J_w was expected. Solution diffusion theory predicts that the experimental J_w should be proportional to the driving force across the membrane (the bulk Δπ). However, the resultant experimental J_w was much lower for the ABM_A01 membrane.

SWW used in this study was made up of weak acids and organic solutes; acetic acid (CH_3COOH), gallic acid ($C_7H_6O_5$), glucose ($C_6H_{12}O_6$), vanillin ($C_8H_8O_3$) and ethanol (C_2H_6O). Membrane selectivity guidelines proposed by Rautenbach and Albrecht (1989) state that the rejection of weak acids (CH_3COOH and $C_7H_6O_5$) is highly pH dependent. When the acid is in the ionized form, rejection will be high, while in the non-ionized form rejection will be low. At pHs above the acid dissociation constant (pK_a), the solute rejection increases significantly, but at pHs below the pK_a value, when the acid is in its neutral form, the rejection rate decreases. Both CH_3COOH and $C_7H_6O_5$ are weak electrolytes ionizing only partially, in principle, the species in the solution of the weak electrolytes were the un-ionized compounds, itself resulting in low rejection of the weak acids. Similarly, with organic solutes, membrane rejection generally increases when the molecular weight of the solute increases. The order of rejection for organic solutes in the SWW was $C_6H_{12}O_6$ > $C_8H_8O_3$ > C_2H_6O. Table 4.7 illustrates the physico-chemical properties of the SWW components. Figure 4.11 illustrates the pH of the SWW FS for the CTA, ABM_A01 and ABM_A02 membranes. It was observed that the pH of the SWW FS for the CTA and ABM_A02 membranes were well above the pK_a for CH_3COOH and $C_7H_6O_5$, resulting in high rejection of the feed solutes despite being weak electrolytes. The opposite was evident for the ABM_A01 membrane: in addition to its being a weak electrolyte, the pH of the SWW FS fell below the pK_a of CH_3COOH, resulting in low rejection and allowing the permeation of CH_3COOH solutes. This negatively affected the FO process, resulting in lower experimental J_w.

Table 4.7: Physico-chemical properties of SWW components

Compound	**Chemical formula**	**M_w (g.mol^{-1})**	**pK_a at 25^{0}C**	**Reference**
Acetic acid	CH_3COOH	60.05	4.76	(Perrin *et al*., 1981)
Gallic acid	$C_7H_6O_5$	170.12	4.41	(Perrin *et al*., 1981)
Glucose	$C_6H_{12}O_6$	180.16	n.a	-
Vanillin	$C_8H_8O_3$	152.15	n.a	-
Ethanol	C_2H_6O	46.07	n.a	-

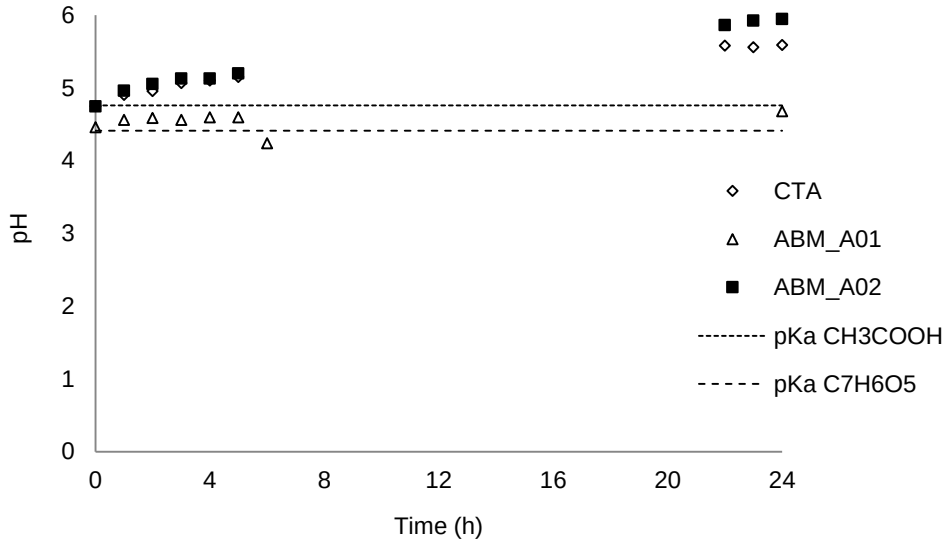

Figure 4.11: pH curve for DS 1 M KCl and FS SWW for the CTA, ABM_01 and ABM_A02 membranes

The experimental J_w of 6.77 $L.m^{-2}.h^{-1}$ generated with the CTA membrane when SWW was used as FS compared well with the experimental J_w of 8.38 and 7.23 $L.m^{-2}.h^{-1}$ generated when DI water and BW5 were used as FSs, respectively. The CTA membrane generated an experimental J_w 6% less than that of the experimental J_w generated when BW5 was used as a FS. An initial flux decline of 20 and 34% after a one h filtration period was experienced for the CTA and ABM_A02 membranes, respectively. Unlike the CTA and ABM_A02 membranes, the ABM_A01 membrane experienced an experimental J_w increase of 5% after one h of operation. After a 24 h filtration period, flux decline was 47, 46 and 68% for the CTA, ABM_A01 and ABM_A02 membranes, respectively. Membrane flux recovery after simple cleaning was 89, 76 and 84% for the CTA, ABM_A01 and ABM_A02 membranes, respectively. Water recovery rates after a 24 h filtration period were 45, 32 and 56% for the CTA, ABM_A01 and ABM_A02 membranes. Figure 4.12 illustrates the SEMs of the used CTA, ABM_A01 and ABM_A02 membranes.

SEM images for the used (KCl: SWW) CTA, ABM_A01 and ABM_A02 membranes illustrate salt concentrations (KCl) in the membrane support layers. Significant salt concentrates can be seen in the support layer of the ABM_A01 membrane. The increased salt concentration in the ABM_A01 support layer corroborates the low experimental J_w recorded when SWW was used as a FS. The reverse diffusion of draw solutes (KCl) lowers the OP of the DS, which in turn reduces the bulk $\Delta\pi$ of the FO system. Salt concentrations in the support layer of the ABM_A02 membrane appear to be less severe when compared to the salt concentrations observed in the support layer when BW5 was used as a FS.

CTA

a) b) c)

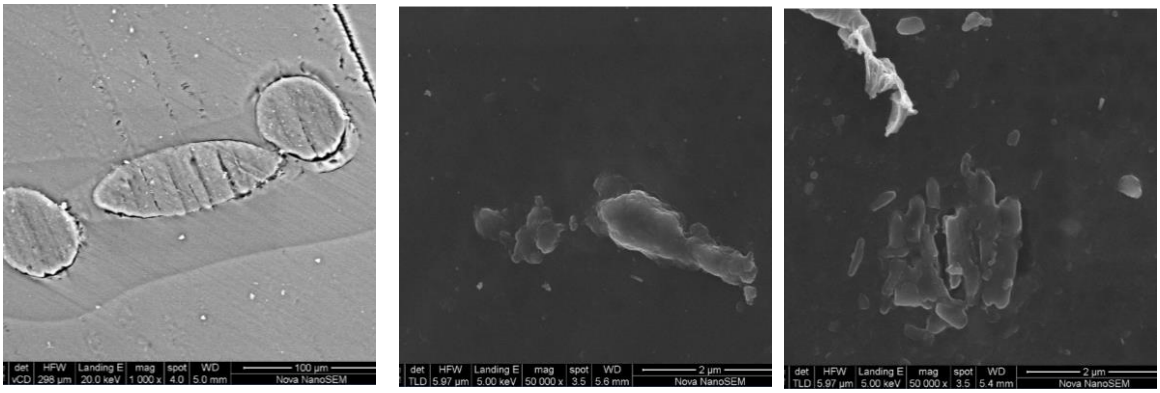

ABM_A01

a) b) c)

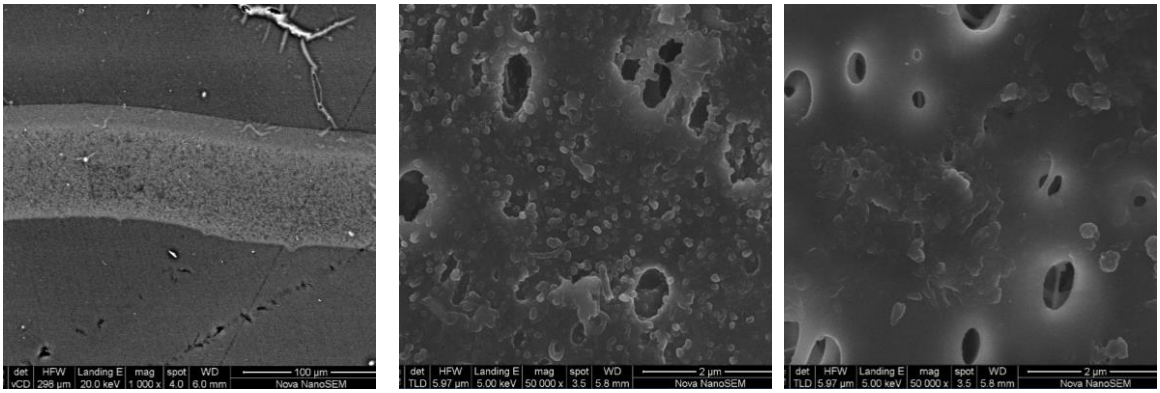

ABM_A02

a) b) c)

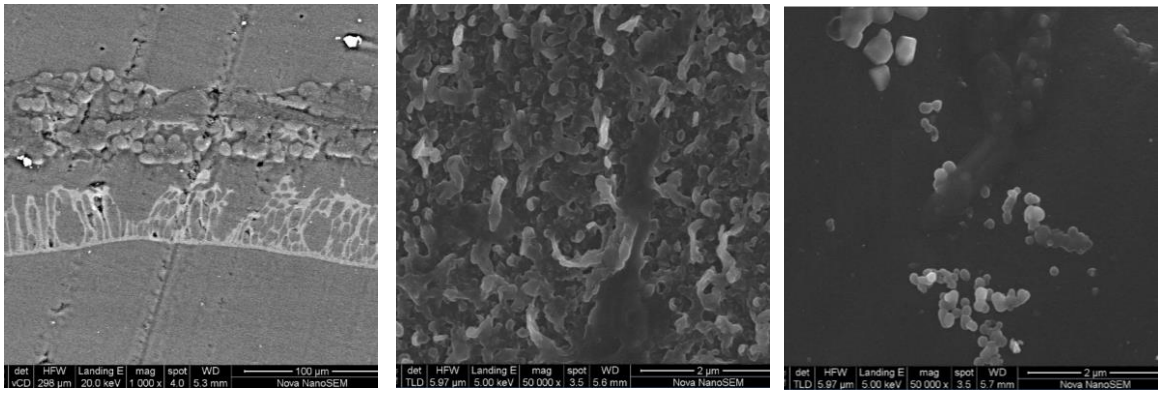

Figure 4.12: KCl & SWW: (a) cross section, (b) active layer and (c) support layer [magnification (a) 100 µm x 1000 and (b and c) 2 µm x 50 000]

The results from the FDFO experiments with a 1 M KCl fertiliser DS, and FSs of DI water, BW5 and SWW, demonstrated that the ABM_A02 membrane was superior for the reclamation of water, with the purpose of reducing the final nutrient concentration for direct fertigation using a single fertiliser 1 M KCl DS. Despite generating a low

experimental J_w of 4.33 $L.m^{-2}.h^{-1}$ with FS BW5, the ABM_A02 membrane generated higher experimental J_w than the commercial CTA membrane and the ABM_A01 membrane. It can be assumed that the performance of the ABM_A02 membrane in terms of experimental J_w was limited with regard to feed waters containing strong electrolytic species. Membrane flux recovery after periodic rinses was consistent at 84% for the ABM_A02 membrane. Water recovery rates for the CTA and ABM_A01 membranes were consistent at 43 and 34%. An average water recovery rate of 52% was observed for the ABM_A02 membrane.

Results obtained from the FDFO experiments with the CTA membrane compare well with fluxes previously reported in literature. Phuntsho (2012) achieved experimental J_w of 9.83 and 8.73 $L.m^{-2}.h^{-1}$ when a 1 M KCl fertiliser DS was used with FSs DI water and BW5, respectively. A variation of 16% was observed for the experimental J_w achieved for this FDFO study.

It needs to be noted that batch ABM_A01 membranes were not evaluated for comparative studies with a N/P/K fertiliser DS.

4.5.1.4. Draw solution (DS) N/P/K blend and feed solution (FS) deionised (DI) water

Target concentrations for N/P/K fertigation in the Boland (Cape Winelands) region of SA vary according to the individual fertilisers that make up the N/P/K blended fertiliser solution. The N/P/K blended fertiliser DS used in the FDFO desalination study comprised $CO(NH_2)_2$, H_3PO_4 and KCl blended in molar concentrations of 2/0.15/1 M, respectively. As stated earlier under Section 4.5.1.1, the DS should be able to extract water across the semi-permeable membrane until OE occurs. Thus, diluting the N/P/K fertiliser solution from molar concentrations of 2/0.15/1 M to 1.57/0.1/0.69 M resulted in an OP of 6 944 kPa. Figure 4.13 illustrates the OP of the N/P/K blended fertiliser DS over 24 h. The target concentration for N/P/K fertigation was achieved at hours 7.07 and 8.96 for the CTA and ABM_A02 membranes, respectively.

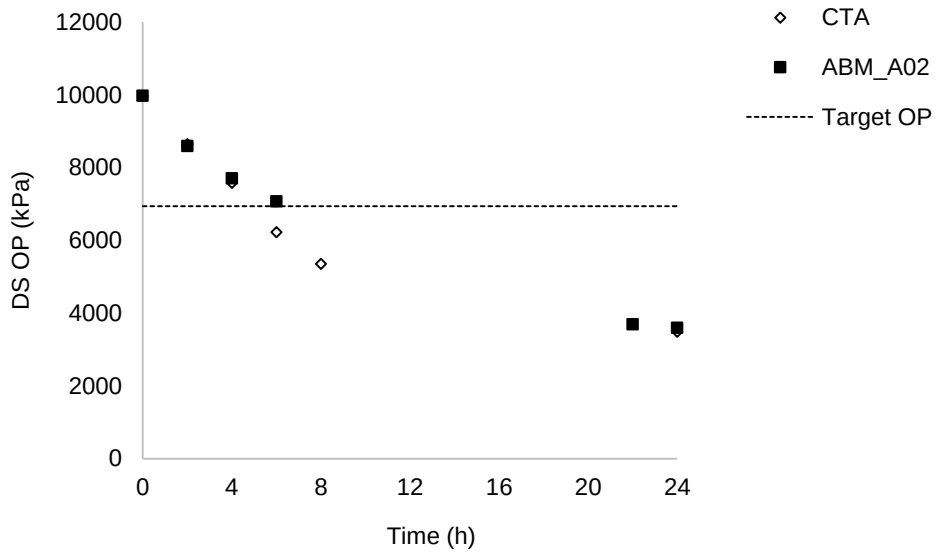

Figure 4.13: DS OP and targeted OP for N/P/K fertigation with FS DI water over 24 h

Table 4.6 illustrates the experimental J_w at various times for the CTA and ABM_A02 membranes with N/P/K blended fertiliser DS and DI water as the controlled FS. Of the two FO membranes, the CTA membrane generated the higher experimental J_w: its experimental J_w of 15.54 $L.m^{-2}.h^{-1}$ was 25% greater than the experimental J_w of 11.62 $L.m^{-2}.h^{-1}$ observed for the ABM_A02 membrane. The driving force in the FO process is the bulk Δπ across the FO membrane. The bulk Δπ of 9 978 kPa when using a N/P/K blended fertiliser DS was double that of the bulk Δπ of 4 668 kPa when a 1 M KCl fertiliser solution was used as a DS. The experimental J_w of 15.54 $L.m^{-2}.h^{-1}$ observed for the CTA membrane was 46% greater than the experimental J_w of 8.38 $L.m^{-2}.h^{-1}$ observed when using a 1 M KCl fertiliser DS. This increase in the experimental J_w for the CTA membrane was corroborated by the comparative increase in the bulk Δπ of the FO system. However, despite the significant difference in bulk Δπ, the ABM_A02 membrane generated an experimental J_w 18% lower than the experimental J_w generated with a 1 M KCl DS. This low experimental J_w recorded for the ABM_A02 membrane may have been the result of dilutive internal concentration polarization (ICP). As water is permeated though the active layer from the DI FS and dilutes the DS at the interface between the active layer and the porous membrane support layer, the driving force for water permeation decreases. Mass transfer resistance at the interface may be attributed to the dilution of DS with the simultaneous reverse diffusion of draw solutes from the bulk DS. The effects of ICP have been attributed to thick and hydrophobic support layers. Support layer properties are crucial in minimising the effects of ICP. Table 3.5 (see Chapter 3, Section 3.4) illustrates the membrane thickness (structural parameter (S)) of the CTA and ABM (ABM_A01 and ABM_A02) membranes in micrometers (µm). The ABM membrane has a S of 110 $\pm$ 5 µm, 15% thicker than that of the CTA membrane with a S

of only 93 $\pm$ 3 µm. The variation in membrane thickness for the CTA and ABM_A02 membranes suggests that the low experimental J_w observed for the ABM_A02 membrane was the result of dilutive ICP caused by the thick support layer.

An initial flux decline of 20 and 14% was experienced for the CTA and ABM_A02 membranes, respectively, after a one h filtration period. After a 24 h filtration period, the experimental J_w had declined 53 and 58% for the CTA and ABM_A02 membranes, respectively. After simple membrane cleaning, the CTA and ABM_A02 membranes achieved membrane flux recoveries of 69 and 85%, respectively. Despite generating an experimental J_w 25% lower than that of the CTA membrane, the ABM_A02 membrane displayed gradual flux decline rates and greater membrane flux recovery. Water recovery rates for the CTA and ABM_A02 membranes were 69 and 68%, respectively. Figure 4.14 illustrates the SEMs of the used CTA and ABM_A02 membranes. SEM images of the used (N/P/K: DI water) CTA and ABM_A02 membranes illustrates minimal salt concentration (N/P/K – $CO(NH_2)_2/H_3PO_4/KCl$) in the support layer. Salt concentration in the membrane active layer for the CTA and ABM_A02 membranes is evident but minimal.

CTA

a) b) c)

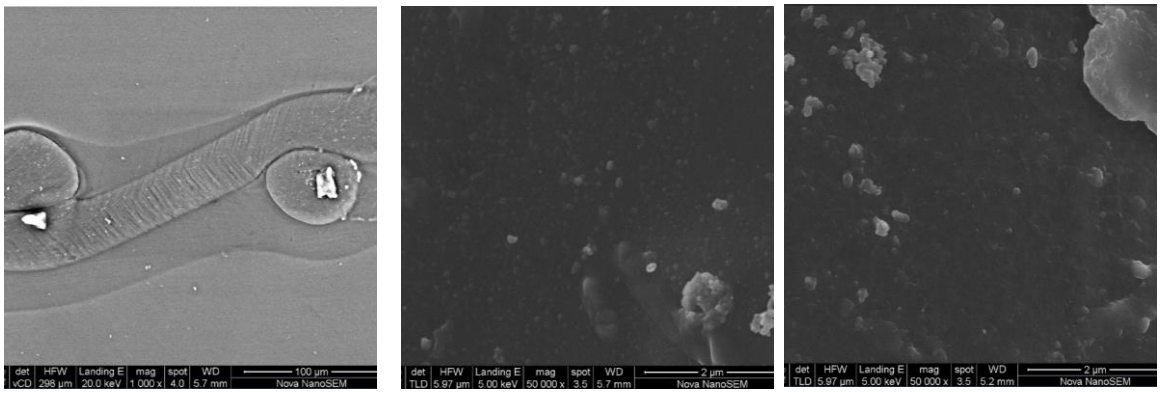

ABM_A02

a) b) c)

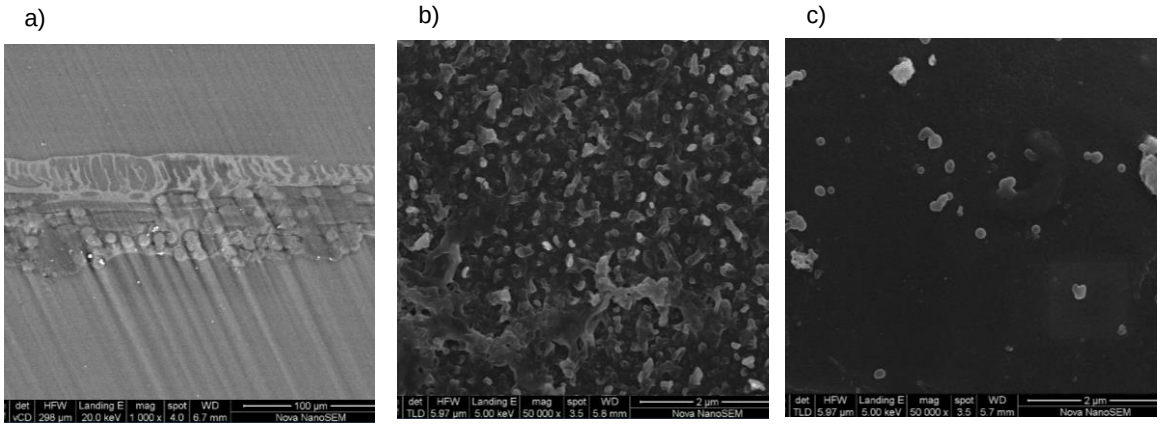

Figure 4.14: N/P/K & DI water: (a) cross section, (b) active layer and (c) support layer [magnification (a) 100 µm x 1000 and (b and c) 2 µm x 50 000]

4.5.1.5. Draw solution (DS) N/P/K blend and feed solution (FS) synthetic brackish water (BW5)

Figure 4.15 illustrates the OP of the N/P/K blended fertiliser DS over 24 h. As indicated above in Section 4.5.1.4, an N/P/K blended fertiliser DS with molar concentration 2/0.15/1 M was used in the FDFO desalination study. An N/P/K blended fertiliser DS with increased molar concentrations was used as a DS, with the objective of reducing the concentration of N/P/K nutrients to molar concentrations of 1.57/0.1/0.69 M in the final product water from the FDFO process. The times taken to achieve the target concentration for N/P/K fertigation for the CTA and ABM_A02 membranes were 12.61 and 10.94 h, respectively.

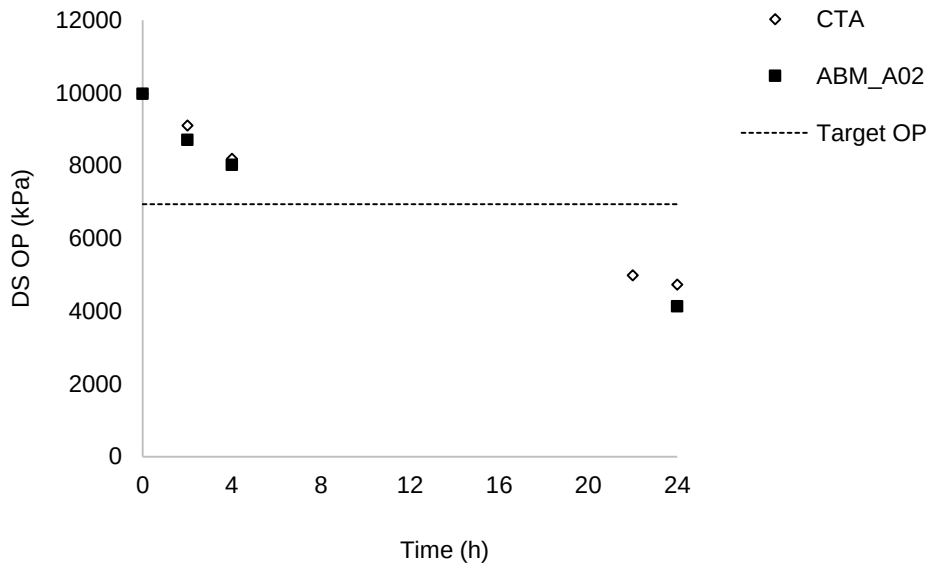

Figure 4.15: DS OP and targeted OP for N/P/K fertigation with FS BW5 over 24 h

Table 4.6 illustrates the bulk Δπ with experimental J_w for the CTA and ABM_A02 membranes, with a N/P/K blended fertiliser DS and BW5 as FS. Similarly, to the experimental J_w of 4.33 $L.m^{-2}.h^{-1}$ observed for the ABM_A02 membrane when a 1 M KCl fertiliser DS with BW5 FS was used, a lower experimental J_w was expected when an N/P/K blended fertiliser DS with BW5 FS was used. The lower experimental J_w observed was the result of the need for the FO process to overcome the additional OP of the BW5 FS (BW5 – 414 kPa). A vast difference was observed for the experimental J_w generated with the ABM_A02 membrane when BW5 was used as a FS with varying fertiliser DSs (1 M KCl and N/P/K blend). The ABM_A02 membrane generated an experimental J_w of 11.31 $L.m^{-2}.h^{-1}$, 62% greater than the experimental J_w observed with a 1 M KCl fertiliser DS. The increased experimental J_w observed when an N/P/K blended fertiliser was used as a DS was the result of the increased bulk Δπ: The N/P/K fertiliser solution generated an OP of 9 978 kPa, double that generated with a 1 M KCl fertiliser DS. An increase in DS OP was imperative for overcoming the additional OP of the FS (BW5), thus generating high fluxes. The CTA membrane, which had generated an experimental J_w much greater than the ABM_A02 membrane when DI water was used as a controlled FS, generated an experimental J_w of 7.85 $L.m^{-2}.h^{-1}$, 31% lower than the experimental J_w observed for the ABM_A02 membrane. The experimental J_w observed for the CTA membrane was comparable with the experimental J_w of 7.23 $L.m^{-2}.h^{-1}$ generated with a 1 M KCl fertiliser DS, despite the significant difference in bulk Δπ.

Initial flux decline of 18 and 15% was experienced for the CTA and ABM_A02 membranes after a one h filtration period. After a 24 h filtration period, the experimental J_w of the CTA and ABM_A02 membranes had decreased by 51 and 44%, respectively.

Membrane flux recoveries after simple cleaning were 71 and 83% for the CTA and ABM_A02 membranes, respectively. Water recovery rates for the CTA and ABM_A02 membranes for a filtration period of 24 h was 51 and 55%, respectively. Despite generating a comparatively superior flux to the CTA membrane, the ABM_A02 membrane only managed to achieve a 4% increased water extraction capacity. Figure 4.16 illustrates the SEMs of the used CTA and ABM_A02 membranes.

SEM images of the used (N/P/K: BW5) CTA and ABM_A02 membranes illustrate salt concentration (N/P/K – $CO(NH_2)_2/H_3PO_4/KCl$) clusters in the support layer. Salt concentrations seen in the support layer of the CTA and ABM_A02 membranes appear to be more significant for FS, BW5 than for FS, DI water. Salt concentrations (NaCl) are also apparent in the active layer of the CTA membrane.

CTA

a) b) c)

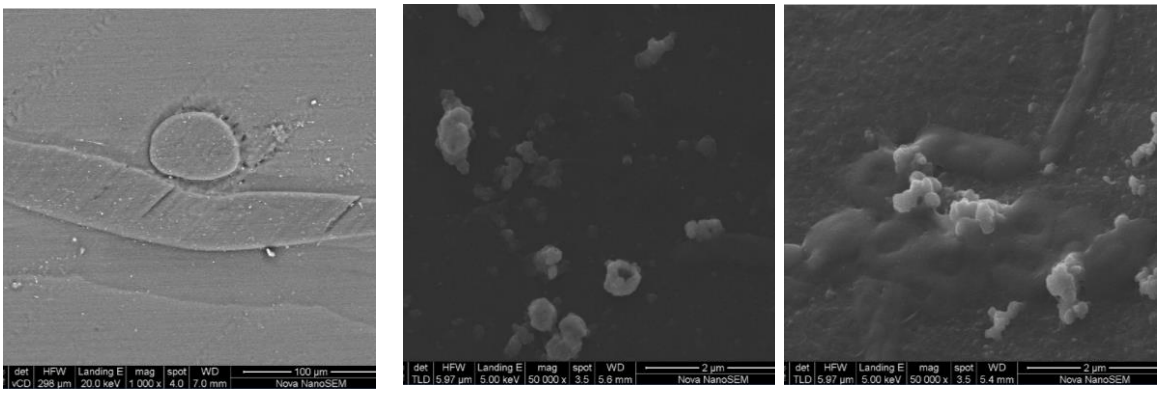

ABM_A02

a) b) c)

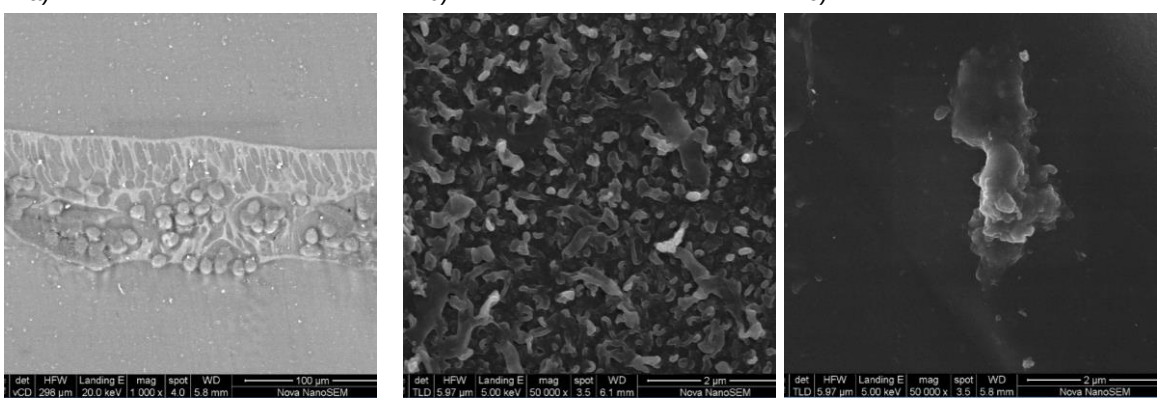

Figure 4.16: N/P/K & BW5: (a) cross section, (b) active layer and (c) support layer [magnification (a) 100 µm x 1000 and (b and c) 2 µm x 50 000]

4.5.1.6. Draw solution (DS) N/P/K blend and feed solution (FS) synthetic winery wastewater (SWW)

Targeted molar concentrations for N/P/K fertigation were selected as 1.57/0.1/0.69 M. Data extrapolated from Figure 4.17 was used to determine the time at which the target concentration OP of 6 944 kPa was achieved. Target concentrations for N/P/K fertigation were achieved at 12.13 and 11.81 h for the CTA and ABM_A02 membranes.

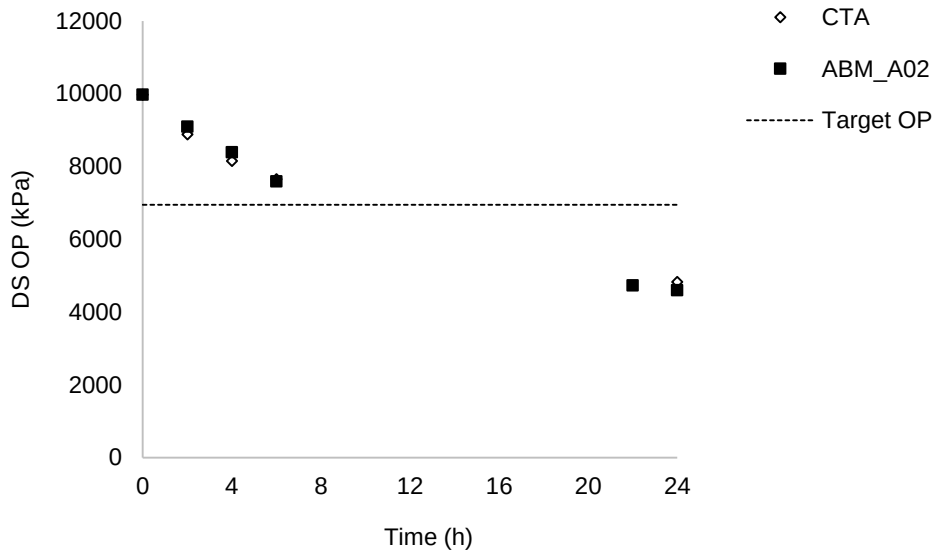

Figure 4.17: DS OP and targeted OP for N/P/K fertigation with FS SWW over 24 h

Table 4.6 illustrates the experimental J_w at various times for the CTA and ABM_A02 membranes with N/P/K blended fertiliser DS and SWW FS. The experimental J_w values observed for the CTA and ABM_A02 membranes were comparable at 8.8 and 8.86 $L.m^{-2}.h^{-1}$, respectively. When considering solution diffusion theory and the proportionality of the experimental J_w to the bulk $\Delta\pi$ of the two independent solutions (FS and DS), it was observed that the CTA membrane generated an experimental J_w 11% greater than the experimental J_w of 7.85 $L.m^{-2}.h^{-1}$ generated when BW5 was used as a FS. However, the experimental J_w observed for the ABM_A02 membrane was not proportional to the bulk $\Delta\pi$ of the two independent solutions. Despite generating a bulk $\Delta\pi$ of 9 917 kPa when SWW was used as a FS, the resultant experimental J_w for the ABM_A02 membrane was 22% less than the experimental J_w of 11.31 $L.m^{-2}.h^{-1}$ generated when BW5 was used as a FS with a bulk $\Delta\pi$ of 9 564 kPa.

As stated earlier under Section 4.5.1.3, the SWW used in this study was made up of weak acids (CH_3COOH and $C_7H_6O_5$) and organic solutes ($C_6H_{12}O_6$, $C_8H_8O_3$ and C_2H_6O). The rejection of weak acids is said to be highly pH dependent (Rautenbach & Albrecht, 1989). For strong electrolytic acids, rejection is high but for weak electrolytic acids,

rejection is low but at pHs above the pK_a rejection rises significantly. Figure 4.18 illustrates the pH curve of the SWW FS for the CTA and ABM_A02 membranes. From Figure 4.18 it is evident that the pH of the SWW FS surpassed the pK_a for both weak acids, CH_3COOH and $C_7H_6O_5$, resulting in high rejection. The pH of a solution is determined by the effect of hydrogen ions (H^+) and hydroxyl ions (OH^{-1}). Greater H^+ concentrations lower the pH (acidic) and greater OH^{-1} concentrations increase the pH (alkaline). Section 4.6.1.4 elaborated on the effects of dilutive ICP that may have affected the performance of the ABM_A02 membrane due to the thick support layer. Dilutive ICP results in the reverse diffusion of draw solutes across the semi permeable membranes. $CO(NH_2)_2$, which is found at elevated concentrations in the N/P/K blended fertiliser DS, increases the measured pH of aqueous solutions (Bull *et al*., 1964). Bull *et al.* (1964) postulate that $CO(NH_2)_2$ at high concentrations (2 M) drastically reduces the activity of H^+ ions, thus leaving the activities of the other ions more or less charged. The increased pH of the SWW FS for the ABM_A02 membrane may be corroborated by the effects of dilutive ICP and the effect of $CO(NH_2)_2$ on the measured pH of SWW solution.

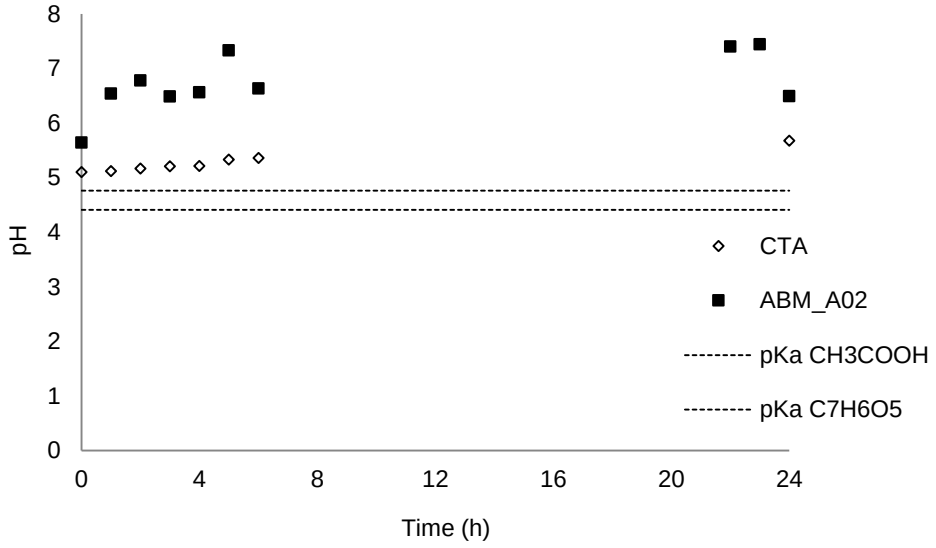

Figure 4.18: pH curve for N/P/K blended fertiliser DS and FS SWW over 24 h

An initial experimental J_w decline of 21% and 16% was observed after a one h filtration period for the CTA and ABM_A02 membranes, respectively. Despite having a lower initial experimental J_w decline, the ABM_A02 membrane had an overall flux decline of 53%, 10% more than the CTA membrane. Water recovery rates for the CTA and ABM_A02 membranes over a 24 h filtration period were 51 and 55%, respectively. Figure 4.19 illustrates the SEMs of the CTA and ABM_A02 membranes.

SEM images of the (N/P/K: SWW) CTA membrane indicate minimal salt concentration in the membrane's active and support layers. Salt concentration in the active layer of the

CTA and ABM_A02 membranes is attributed to the permeation of weak acids (CH_3COOH and $C_7H_6O_5$) and organic solutes ($C_6H_{12}O_6$, $C_8H_8O_3$ and C_2H_6O) found in the SWW. Salt concentration in the membrane support layer is attributed to reverse permeation of the $CO(NH_2)_2$, H_3PO_4 and KCl straight fertilisers used to make up the N/P/K blend.

CTA

a) b) c)

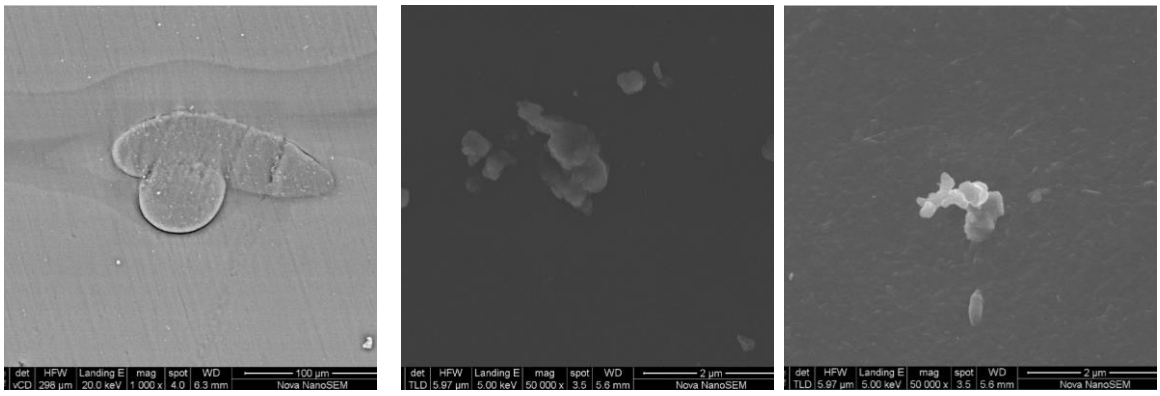

ABM_A02

a) b) c)

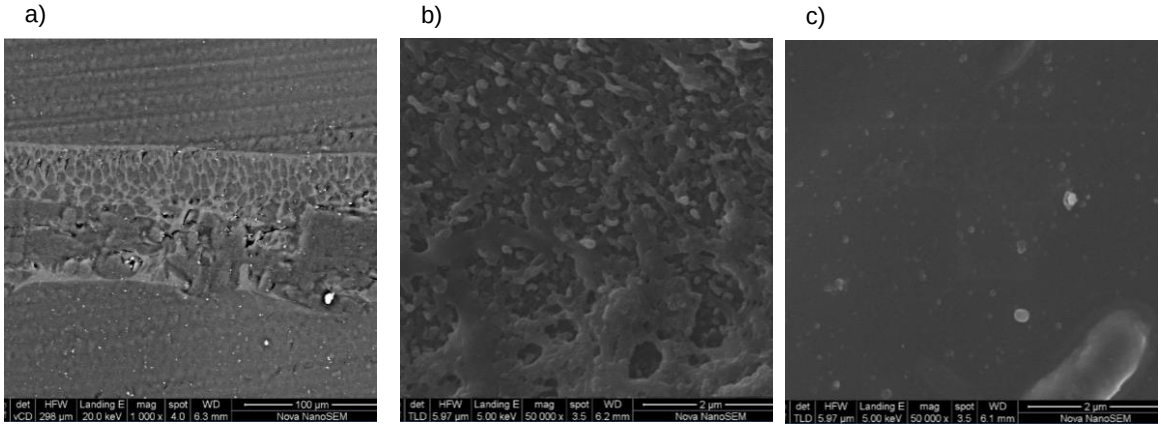

Figure 4.19: N/P/K & SWW: (a) cross section, (b) active layer and (c) support layer [magnification (a) 100 µm x 1000 and (b and c) 2 µm x 50 000]

The results of the FDFO experiments with N/P/K blended fertiliser DS and FSs; DI water, BW5 and SWW, demonstrated that despite an initial bulk Δπ of 9 978 kPa, two times greater than the bulk Δπ of 4 668 kPa generated by a 1 M KCl fertiliser DS, the N/P/K blended fertiliser DS generated initial experimental J_w less than the 1 M KCl fertiliser DS with FSs, DI water and SWW for the ABM_A02 membrane. A substantial increase in the experimental J_w was only observed for the CTA membrane with FS DI water, and for the ABM_A02 membrane with FS BW5. The poor performance of the N/P/K blended fertiliser DS in terms of experimental J_w may be attributed to the high concentration of $CO(NH_2)_2$. Despite $CO(NH_2)_2$ being highly soluble in water, it is a weak electrolyte and does not

dissociate to form any charged species in water. As such the OP of 4 923 kPa at 2 M for $CO(NH_2)_2$ was significantly lower than that of the less soluble KCl fertiliser (9 027 kPa at 2 M). $CO(NH_2)_2$ in a solution has a tendency to self-aggregation due to the hydrophobic effect, with $CO(NH_2)_2$ - $CO(NH_2)_2$ associations increasing at increased concentrations. The ABM_A02 membrane once again proved to be superior for the reclamation of water with the purpose of reducing the final nutrient concentration from 2/0.15/1 M (initial N/P/K blended fertiliser DS) to 1.57/0.1/0.69 M (final product water DS) for direct N/P/K fertigation. The ABM_A02 membrane generated increased experimental J_w in comparison to the commercial CTA membrane, with the exception of when DI water was used as a controlled FS. Membrane flux recovery for the ABM_02 membrane was consistent, ranging from 80 to 85%. Water recovery rates for the FO membranes varied by a mere 7%, with the CTA membrane extracting an average of 638 mL of water and the ABM_02 membrane extracting an average of 684 mL of water.

4.5.2. Comparison of forward osmosis (FO) membrane performance: Reverse solute flux (J_s)

Reverse solute flux (J_s) in FO technology is inevitable. The phenomenon increases operational costs and decreases the FO driving force. When the membrane is in the FO mode (FS-AL), draw solutes which diffuse from the DS into the porous support layer result in intensified cake layer OP within the fouling layer of the membrane and elevated OPs at the membrane boundary layer. The average J_s over 24 h for the CTA, ABM_A01 and ABM_A02 membranes using 1 M KCl fertiliser DS and DI feed water was 0.94, 36.18 and 6.72 $g.m^{-2}.h^{-1}$, respectively. The average J_s at the respective target concentration time for the CTA, ABM_A01 and ABM_A02 membranes was 0.99, 32.99 and 7.83 $g.m^{-2}.h^{-1}$. As expected the CTA membrane exhibited a significantly low J_s due to its high solute rejection properties. Special advantages of the CTA membrane include excellent chlorine tolerance. In order to maintain electro neutrality, the cation (K^+) from the dissociated KCl moves to the feed solution via reverse permeation. The ABMs (ABM_A01 and ABM_A02) used in this study form part of the second and third generation Aquaporin Inside^{TM} Membranes developed in Singapore under a research collaboration between the Singapore Membrane Technology Centre (SMTC) under the NEWRI Institute of Nanyang Technological University, DHI Singapore, and Aquaporin A/S (Denmark). Second and third generation ABMs were received from Aquaporin A/S in June 2016 and July 2017, respectively. Data sheets characterising second and third generation ABM by high J_w and low J_s was summarised in Tale 3.5, Chapter 3. Standard testing solutions comprised of DI water FS and 1 M NaCl DS. The increased J_s experienced for the ABM_A01 membrane may be attributed to a deterioration in

membrane performance after the considerable storage time of approximately 1 year which exceeded the 6 month shelf life for second generation ABM. Discrepancies in J_s recorded for the FDFO filtration experiments may be attributed different solution properties of the fertiliser draw solutes in comparison with the 1 M NaCl DS. Ongoing developments in membrane preparation were successful in producing the next generation Aquaporin Inside™ Membranes, Singh *et al.* (2018) conducted a study for the concentration of molasses distillery wastewater using a ABM FO membrane, and reported J_s for the study that was significantly low at 0.36 $g.m^{-2}.h^{-1}$. This part of the study will be redone with new ABMs and be reported in a subsequent study.

Reverse permeation of the fertiliser draw solutes, 1 M KCl and blended N/P/K using BW5 and SWW as FSs were determined from conductivity measurements of the feed waters at the start and end of each filtration, as shown in Table 4.8. Achilli *et al.* (2010) postulated a correlation between reverse permeation of draw solutes and DS concentration, suggesting that the reverse diffusion of draw solutes decreases with decreasing DS concentration. When considering the two DSs, 1 M KCl and blended N/P/K in a 2/0.15/1 molar ratio, reverse permeation for the N/P/K blended fertiliser DS with a combined molar concentration of 3.15 M was considerably higher for the CTA and ABM_A02 membranes. This corroborates the notion that DS concentration has a significant effect on the reverse diffusion of draw solutes. Achilli *et al.* (2010) and Perry *et al.* (2015) concluded that DSs containing divalent ions with comparatively larger sized hydrated ions are less susceptible to reverse permeation when compared to monovalent ions with comparatively smaller hydrated diameters. Both Achilli *et al.* (2010) and Perry *et al.* (2015) suggest that reverse permeation of the draw solutes is affected by the properties of both the anion and cation. When considering the blended fertiliser DS (N/P/K) made up of straight fertilisers, $CO(NH_2)_2$, H_3PO_4 and KCl, H_3PO_4 in the N/P/K blended fertiliser DS dissociates to form H^+ cations and $H_2PO_4^-$ anions. The $H_2PO_4^-$ anion with a large hydrated size cannot diffuse though the negatively charged CTA and ABM_A02 membranes. However, in order to maintain electrical neutrality, smaller cations (H^+) will naturally diffuse back to the DS. For KCl, the J_s of K^+ cations were associated with the diffusion of Cl^- anions since the hydrated diameter of the Cl^- anion is comparatively smaller than that of the $H_2PO_4^-$ anion. When in an aqueous solution, $CO(NH_2)_2$ remains uncharged, resulting in high reverse permeation. Neutral draw solutes ($CO(NH_2)_2$) are not as effectively rejected by the membrane support layer when compared to strong electrolytic species (Phuntsho, 2012; Yong *et al*., 2012). The weak rejection of neutral draw solutes ($CO(NH_2)_2$) results in the rapid permeation of $CO(NH_2)_2$ though the membrane support layer, and in turn may result in ECP on the feed side of

the membrane (active layer). Severe ECP results in a decrease of the bulk Δπ across the FO system while also impeding the permeation of water across the FO membrane.

Table 4.8: Conductivity measurements of the alternative feed water resources with, 1 M KCl and blended N/P/K as DSs before and after 24 h

FO membranes	Conductivity	
	Before filtration (mS.cm^{-1})	After filtration (mS.cm^{-1})
1 M KCl : BW5		
CTA	9.88	11.65
ABM_A01	9.88	16.04
ABM_A02	9.88	11.79
1 M KCl : SWW		
CTA	0.206	0.33
ABM_A01	0.206	1.41
ABM_A02	0.206	1.40
N/P/K blend: DI		
CTA	0.005	0.4
ABM_A02	0.005	3.41
N/P/K blend: BW5		
CTA	9.88	13.32
ABM_A02	9.88	16.69
N/P/K blend: SWW		
CTA	0.206	0.44
ABM_A02	0.206	1.57

4.5.2.1. Loss of nutrients

In the FDFO study, the reverse diffusion of fertiliser draw solutes not only results in the reduction of the FO driving force, but may reduce the amount of essential nutrients in the final product water for direct fertigation. J_s studies of draw solutes in previously reported research are typically done in terms of specific reverse solute flux (SRSF). However, the amount of macro-nutrients in the final product water is critical for direct fertigation. J_s for the FDFO experiments are presented in terms of the loss of macro-nutrients (N/P/K) in g.L^{-1} to feed waters and the final macronutrient concentration in the final product water. Tables 4.9 and 4.10 illustrate the reverse permeation of the straight and blended fertiliser solutes as well as the final nutrient concentration in the final product water for FSs DI water, BW5 and SWW.

It is evident from Table 4.9 that for the straight fertiliser DS, 1 M KCl (single nutrient – K) the final nutrient concentration was dependent on the type of feed water used. When

FSs, BW5 and SWW were used, with total dissolved solids (TDS) of 6 823 and 120 mg.L^{-1}, respectively, a proportional increase in the final nutrient concentration of the product water was observed. A similar correlation was not observed for the blended N/P/K fertiliser DS when total nitrogen (N) was determined though empirical means (see Appendix F). However, the theoretically determined total N illustrated a proportional increase in the final N concentration with increased TDS in feed water. Figure 4.20 compares proportional N concentration with varying feed waters determined empirically and theoretically.

Table 4.9: Final N/P/K concentration and loss of N/P/K by reverse permeation in $g.L^{-1}$ for single fertiliser DS, 1 M KCl. N/P/K concentrations determined though theoretical calculations

FDFO experiments	DS (KCl) : FS (DI water)			DS (KCl) : FS (BW5)			DS (KCl) : FS (SWW)		
	CTA	ABM_A01	ABM_A02	CTA	ABM_A01	ABM_A02	CTA	ABM_A01	ABM_A02
N/P/K loss by RSF ($g.L^{-1}$)	0/0/18.43	0/0/12.79	0/0/27.54	0/0/17.5	0/0/11.36	0/0/11.85	0/0/19.9	0/0/9.79	0/0/25.12
N/P/K concentration in final product ($mg.L^{-1}$)	0/0/26.31	0/0/31.95	0/0/17.20	0/0/27.27	0/0/33.38	0/0/32.89	0/0/24.85	0/0/34.95	0/0/19.62

Table 4.10: Final N/P/K concentration and loss of N/P/K by reverse permeation in $g.L^{-1}$ for blended fertiliser DS, N/P/K. N/P/K concentrations determined though theoretical calculations and empirical methods

FDFO experiments	DS (N/P/K) : FS (DI water)		DS (N/P/K) : FS (BW5)		DS (N/P/K) : FS (SWW)	
	CTA	ABM_A02	CTA	ABM_A02	CTA	ABM_A02
N/P/K loss by RSF ($g.L^{-1}$)	1.82/0.0017/6.16	1.22/0.0047/6.05	1.83/0.0032/0.23	1.1/0.0084/3.73	2.1/0.0028/0.44	0.77/0.0042/1.85
N/P/K concentration in final product ($g.L^{-1}$)	24.6/0.94/16.21	20.21/0.87/16.32	21.02/0.93/22.14	20.58/0.96/18.64	20.83/1.08/21.93	26.23/0.53/20.52

Table 4.11: Final N/P/K concentration and loss of N/P/K by reverse permeation in $g.L^{-1}$ for blended fertiliser DS, N/P/K. N/P/K concentrations determined though theoretical calculations

FDFO experiments	DS (N/P/K) : FS (DI water)		DS (N/P/K) : FS (BW5)		DS (N/P/K) : FS (SWW)	
	CTA	ABM_A02	CTA	ABM_A02	CTA	ABM_A02
N/P/K loss by RSF ($g.L^{-1}$)	35.24/2.53/28.53	32.09/2.52/28.42	27.91/2/22.6	32.24/2.31/26.1	28.17/2.02/22.81	29.91/2.15/24.22
N/P/K concentration in final product ($g.L^{-1}$)	20.02/1.43/16.21	20.17/1.44/16.32	27.35/1.96/22.14	23.02/1.65/18.64	27.09/1.94/21.93	25.35/1.81/20.52

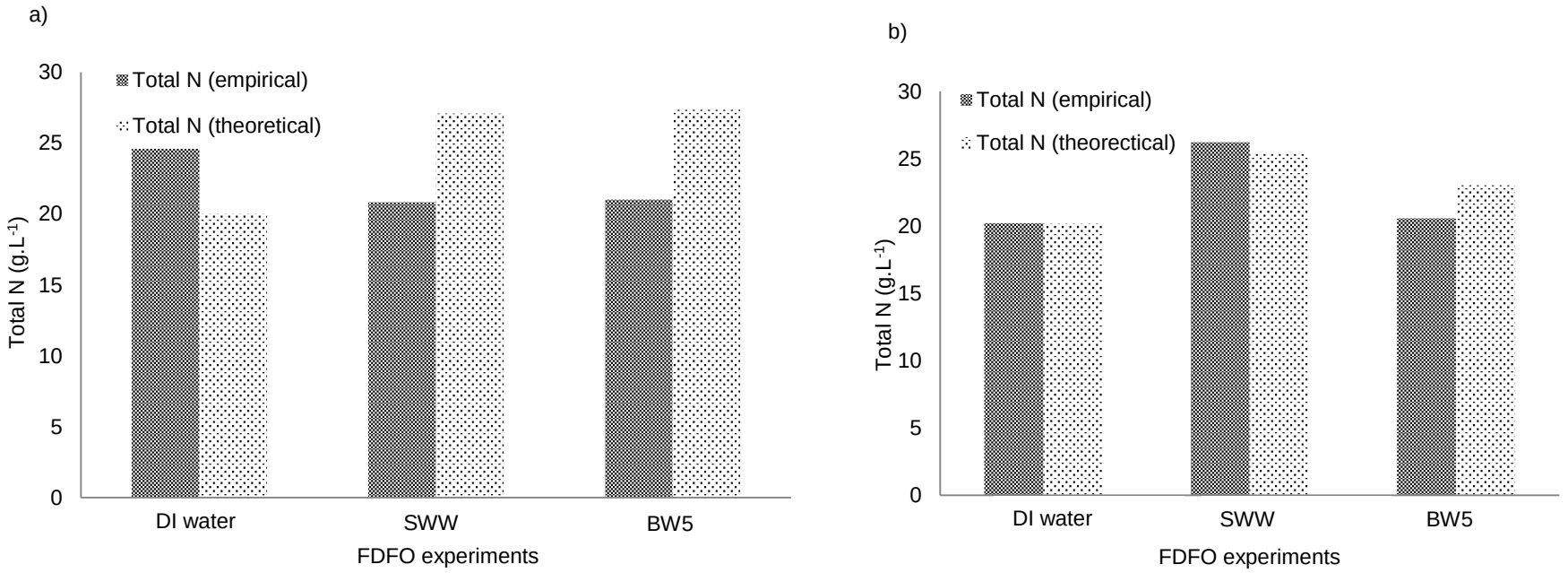

Figure 4.20: Comparison of the empirical and theoretical total N for the (a) CTA and (b) ABM_A02 membranes in the final product water with varying TDS feed water, DI water; BW5 and SWW

CHAPTER FIVE
CONCLUSION AND RECOMMENDATIONS

5.1. Conclusions

This study evaluated the performance and compatibility of forward osmosis (FO) membranes cellulose triacetate (CTA) and aquaporin biomimetic membrane (ABM), with fertilisers for direct fertigation commonly employed within the South African (SA) wine industry, using a fertiliser drawn forward osmosis (FDFO) system.

Alternative feed solutions (FSs) were evaluated for their potential in the FDFO desalination process. Osmotic pressure (OP) generated for the alternative FSs suggested that the total dissolved solids (TDS) concentration had a pronounced effect on the OP generated for alterative FSs. OP is a colligative property and is dependent on the number of dissolved particles in a solution, not the identity of the particles. The measured OP of FSs, DI water, synthetic winery wastewater (SWW) and synthetic brackish water (BW5) was 0, 61 and 414 kPa, respectively. Seawater (SW) samples from the Atlantic Ocean seaboard (AOSB) with an average TDS concentration of 30 617 $mg.L^{-1}$ (20 021 NaCl $mg.L^{-1}$), generated an OP of 2 574 kPa, while SW samples from the Indian Ocean seaboard (IOSB) with an average TDS concentration of 29 933 $mg.L^{-1}$ (20 986 NaCl $mg.L^{-1}$), generated an OP of 2 510 kPa.

Six different straight inorganic fertilisers were evaluated as potential draw solutions (DSs) for the FDFO desalination study. It was observed that all soluble fertilisers generated an OP, thus making them suitable DSs when their respective OP generated was in excess of the OP generated by the alternative FSs. The six fertiliser solutions evaluated for the FDFO desalination study had instinct solution properties, and the OP that they generated was dependent on these properties. K_2SO_4 generated the highest OP of 55 490 kPa at 10 M, while $CO(NH_2)_2$ generated the lowest OP of 2 530 kPa at 1 M, despite being highly soluble. A linear correlation was observed for the fertiliser DS concentration and the respective OP that they generated.

Fertiliser blends were also evaluated as potential DSs for the FDFO desalination study. Straight fertilisers were blended in equal molar concentrations ranging from 0 to 2 M. The blending of fertiliser solutions generally resulted in reduced OP generation in comparison to the OP calculated from the sum of the individual fertiliser DSs' OPs. The

low OP generated for the blended fertiliser DSs was the result of the formation of precipitate that reduced the overall solubility of the blended fertiliser solution.

The two FO membranes (CTA and ABM) were comparatively evaluated in terms of experimental water flux (J_w), reverse solute flux (J_s) and water recovery for straight fertiliser DS, 1 M KCl, and blended fertiliser DS, N/P/K against alternative FSs, namely DI water, SWW and BW5. Two batches of ABM membranes were evaluated in the FDFO study, ABM_A01 and ABM_A02.

The ABM_A02 membrane proved superior for the reclamation of water with the purpose of reducing the final nutrient concentration of fertiliser DSs for direct fertigation. The performance of the ABM_A02 membrane in terms of J_w was significantly higher than that of the commercial CTA membrane. It was concluded that the performance of the ABM_A02 membrane in terms of experimental J_w is limited to feed waters with a high total dissolved solids (TDS) concentration when single 1 M KCl fertiliser DS was used. Despite exceptional experimental J_w generation, the average J_s of the ABM_A02 membrane was significantly higher than that of the commercial CTA membrane. The average J_s observed for the CTA membrane was notably low in comparison to the ABMs (ABM_A01 and ABM_A02).

5.2. Recommendations

The following recommendations are made, based on the challenges experienced and results obtained.

1. Although scanning electron microscopy (SEM) images illustrate scaling on membrane surfaces, in-depth membrane autopsy such as energy-dispersive x-ray spectroscopy (EDS) analysis can be conducted to identify the scaling composition. The composition of the scaling layer will provide insight into the reverse solute diffusion of draw solutes.
2. Despite significantly increased OP when a N/P/K fertiliser DS was used, the experimental J_w observed was not proportional to the bulk OP difference ($\Delta\pi$) of the FO system. The performance of individual straight fertiliser solutes $CO(NH_2)_2$ and H_3PO_4, as found in the N/P/K blended fertiliser DS, should be assessed in terms of experimental J_w. The performance of the individual straight fertiliser solutes ($CO(NH_2)_2$ and H_3PO_4) could provide insight into the performance of the blended fertiliser DS.

3. Placing the DS on a weight balance and FS on a magnetic stirrer could result in a constant homogenous FS and hence more accurate electrical conductivity (EC) measurements.
4. J_s for the ABM_A01 and ABM_A02 was higher than < 2 $g.m^{-2}.h^{-1}$ as in the datasheet, therefore experiments for J_s should be repeated with the latest developed ABM, that is still within its respective shelf life.

REFERENCES

Achilli, A., Cath, T.Y. & Childress, A.E. 2010. Selection of inorganic-based draw solutions for forward osmosis applications. *Journal of Membrane Science*, 364(1-2):233-241.

Achilli, A., Cath, T.Y., Marchand, A.E. & Childress, A.E. 2009. The forward osmosis membrane bioreactor: A low fouling alternative to MBR processes. *Deslination*, 239(1-3):10-21.

Agustina, T.E., Ang, H.M. & Pareek, V.K., 2008. Treatment of winery wastewater using a photocatalytic/photolytic reactor. *Chemical Engineering Journal,* 135:151-156.

Akther, N., Sodiq, A., Giwa, A., Daer, S., Arafat, H.A. & Hasan, S.W. 2015. Recent advancements in forward osmosis desalination: A review. *Chemical Engineering Journal,* 281:502-522.

Alexander, M. 1981. *Advances in Microbial Ecology*. Volume 5. Berlin: Springer.

Al-Hemiri, A.A., Sharif, A.O. & Hussein, M. 2009. A study of forward osmosis using various drawing agents. *Iraqi Journal of Chemical and Petrochemical Engineering*, 10(3):51-56.

Alsvik, I.L. & Hägg, M. 2013. Pressure retarded osmosis and forward osmosis membranes: Materials and Methods. *Polymers*, 5:303-327.

Alva, A.K., Mattos, D. & Quaggio, J.A. 2008. Advances in nitrogen fertigation of Citrus. *Journal of Crop Improvement*, 22(1):121-146.

Atkinson, S. 2002. Nanofiltration concentrates coloured wastewater and produces potable water. *Membrane Technology*, 2002(7):11-12.

Arienzo, M., Chisten, E.W. & Quayle, W.C. 2009. Phytotoxicity testing of winery wastewater for constructed wetland treatment. *Journal of Hazardous Matter*, 169:94-99.

Benavides, S. & Phillip, W.A. 2016. Water recovery and solute rejection in forward osmosis modules: Modelling and bench-scale experiments. *Journal of Membrane Science*, 505:26-35.

Bassa, F. & Chetty, S. 2002. Determination of biodegradable COD fraction of industrial effluents by measurement of BOD and COD. Paper presented at the Biennial Conference of the Water Institute of Southern Africa (WISA), Durban, South Africa, 19–23 May 2002.

Besada, H. & Werner, K. 2015. An assessment of the effects of Africa's water crisis on food security and management. *International Journal of Water Resources Development*, 31(1):120-133.

Blossey, R. 2003. Self-cleaning surfaces – virtual realities. *Nature Matter,* 2:301-306.

Boo, C., Elimelech, M. & Hong, S. 2013. Fouling control in forward osmosis process integrating seawater desalination and wastewater reclamation. *Journal of Membrane Science*, 444:148-156.

Brito, A.G., Peixoto, J., Oliveira, J.M., Oliveira, J.A., Costa, C., Nogueira, R. & Rodrigues, A. 2006. Brewery and winery wastewater treatment: Some focal points of design and operation. University of Minho, Centre for Biological Engineering, School of Engineering, Campus de Gualtar, 4710-057 Braga, Portugal.

Bull, H.B., Breese, K., Ferguson, G.L. & Swenson, C.A. 1964. The pH of urea solutions. *Archives of Biochemistry and Biophysics*, 104(2):297-304.

Calzadilla, A., Zhu, T., Rehdanz, K., Tol, R.S.J. & Ringler, C. 2014. Climate change and agriculture: Impacts and adaptation options in South Africa. *Water Resources and Economics*, 5:24-48.

Cath T.Y., Adams D. & Childress A.E. 2005. Membrane contactor processes for wastewater reclamation in space. Part II: Combined direct osmosis, osmotic distillation, and membrane distillation for treatment of metabolic wastewater. *Journal of Membrane* Science, 257:111–119.

Cath, T.Y., Childress, A.E. & Elimelech, M. 2006. Forward Osmosis: Principles, applications and recent development: Review. *Journal of Membrane Science*, 281:70-87.

Cath, T.Y., Hancock, N.T., Lundin, C.D., Hoppe-Jones, C. & Drewes, J.E. 2010. A multi-barrier osmotic dilution process for simultaneous desalination and purification of impaired water. *Journal of Membrane Science*, 362:417-426.

Chekli, L., Phuntsho, S., Kim, J.E., Kim, J., Choi, J.Y., Choi, J., Kim, S., Kim, J.H., Hong, S., Sohn, J. & Shon, H.K. 2016. A comprehensive review of hybrid forward osmosis systems: Performance, applications and future prospects. *Journal of Membrane Science*, 497:430-449.

Chen, X., Xu, J., Lu, J., Shan, B. & Gao, C. 2017. Enhanced performance of cellulose triacetate membranes using binary mixed additives for forward osmosis desalination. *Desalination*, 405:68-75.

Chung, T.S., Li, X., Ong, R.C., Ge, Q., Wang, H. & Han, G. 2012. Emerging forward osmosis (FO) technologies and challenges ahead for clean water and clean energy applications. *Current Opinion Chemical Engineering*, 3:246-257.

Coday, B.D., Beaudry, E.G., Herron, J., Lampi, K., Hancock, N.T. & Cath, T.Y. 2014. The sweet spot of forward osmosis: Treatment of produced water, drilling water and other complex and difficult liquid streams. *Desalination*, 333(1):23-35.

Conradie, W.J. & Myburgh, P.A. 2000. Fertigation of *Vitis vinifera* L. cv. Bukettraube/110 Richter on a sandy soil. *South African Journal of Enology and Viticulture*, 21:63-66.

Conradie, A., Sigge, G.O. & Cloete, T.E. 2014. Influence of winemaking practices on the characteristics of winery wastewater and water usage of wineries. *South African Journal of Enology and Viticulture,* 35(1):10-19.

Costa, A.R. & De Pinho, M.N. 2006. Comparison of the performance of ultrafiltration and nanofiltration in surface water treatment. *Desalination*, 199(1-3):73-75.

DAFF (Department of Agriculture, Forestry and Fisheries). 2012. Production guideline: Grapes. Available online at http:/www.nda.agric.za/docs/Brochures/grapesprod.pdf

[30 June 2016].

DAFF (Department of Agriculture, Forestry and Fisheries). 2015a. Economic Review of the South African Agriculture. Available online at http://www.agrisa.co.za/wp-content/uploads/2016/03/Economic-Review-of-the-South-African-agriculture-2015.pdf.
[24 June 2016].

DAFF (Department of Agriculture, Forestry and Fisheries). 2015b. South African fertilizers market analysis report. Available online at http://www.nda.agric.za/doaDev/sideMenu/Marketing/Annual%20Publications/Commodity%20Profiles/field%20crops/South%20African%20Fertilisers%20Market%20Analysis%20Report%202015.pdf [24 June 2016].

Devesa-Rey, R., Vecino, X., Varela-Alenda, J.L., Barral, M.T., Cruz, J.M. & Moldes, A.B. 2011. Valorization of winery waste vs. cost of not recycling. *Waste Management*, 31:2327-2335.

Dillon, C. 2011. Waste management in the South African wine industry. Dissertation submitted for the diploma of Cape Wine Master to the Cape Wine Academy, South Africa.

Dryden, M. & Campbell, V. 2013. Opportunities to reduce water and carbon footprints of Western Cape produce-A focus on irrigation. Unpublished final year project. Department of Chemical Engineering, University of Cape Town, South Africa.

Erdogan, I.G. 2014. Treatment of softdrink industry wastewater using an integrated anaerobic/aerobic membrane bioreactor. Unpublished Master's Thesis. Department of Chemical Engineering, Cape Peninsula University of Technology, South Africa.

Fang, W., Wang, R., Chou, S., Setiawan, L. & Fane, A.G. 2012. Composite forward osmosis hollow fiber membranes: Integration of RO- and NF-like selective layers to enhance membrane properties of anti-scaling and anti-internal concentration polarization. *Journal of Membrane Science*, 394:140-150.

Fleming, E., Mounter, S., Grant, B., Griffith, G. & Villano, R. 2014. The New World challenge: Performance trends in wine production in major wine-exporting countries

in the 2000s and their implications for the Australian wine industry. *Wine Economics and Policy*, 3:115-126.

Fritzmann, C., Löwenberg, J., Wintgens, T. & Melin, T. 2007. State-of-the-art reverse osmosis desalination. *Desalination*, 216(1-3):1-76.

Garcia, N., Moreno, J., Cartmell, E., Rodriguez-Roda, I. & Judd, S. 2013. The cost and performance of a MF-RO/NF plant for trace metal removal. *Desalination*, 309:181-186.

Ge, Q., Ling, M. & Chung, T. 2013. Draw solutions for forward osmosis processes: Developments, challenges, and prospects for the future. *Journal of Membrane Science*, 442:225-237.

Goga, S. & Pegram, G. 2014. A review of integrated planning in South Africa. *Understanding the Food Energy Water Nexus.* WWWF SA. Pretoria: British Commission.

Goldammer, T. 2015. *Grape Grower's Handbook: A Guide to Viticulture for Wine Production*. Centreville, VA: Apex Publishers.

Goldblatt, A. 2010. WWWF: Agriculture: Facts and trends South Africa. Available online at http://www.worldwildlife.org/cci/agriculture.cfm [12 April 2016].

Gonotec. 2014. User Guide: Osmomat 3000. Version 1.05. Available online at http://www.gonotec.com/ [8 September 2016].

Grain SA. 2011. Fertiliser Report. Available online at http://www.grainsa.co.za/upload/report_files/Kunsmisverslag-Volledig.pdf [1 September 2017].

Grattoni, A. & Merlo, M. 2007. Osmotic pressure beyond concentration restriction. *Journal of Physical Chemistry*, 111:11770-11775.

Gray, G.T., McCutcheon, J.R. & Elimelech, M. 2006. Internal concentration polarization in forward osmosis: Role of membrane orientation. *Desalination*, 197:1-8.

Greenlee, L.F., Lawler, D.F., Freeman, B.D., Marrot, B. & Moulin P. 2009. Reverse osmosis desalination: Water sources, technology and today's challenges. *Water Research*, 43(9):2317-2348.

Grismer, M.E., Carr, M.A. & Sheperd, H.L. 2003. Evaluation of constructed wetland treatment performance for winery wastewater. *Water Environmental Research,* 75(5):412-421.

Guglielmi, G., Andreottola, G., Foladori, P. & Ziglio, G. 2009. Membrane bioreactors for winery wastewater treatment: Case studies at full scale. *Water Science Technology*, 60(5):1201-1206.

Hagin, J., Sneh, M. & Lowengart-Aycicegi, A. 2002. Fertigation – Fertilization though irrigation. IPI Research Topics No. 23. Ed. by A.E. Johnston. Basel, Switzerland: International Potash Institute.

Han, G., Liang, C., Chung, T., Weber, M., Staudt, C. & Maletzko, C. 2016. Combination of forward osmosis (FO) process with coagulation/flocculation (CF) for potential treatment of textile wastewater. *Water Research*, 91:361-370.

Hélix-Nielsen, C. 2009. Biomimetic membranes for sensor and separation applications. *Analytical and Bioanalytical Chemistry*, 395:697-718.

Huang, H. & Yang, S. 2006. Filtration characteristics of polysulfone membrane filters. *Journal of Aerosol Science*, 37:1198-1208.

Huang, L. & McCutcheon, J. 2015. Impact of support layer pore size on performance of thin film composite membranes for forward osmosis. *Journal of Membrane Science*, 483:25-33.

Huei, L.C. 2005. Biodegradation of brewery effluent using packed-bed upflow anaerobic reactor (PBUAR) and membrane bioreactor (MBR). Unpublished Bachelor's thesis, Faculty of Civil Engineering, University Teknologi. Kuala Lumpur, Malaysia.

Ioannou, L.A., Michael, C., Vakondios, N., Drosou, K., Xekoukoulotakis, N.P., Diamadopoulos, E. & Fatta-Kassinos, D. 2013. Winery wastewater purification by

reverse osmosis and oxidation of the concentrate by solar photo-fenton. *Separation and Purification Technology*, 118:659-669.

Jin, X., Shan, J., Wang, C., Wei, J. & Tang, C.Y. 2012. Rejection of pharmaceuticals by forward osmosis membranes. *Journal of Hazardous Materials*, 227-228:55-61.

Judd, S. 2011. *The MBR Book: Principles and Applications of Membrane Bioreactors for water and wastewater treatment.* Oxford: Butterworth-Heinemann.

Kafkafi, U. & Tarchitzky, J. 2011. *Fertigation: A tool for efficient fertilizer and water management*. International Fertilizer Industry Association (IFA). International Potash Institute (IPI). Paris, France

Klaysom, C., Cath, T.Y., Depuydta, T. & Vankelecom, I.F.J. 2013. Forward and pressure retarded osmosis: Potential solutions for global challenges in energy and water supply. *The Royal Society of Chemistry*, 42:6959-6989.

Korenak, J., Basu, S., Balakrishnan, M., Hélix-Nielsen, C. & Petrinić, I. 2017. Forward Osmosis in Water Treatment Processes. *Acta Chimica Solvenica*, 64:83-94.

Kumar, M., Grzelakowski, M., Zilles, J., Clark, M. & Meier. 2007. Highly permeable polymeric membranes based on the incorporation of the functional water channel protein Aquaporin Z. *Proceedings of the National. Academy of Sciences U.S.A*, 104:20719-20724.

Kyzas, G.Z., Symeonidou, M.P. & Matis, K.A. 2014. Technologies of winery wastewater treatment: A critical approach. *Desalination and Water Treatment*, 57(8): 1-15.

Laing, M. 2016. Investigating the performance of a novel anaerobic sequencing batch reactor (ANSBR) and optimisation of operational parameters to treat synthetic winery wastewater. Unpublished Master's Thesis. Department of Food Science, Stellenbosch University, Stellenbosch, South Africa.

Larcher, W. 2003. *Physiology Plant ecology: ecophysiology and stress physiology of functional groups*. 4th Edition. New: York: Springer.

Linares, R.V., Li, Z., Elimelech, M., Amy, G. & Vrouwenvelder, H. 2017. Recent developments in forward osmosis processes. Available online at http://www.iwaponline.com [13 September 2017].

Logan, B.E. & Elimelech, M. 2012. Membrane-based processes for sustainable power generation using water. *Nature,* 488:313-319.

Low, Z., Liu, Q., Shamsaei, E., Zhang, X. & Wang, H. 2015. Preparation and characterization of thin-filmed composite membrane with nanowire-modified support for forward osmosis process. *Membranes*, 5:136-149.

Lutchmiah, K., Verliefde, A.R.D., Roest, K., Rietveld, L.C. & Cornelissen, E.R. 2014. Forward osmosis for application in wastewater treatment: A review. *Water Research*, 58:179-197.

Madsen, H.T., Bajraktari, N., Hélix-Nielsen, C., Van der Bruggen, B. & Søgaard, E.G. 2015. Use of biomimetic forward osmosis membrane for trace organics removal*. Journal of Membrane Science*, 476:469-474.

Maguire, R. 2009. Fertiliser type and calculating application rates. *Virginia Cooperative Extension Publications* No. 424-035. Virginia State University, Petersburg VA.

Mahajan. C.S., Jadhav, R.N., Narkhede, S.D., Ingle, S.T. & Attarde, S.B. (2009). Assessment of winery wastewater and its impact on irrigated soil. *Journal of Environmental Research and Development*, 4(2):365-371.

Martinetti, C.R., Childress, A.E. & Cath, T.Y. 2009. High recovery of concentrated RO brines using forward osmosis and membrane distillation. *Journal of Membrane Science*, 331(1-2):31-39.

McCutcheon, J.R., McGinnis, R.L. & Elimelech, M. 2006. Desalination by ammonia-carbon dioxide forward osmosis: Influence of draw and feed solution concentrations on process performance. *Journal of Membrane Science*, 278:114-123.

McCutcheon, J.R. & Elimelech, M. 2006. Influence of concentrative and dilutive internal concentration polarization on flux behaviour in forward osmosis. *Journal of Membrane Science*, 284:237-247.

McGovern, R. K. 2014. The Economics of future membrane desalination processes and applications. Unpublished PhD thesis, Massachusetts Institute of Technology, Cambridge MA.

Melamane, X. L. 2007. Treatment of wine distillery wastewaters by high rate anaerobic digestion and submerged membrane systems. Doctoral dissertation, Rhodes University, Grahamstown, SA.

Melamane, X.L., Strong, P.J. & Burgess, J.E. 2007. Treatment of wine distillery wastewater: A review with emphasis on anaerobic membrane reactors. *South African Journal for Enology and Viticulture*, 28(1):25.

Miyaki, H., Adachi, S., Suda, K. & Kojima, Y. 2000. Water recycling by floating media filtration and nanofiltration at a soft drink factory. *Desalination,* 131(1):47-53.

Mosse, K.P.M., Patti, A.F., Chisten, E.W. & Cavagnaro, T.R. 2011. Review: Winery wastewater quality and treatment options in Australia. *Australian Journal of Grape and Wine Research*, 17(2):111-121.

Motsa, M.M., Mamba, B.B., Hoek, E.M.V. & Verliefde, A.R.D. 2014. Organic fouling in forward osmosis membranes: The role of feed solution chemistry and membrane structural properties. *Journal of Membrane Science*, 460:99-109.

Mozell, M.R. & Thach, L. 2014. The impact of climate change on the global wine industry: Challenges & solutions. *Wine Economics and Policy*, 3(2):81-89.

Mpelasoka, B.S., Schachtman, D.S., Treeby, M.T. & Thomas, M.R. 2003. A review of potassium nutrition in grapevines with special emphasis on berry accumulation. *Australian Journal of Grape and Wine Research*, 9:154-168.

Musee, N., Lorenzen, L. & Aldrich, C. 2007. Cellar waste minimization in the wine industry: A systems approach. *Journal of Cleaner Production*, 15:417-431.

Myburgh, P.A. & Howell, C.A. 2014. The impact of wastewater irrigation by wineries on soils, crop growth and product quality. Report to the Water Research Commission and Winetech by ARC Infruitec-Nietvoorbij. Stellenbosch, SA.

Naidu, L.D., Saravanan, S., Chidambaram, M., Goel, M., Das, A. & Sarat Chandra Babu, J. 2015. Nanofiltration in transforming surface water into healthy water: comparison with reverse osmosis. *Journal of Chemistry*, 15:1-6.

Nkondo, M., Van Zyl, F., Keuris, H. & Scheiner, B. 2012. Proposed National Water Research Strategy (NWRS 2). Summary: Managing water for an equitable and sustainable future. (2). Pretoria, SA: Department of Water Affairs.

NOAA (National Oceanic and Atmospheric Administration). 2017. Why is the ocean so salty? Available online at https://www.oceanservice.noaa.gov/facts/whysalty.html [14 September 2017].

Perrin, D.D., Dempsey, B. & Serjeant, E.P. 1981. *pK_a – prediction for organic acids and bases*. London: Chapman & Hall.

Perry, M., Madsen, S.U., Jorgensen, T., Braekevelt, S., Lauritzen, K. & Hélix-Nielsen, C. 2015. Challenges in commercializing biomimetic membranes. *Membranes*, 5:685-701.

Perry, R.H., Green, D.W. & Maloney, J.O. 1997. *Perry's chemical engineers' handbook*. 7th Edition. New York: McGraw-Hill.

Petruccioli, M., Duarte, J. C., Eusebio, A. & Federici, F. 2002. Aerobic treatment of winery wastewater using a jet-loop activated sludge reactor. *Process Biochemistry*, 37(8):821-829.

Petruccioli, M., Duarte, J.C. & Federici, F. 2000. High rate aerobic treatment of winery wastewater using bioreactors with free immobilized activated sludge. *Journal of Bioscience Bioengineering,* 90(4):381.

Proffitt, T. & Campbell-Clause, J. 2012. *Managing grapevine nutrition and vineyard soil health.* http://www.winewa.asn.au. [13 June 2016].

Phuntsho, S., Shon, H.K., Hong, S., Lee, S. & Vigneswaaran, S. 2011. A novel low energy fertiliser-driven forward osmosis desalination for direct fertigation: Evaluating the performance of fertiliser draw solutions. *Journal of Membrane Science*, 375:172-181.

Phuntsho, S. 2012. A novel fertiliser drawn forward osmosis desalination for fertigation. Unpublished PhD Thesis. School of Civil and Environmental Engineering, Faculty of Engineering and Information Technology. University of Technology, Sydney (UTS), New South Wales, Australia.

Phuntsho, S., Shon, H.K., Hong, S., Lee, S., Vigneswaaran, S. & Kandasamy, J. 2012. Fertiliser drawn forward osmosis desalination: The concept, performance and limitations of fertigation. *Reviews in Environmental/Science Biotechnology*, 11:147-168.

Phuntsho, S., Lotfi, F., Hong, S., Shaffer, D.L., Elimelech, M. & Shon, H.K. 2014. Membrane scaling and flux decline during fertiliser drawn forward osmosis desalination of brackish groundwater. *Water Research*, 57:172-182.

Phuntsho, S, Kim, J.E., Johir, M.A.H., Hong, S., Li, Z., Ghaffour, N., Leiknes, T. & Shon, H.K. 2016. Fertiliser drawn forward osmosis process: Pilot-scale desalination of mine impaired water for fertigation. *Journal of Membrane Science*, 508:22-31.

Qasim, M., Darwish, N.A., Sarp, S. & Hilal, N. 2015. Water desalination by forward (direct) osmosis phenomenon: A comprehensive review. *Desalination*, 374:47-69.

Qi, S., Wang, R., Chaitra, G.K.M., Torres, J., Hu, X. & Fane, A.G. 2016. Aquaporin-base biomimetic reverse osmosis membranes: Stability and long term performance. *Journal of Membrane Science*, 508:94-103.

Qui, C., Setiawan, L., Wang, R., Tang, C.Y. & Fane, A.G. 2012. High performance flat sheet forward osmosis membrane with an NF-like selective layer on a woven fabric embedded substrate. *Desalination,* 287:266-270.

Quist-Jensen, C.A, Macedonio, F. & Drioli, E. 2015. Membrane technology for water production in agriculture: Desalination and wastewater reuse. *Desalination,* 364:17-32.

Raath, P.J. 2012. Effect of varying levels of nitrogen, potassium and calcium nutrition on table grape vine physiology and berry quality. Unpublished PhD Thesis. Department of Viticulture and Oenology, Faculty of AgriSciences. University of Stellenbosch, Stellenbosch, SA.

Ramond, J.B., Welz, P.J., Tuffin, M.I., Burton, S.G. & Cowan, D.A. 2013. Assessment of temporal and spatial evolution of bacterial communities in a biological sand filter mesocosm treating winery wastewater. *Journal of Applied Microbiology*, 115:91-101.

Rapheal, S., Sapoznik, J. & Hassan, D. 2010. Energy aspects in osmotic processes. *Desalination and Water Treatment*, 15:228-235.

Rautenbach, R. & Albrecht, R. 1989. *Membrane Processes*. London: John Wiley.

Rautenbach, R. & Groeschl, A. 1990. Separation potential of nanofiltration membranes. *Desalination*, 77(1-3):73-84.

Said, R.R. 2011. Forward osmosis process for the treatment of wastewater from textile industries. Unpublished MSc. The College of Engineering, University of Baghdad, Baghdad, Iraq.

Shaffer, D.L., Werber, J.R., Jaramillo, H., Lin, S. & Elimelech, M. 2015. Forward osmosis: Where are we now? *Desalination,* 356:271-284.

Shen, Y., Saboe, P.O., Sines, I.T., Erbakan, M. & Kumar, M. 2014. Biomimetic membranes: A review. *Journal of Membrane Science,* 454:359-381.

Sheridan, C.M., Glasser, D., Hildebrandt, D., Petersen, J. & Rohwer, J. 2011. An annual and seasonal characterisation of winery effluent in South Africa. *South African Journal of Enology and Viticulture*, 32(1):1-8.

Simate, G.S., Cluett, J., Iyuke, S.E., Musapatika, E.T., Ndlovu, S., Walubita, L.F. & Alvarez, A.E. 2011. The treatment of brewery wastewater for reuse: State of the art. *Desalination*, 273(2):235-247.

Singh, N., Petrinić, I., Hélix-Nielsen, C., Basu, S. & Balakrishnan, M. 2018. Concentrating molasses distillery wastewater using biomimetic forward osmosis (FO) membranes. *Water Research*, 130:271-280.

SAWIS (South African wine industry information & systems). 2016. *South African wine exports analysis*. Available online at wosa.co.za/The-Industry/Statistics/Sawis-Annual-Statistics/.

Sterlitech Corporation. 2016. Forward osmosis (FO) Membranes. Available online at http://www.sterlitech.com/membrane-process-development/flat-sheet-membranes/forward-osmosis-membranes.html. [5 July 2016].

Strong, P.J. & Burgess, J.E. 2008. Treatment methods for wine-related and distillery wastewaters: A review. *Bioremediation Journal,* 12(2):70-87.

Sunohara, T. & Masuda, T. 2011. Cellulose triacetate as a high-performance membrane. *Contributions to Nephology*, 173:156-163.

Tan, C.H. & Ng, H.Y. 2010. A novel hybrid forward osmosis-nanofiltration (FO-NF) process for seawater desalination: Draw solution selection and system configuration. *Desalination and Water Treatment*, 13:356-361.

Tang, C.Y., Zhao, Y., Wang, R., Hélix-Nielsen, C. & Fane, A.G. 2013. Desalination by biomimetic aquaporin membranes: Review of status and prospects. *Desalination*, 308:34-40.

Tang, C., Wang, Z., Petrinić, I., Fane, A.G. & Hélix-Nielsen, C. 2015. Biomimetic aquaporin membranes coming of age. *Desalination*, 368: 89-105.

Thiam, D.R., Muchapondwa, E., Kirsten, J. & Bourblanc, M. 2015. Implications of water policy reforms for agricultural productivity in South Africa: Scenario analysis based on the Olifants river basin. *Water Resources and Economics,* 9:60-79.

Thorsen, T. & Fløgstad, H. 2006. Nanofiltration in drinking water treatment: Literature review. *Techne*au D5.3.4B.

Thopil, G.A. & Pouris, A. 2016. A 20 year forecast of water usage in electricity generation for South African amidst water scarce conditions. *Renewable and Sustainable Energy Reviews*, 62:1106-1121.

Treeby, M.T., Beckinham, C.R. & Cross, N. 2004. Fertigation. In *Drip irrigation: A Grapegrower's Guide*. 3rd Edition. Ed. J. Giddings. Orange, Australia: NSW Agriculture. 89-99.

Treeby, M. 2006. Manipulating grapevine annual shoot growth, yield, and composition of grapes using fertigation. CSIRO Plant Industry, Horticulture Unit, River Avenue, Merbein, Victoria, Australia.

Tu, K.L., Nghiem, L.D. & Chivas, A.R. 2010. Boron removal by reverse osmosis membranes in seawater desalination application. *Separation and Purification Technology*, 75(2):87-101.

Turner, K.N., Naidoo, K., Theron, J.G. & Broodryk, J. 2015. Investigation into the coast and operation of Southern African desalination and water reuse plants. Volume 2: Current Status of Desalination and Water Reuse in Southern Africa. Report to the Water Research Commission, Pretoria, SA.

Van der Bruffen, B. & Vandecasteele, C. 2003. Removal of pollutants from surface water and groundwater by nanofiltration: Overview of possible applications in the drinking water industry. *Environmental Pollution*, 122(3):435-445.

Van Schoor, L.H. 2005. *Guidelines for the management of wastewater and solid waste at existing wineries*. Paarl, SA: WineTech.

Vinexpo. 2013. *South African wines increase in popularity on the international markets*. Available at http://www.vinexpo.com/en/news/archives/2013/?page=4. [21 July 2016].

VinPro. 2015. *Agro-economy: Financial benchmarking and feasibility studies for wine grape production.* Available at http://www.vinpro.co.za/services/agro-economy. [5 April 2016].

Von Bormann, T. & Gulati, M. 2014. The food energy water nexus: Understanding South Africa's most urgent sustainability challenge. WWWF SA. Pretoria, SA: British Commission. 1-35.

Welz, P.J., Palmer, Z., Isaacs, S., Kirby, B. & le Roes-Hill, M. 2014. Analysis of substrate degradation, metabolite formation and microbial community response in sand bioreactors treating winery wastewater: A comparative study. *Journal of Environmental Management*, 145:147-156.

Welz, P.J., Ramond, J.B., Cowan, D.A. & Burton, S.G. 2012. Phenolic removal process in biological sand filters, sand columns and microcosms. *Bioresource Technology*, 119:262-269.

Welz, P.J. & le Roes-Hill, M. 2014. Biodegradation of organics and accumulation of metabolites in experimental biological sand filters used for the treatment of synthetic winery wastewater: A mesocosm study. *Journal of Water Process Engineering*, 3:155-163.

Wicaksana, F., Fane, A.G., Tang, C. & Wang, R. 2012. Nature meets technology: Forward osmosis membrane technology. In C. Hélix-Nielsen (Ed.), *Biomimetic membranes for sensor and separation applications*. Berlin: Springer. 21-42.

Wilson, A.D. & Stewart, F.F. 2013. Deriving osmotic pressures of draw solutes used in osmotically driven membrane processes. *Journal of Membrane Science*, 431:205-211.

WOSA (Wines of South Africa). 2016. *The Industry-Overview*. http://www.wosa.co.za/The-Industry/Overview/ [5 April 2016].

Woltersdorf, L., Scheidegger, R., Lieh, S. & Döll, P. 2016. Municipal water reuse for urban agriculture in Namibia: Modelling nutrient and salt flows as impacted by sanitation user behaviour. *Journal of Environmental Management,* 169:272-284.

Yong, J.S., Phillip, W.A. & Elimelech, M. 2012. Coupled reverse draw solute permeation and water flux with neutral draw solutes. *Journal of Membrane Science*, 392-393:9-17.

Zaviska, F. & Zou, L. 2014. Using a modelling approach to validate a bench scale forward osmosis pre-treatment process for desalination. *Desalination*, 350:1-13.

Zhang, H., Cheng, S. & Yang, F. 2014a. Use of a spacer to mitigate concentration polarization during forward osmosis process. *Desalination,* 347:112-119.

Zhang, X., Ning, Z., Wang, D.K. & Diniz da Costa, J.C. 2014b. Processing municipal wastewaters by forward osmosis using CTA membrane. *Journal of Membrane Science*, 468:269-275.

Zhao, P., Gao, B., Xu, S., King, J., Ma, D., Shon, H.K., Yue, Q. & Liu, P. 2015. Polyelectrolyte-prompted forward osmosis process for dye wastewater treatment: Exploring the feasibility of using polyacrylamide as draw solution. *Chemical Engineering Journal*, 264:32-38.

Zhao, P., Gao, B., Yue, Q., Liu, S. & Shon, H.K. 2016. Effect of high salinity on the performance of forward osmosis: Water flux, membrane scaling and removal efficiency. *Desalination,* 378:67-73

Zhao, Y., Qiu, C., Li, X., Vararattanavech, A., Shen, W., Torres, J., Hélix-Nielsen, C., Wang, R., Hu, X., Fane, A.G. & Tang, C.Y. 2012. Synthesis of robust and high-performance aquaporin-based biomimetic membranes by interfacial polymerization-membrane preparation and RO performance characterization. *Journal of Membrane Science*, 423-424:422-428.

Zhao, C., Xue, J., Ran, F. & Sun, S. 2013. Modification of polyethersulfone membranes: A review of methods. *Progress in Material Science*, 58:76-150.

Zhao, J., Zhao, X., Jiang, Z., Li, Z., Fan, X., Zhu, J., Wu, H., Su, Y., Yang, D., Pan, F. & Shi, J. 2014. Biomimetic and bioinspired membranes: Preparation and application. *Progress in Polymer Science,* 39:1668-1720.

APPENDIX A: Water Analyses Report

Sample	pH at 25ºC	EC at 25ºC mS.m^{-1}	OP (kPa)	Na (mg.L^{-1})	K (mg.L^{-1})	Ca (mg.L^{-1})	Mg (mg.L^{-1})	Cl (mg.L^{-1})	SO_4 (mg.L^{-1})	B (mg.L^{-1})	TDS (mg.L^{-1})
DI	5.3	0.4	0.14	22.5	0.4	0.6	0.6	3	6	0.34	3
DI	5.4	0.5	0.18	11.7	0.2	0.1	0.2	3	5	0.2	3
BW5	5.6	1 066	384	2 040	0.2	0	0.1	3 140	5	0.13	6 819
BW5	4.7	1 067	384	2 098	0.2	0.1	0	3 040	5	0.09	6 826
SSW	5.8	5 716	2 058	9 390	2.1	7.8	1	23 660	5	0.05	36 364
SSW	5.8	5 713	2 057	9 445	0.7	0.3	0	24 120	5	0.02	36 169
AOSB											
C4	7.8	5 020	1 807.2	8 476.3	381.4	329.5	202.1	18 845.4	2 989	3.8	29 800
C4	7.8	5 080	1 828.8	8 529.4	380.1	332.3	224.8	19 594	3 035	3.84	30 200
SP	7.9	5 170	1 861.2	8 535	382.6	332.1	220.3	19 766.8	3 028	3.8	31 000
SP	7.9	5 140	1 850.4	8 352.6	379.2	326.9	224.6	19 781.1	2 976	3.76	30 700
CB	7.9	5 140	1 850.4	6 861.8	318.4	312.5	204.7	20 141.1	2 351	5.61	30 800
CB	7.8	5 200	1 872	6 913.5	316.7	324.8	210.7	19 781.1	2 391	5.32	31 200
IOSB											
STR B	7.5	4 760	1 713.6	7 922.5	362.3	306.7	230.3	18 298.3	2 779	3.51	28 400
STR B	7.5	4 740	1 706.4	7 896.9	364.1	307.5	226.8	18 197.5	2 800	3.53	28 200
GB	7.9	5 120	1 843.2	8 464.7	383.3	331.3	220.2	19 881.9	3 002	3.76	30 600
GB	7.9	5 140	1 850.4	8 591.5	381.3	335.9	211.6	19 738	3 044	3.84	30 700
STR A	8	5 160	1 857.6	8 546	390.8	332.1	220.8	19 766.8	3 020	3.85	30 800
STR A	7.9	5 160	1 857.6	8 544.1	386.5	335	222.6	19 795.5	3 048	3.86	30 900

*Note: C4: Clifton 4th; SP: Sea Point; CB: Camps Bay; STR B: Strand B; STR A: GB: Gordons Bay; Strand A

APPENDIX B: Biomimetic membrane handling, storage, and cleaning

B 1. Membrane preparation

Prior use of the aquaporin biomimetic membrane (ABM), ABMs should be soaked in deionised (DI) water for a minimum of 30 minutes. Once wet, the membrane should not be dried again.

B 2. Membrane handling

When handling the membrane it is advised to do so with gloves so as to not compromise the integrity of the membrane surface.

B 3. Membrane cleaning after use

Membrane cleaning can be accomplished by periodic rinses achieved by running DI water though the CF042D-FO cell counter currently for 2 h at elevated flow rates.
Cleaning procedure may vary depending on feed water used.

B 3.1. Cleaning procedure for stained membranes

Cleaning procedure with citric acid:

- Procedure
  a. Prepare citric acid solution (10% weight).
  b. Rinse the membrane with the citric acid solution for 40 minutes.
  c. Thereafter, rinse the membrane with DI water to remove any excess citric acid solution.

B 4. Membrane storage

The ABM can be stored at room temperature; recommend storage in a dark place at 4 °C. Do not allow the membrane to dry as this will compromise membrane performance and integrity. After cleaning, the membrane should be stored in DI water until next use. When reusing the ABM, it should be removed from the DI water carefully while wearing gloves and placed directly into the FO cell from the solution. (Sterlitech Corporation, 2016).

Membrane shelf life: Minimum 6 months. (Sterlitech Corporation, 2016).

B 5. Membrane cutting

ABMs are not cut to exact CF042D-FO cell dimensions. ABMs are fragile; the use of scissors is preferred when cutting. Membrane edges should be cut smooth carefully using a sharp scalpel.

B 6. Recommendations

ABMs are still in the development stage and are relatively fragile; care should be taken when handling. Aquaporin suggests avoiding the use of a spacer on the active side of the membrane (draw side is OK) as it can damage the Aquaporin Inside coating. It is also recommended to run at lower cross flow velocities/flow rates to keep the shear stress low at the membrane surface. If high cross flow velocities/flow rates are not required for fouling control, flow rates should be lowered as much as possible.

APPENDIX C: Methyl violet solution to stain damaged thin film composite (TFC) films

C 1. Standard operating procedure

For forward osmosis (FO) experiments:

1. Preparation of 0.01 % methyl violet solution
2. $\frac{1\ \text{g}\ C_{24}H_{28}N_3Cl}{100\ \text{g solution}\ (1\ \text{g}\ C_{24}H_{28}N_3Cl + 99\ \text{g}\ H_2O)} = 0.01\ \%$
3. Add 3 drops of a 0.01 weight % methyl violet solution to the FO feed solution (FS) during testing.

For staining a minimum of 10 mL of feed has to be transported though the membrane skin.

By investigating the stained areas of the membrane surface, conclusions on the type of imperfection can be drawn. Examples of methyl violet stained membranes are illustrated in Figure 7.1.

Figure 7.1: Examples of methyl violet stained membranes

Remember:
Methyl violet is a very intensive dye! The spilled solution should be wiped off immediately with ethanol.
Keep in mind that the methyl violet can also stain equipment thus be aware of any contamination.

APPENDIX D: Operating procedure and calibration of the Osmomat 3000 osmometer

D 1. Operation

- Switch the Osmometer on. The on/off switch is located at the back of the Osmometer.

See Figure 7.2

- Clean the thermistor probe using a soft paper towel.
- Press "Measure" on the Start menu
- Wait until ice forms on the initiation needle.
- After successful ice formation, the menu for calibration or the measurement menu is displayed (depending on the configured calibration interval).
- If necessary, calibrate the device.
- When the device is ready, tap "Measure.

The measurement menu opens

- Pipette a sample volume of 50 µL into an unused and clean measuring vessel

The sample must be pipetted without air bubbles.

- Position measuring vessel on thermistor probe with cover facing front

NOTE: Check that the measuring vessel is securely attached to the thermistor probe when it clicks into place.

- Press "Printer On" on the measurement menu to output the measurement results to a printer. Make sure that the printer is ready
- To start the measurement, tap "Single Sample"
- If necessary, enter the sample ID using the virtual keyboard.
- The sample ID can be pre-defined in the user preferences. In this case, the system assigns the sample ID automatically
- Move elevator DOWN for measurement to occur

Moving the elevator up during the measurement will abort the measurement.

- The sample measurement is performed automatically. Pay attention to the displays on the touchscreen
- The measurement result displays on the touchscreen (in $mOsmol.kg^{-1}$ H_2O) and, if applicable, prints
- Move elevator up.
- Remove measuring vessel from thermistor probe.
- Dispose of measuring vessel and sample according to local regulations.
- Clean thermistor probe using a soft paper towel.

D 2. Calibration

There are two modes of operation of the OSMOMAT 3000 Cryoscopic Osmometer:

a) Calibrating the system with DI and a calibration standard.
b) Measuring the osmolality of a sample.

The calibration of the OSMOMAT 3000 consists of two or three single-pass or multi-pass measurements. This means that the complete calibration (2 or 3 points) is one process. After all required points are measured the results will be displayed and can be accepted, partly disabled or completely rejected.

- Setting the instrument CAL1 using a calibration solution.
  Purpose: Linearization and fixing of instruments CAL1-point.

  Method:

  a. Choose the osmolality of the standard by pressing the << or >> button until the osmolality of the standard is displayed. The values that are represented are: 300,400, 500, 600, 700, 850, 900, 1200, 1500, 1800, 2000, 2500, 100, 200 and back to 300.
  b. Perform measuring as described in OPERATION.
  c. Depending on the selection in Quality Assurance, the user has to run one, two or three passes to confirm the result.
  d. Continue with Second Standard Calibration after all required measurements are successful.

- Setting the instrument CAL2 using a calibration solution
  Purpose: Linearization and fixing of instruments CAL2-point

  Method:

a. Choose the osmolality of the standard by pressing the << or >> button until the osmolality of the standard is displayed. The values that are represented are: 400, 500, 600, 700, 850, 900, 1200, 1500, 1800, 2000, 2500, 100, 200 and back to 400.
b. Perform measuring as described in OPERATION.

c. Depending on the selection in Quality Assurance, the user has to run one, two or three passes to confirm the result.

- Apply calibration values
  Purpose: Finalize calibration

  Method:

  a. Disable single measurements to prevent that outliers distort calibration.
  b. Apply to calibration or retry.

Figure 7.2: Osmometer OSMOMAT 3000 over view (a) front view and (b) back view

Front view:

1. Touch Screen
2. Upper cooling System
3. Thermistor probe with measuring vessel
4. Lower cooling system
5. Elevator
6. Printer

Back view:

1. Interface
2. Fine-Wire fuses

3. On/off switch
4. Power cord connection
5. Fan outlet

APPENDIX E: Phosphate (PO_4) test

E 1. Method for total phosphate determination (0.5 to 5 mg.L^{-1} PO_4 – P (0.11 to 11.46 mg.L^{-1} P_2O_5)).

Using a Merck Spectroquant Phosphate Test for the determination of orthophosphate, Cat. No. 1.14848.0001.

1. The pH of the sample must be within the range of 0 to 10
   Adjust, if necessary with sulphuric acid (H_2SO_4).
2. Pipette 5 mL of the sample into a test tube with P5000 pipette.
3. Add 5 drops of the PO_4-1 reagent to the test tube.
4. Place a cap on the test tube and mix with a vortex mixer.
5. Add 1 level blue microspoon (in the cap of the PO_4-2 bottle) of the PO_4-2 reagent.
6. Place a cap on the test tube and mix vigorously with vortex mixer until the PO_4-2 reagent has completely dissolved.
7. Leave test tube to stand for 5 minutes for the reaction to occur.
8. Fill sample into a 10 mm cell
9. Place the 10 mm cuvette into the 10 mm slot of the Nova 60 Spectroquant to measure for PO_4.

APPENDIX F: Nitrogen (total) cell test

F 1. Method for total nitrogen determination (10 to 150 mg.L^{-1} N)

Using Merck Spectroquant Nitrogen (total) Cell Test for the determination of nitrogen, Cat. No. 1.14763.0001.

1. Pipette 1 mL of the sample into an empty test cell.
2. Add 9 mL of distilled water.
3. Place a cap on the test cell and mix with a vortex mixer.
4. Add 1 level blue microspoon (in the cap of the N-1K bottle) of the N-1K reagent.
5. Place a cap on the test cell and mix with a vortex mixer.
6. Add 6 drops of the N-2K reagent.
7. Place a cap on the test cell and mix with a vortex mixer.
8. Heat the test cells in the Spectroquant thermoreactor TR 420 at 120˚C for 1 h.
9. Carefully remove the test cells after 1 h and place in a test tube rack to cool down to room temperature.
10. Pipette 1 mL of the digested sample into a reaction cell.
    Do not mix the contents.
11. Pipette 1 mL of reagent N-3K.
12. Place the cap on the reaction cell and mix with a vortex mixer.
    Wear eye protection. The cell becomes hot. The cell must be held by the screw cap.
13. Leave test cell to stand for 10 minutes for the reaction to occur.
14. Place the test cells into the Nova 60 Spectroquant to measure for N.

APPENDIX G: Theoretical total N/P/K determination

G 1. Determining total N in N/P/K DS

1. Using the equation, $C=\frac{n}{V}$
2. C = 2 mol.L^{-1} (Concentration of $CO(NH_2)_2$), V = 0.5 L and n = unknow moles
3. $2\ \text{mol.L}^{-1}=\frac{n}{0.5\ \text{L}}$
4. n = 1 mol
5. Using the equation, $m=n\times M_w$
6. n = 1 mol, M_w = 60.06 g.mol^{-1} and m = unknown mass
7. $m=1\ \text{mol}\times 60.06\text{g.mol}^{-1}$
8. m = 60.06 g
9. Using the equation, $\frac{\text{amount of N in fertiliser}\times 100}{\text{percentage of N in fertiliser}}=\text{mass of fertiliser}$
10. Percentage of N in $CO(NH_2)_2$ = 46 %, mass of fertiliser = 60.06 g, amount of N in fertiliser = unknown
11. $\frac{\text{amount of N in fertiliser}\times 100}{\text{percentage of N in fertiliser}}=\text{mass of fertiliser}$
12. $\frac{\text{amount of N in fertiliser}\times 100}{46\%}=60.06\ \text{g}$
13. Amount of N in fertiliser = 27.63 g per 0.5 L
14. Amount of N in fertiliser = 55.26 g.L^{-1}

G 2. Total N in final N/P/K DS for FDFO experiment, N/P/K: DI water

1. Using the equation, $C_1V_1=C_2V_2$
2. Concentration of the undiluted DS (2 M $CO(NH_2)$ – C_1) = 2 mol.L^{-1}, V_1 = 0.5 L, V_2 = 1.37 L and C_2 = unknown molar concentration.
3. $C_1V_1=C_2V_2$
4. $(2\ \text{mol.L}^{-1})\times(0.5\ \text{L})=C_2\times(1.37\ \text{L})$
5. C_2 = 0.73 mol.L^{-1}
6. Converting from molar concentration to mass concentration
7. C_2 = 0.73 mol.L^{-1}, M_w = 60.06 g .mol^{-1}
8. $C_2\times M_w$
9. $0.73\ \text{mol.L}^{-1}\times 60.06\ \text{g.mol}^{-1}$
10. C_2 = 43.84 g.L^{-1}
11. Using the equation, $\frac{\text{amount of N in fertiliser}\times 100}{\text{percentage of N in fertiliser}}=\text{mass of fertiliser}$
12. Percentage of N in $CO(NH_2)_2$ = 46 %, mass of fertiliser = 43.84 g.L^{-1}, amount of N in fertiliser = unknown

13. $\frac{\text{amount of N in fertiliser} \times 100}{\text{percentage of N in fertiliser}} = \text{mass of fertiliser}$
14. $\frac{\text{amount of N in fertiliser} \times 100}{46\%} = 43.84\ \text{g.L}^{-1}$
15. Amount of N in fertiliser = 20.17 g.L^{-1}